Mechanisms of Molecular Chaperone Surface Binding and Endocytosis:

Insights into the Molecular Basis for GRP94 Immune Function

by

Angela Roberta Jockheck-Clark

Department of Cell Biology
Duke University

Date:_____

Approved:

_____
Dr. Christopher V. Nicchitta, Supervisor

_____
Dr. Marc G. Caron, Chair

_____
Dr. Soman N. Abraham

_____
Dr. Alejandro Aballay

Dissertation submitted in partial fulfillment of
the requirements for the degree of Doctor
of Philosophy in the Department of
Cell Biology in the Graduate School
of Duke University

2010

ABSTRACT

Mechanisms of Molecular Chaperone Surface Binding and Endocytosis:

Insights into the Molecular Basis for GRP94 Immune Function

by

Angela Roberta Jockheck-Clark

Department of Cell Biology
Duke University

Date:_____
Approved:

_____
Dr. Christopher V. Nicchitta, Supervisor

_____
Dr. Marc G. Caron, Chair

_____
Dr. Soman N. Abraham

_____
Dr. Alejandro Aballay

An abstract of a dissertation submitted in partial
fulfillment of the requirements for the degree
of Doctor of Philosophy in the Department of
Cell Biology in the Graduate School
of Duke University

2010

Abstract

Extracellular GRP94 can elicit both innate and adaptive immune responses by interacting with endocytic and signaling receptors on professional antigen presenting cells (pAPCs). CD91 was the first receptor proposed to facilitate GRP94-mediated immune responses. Using a GRP94 affinity matrix, a CD91 fragment was isolated from the detergent-solubilized membranes of a pAPC cell line. It was then demonstrated that CD91 ligands could inhibit GRP94-mediated peptide cross-presentation, suggesting that CD91 played a critical role in this process. While these studies implied that CD91 could function as a GRP94 endocytic receptor, later works suggested that CD91 may not recognize GRP94 at the cell surface. These opposing observations have lead to a significant controversy surrounding the identity of CD91 as an endocytic receptor for GRP94. Because the ability of CD91 to directly mediate GRP94 surface binding and uptake has not been established, the studies included in this dissertation have focused on evaluating the ability of CD91 to facilitate three processes that are necessary for GRP94-mediated peptide cross-presentation: surface binding, internalization, and processing.

These studies utilized a recombinantly-expressed N-terminal domain of GRP94 (GRP94.NTD), which was previously shown to have nearly identical biological activity

to full length GRP94. The ability of CD91 to directly bind and internalize GRP94.NTD was examined using murine embryonic fibroblast (MEF) cell lines whose expression of CD91 was either reduced via siRNA, or eliminated by genetic disruption of the CD91 locus. Binding competition experiments were also conducted. Together, these studies reveal that CD91 does not directly interact with GRP94 at the cell surface. The ability of CD91 to directly facilitate GRP94 internalization was examined using various internalization and internalization competition assays. These studies demonstrated that GRP94.NTD and the CD91 ligand RAP were internalized through spatially and kinetically distinct pathways, that CD91 was not necessary for GRP94.NTD internalization, and that RAP did not inhibit GRP94 endocytosis. Together, these studies strongly suggest that CD91 does not directly facilitate GRP94 internalization. When these studies were extended to DC2.4 mouse dendritic cells, the CD91 ligand RAP reduced GRP94.NTD internalization/process by ~15%. This suggests that CD91 may indirectly facilitate GRP94 internalization in pAPC cell lines. Lastly, cross-presentation studies were utilized to examine the ability of various CD91 ligands to influence GRP94.NTD-mediated peptide cross-presentation through a post-uptake mechanism using the DC2.4/OT-1 system. Although it was discovered that DC2.4 cells can internalize and process GRP94.NTD/peptide complexes through fluid-phase endocytosis, CD91 ligands did not significantly inhibit GRP94-mediated peptide cross-

presentation by DC2.4 cells. These studies demonstrate that CD91 does not play a primary role in GRP94-mediated peptide cross-presentation.

In the course of these studies, cell surface heparan sulfate proteoglycans (HSPGs) were identified as novel cell surface binding sites for GRP94.NTD on MEF cells. This conclusion was established using three distinct experimental approaches. GRP94.NTD surface binding was significantly decreased following heparin pre-treatment, following incubation with the sulfation inhibitor sodium chlorate, and following digestion with extracellular heparinase II. Conversely, these treatments did not significantly influence GRP94.NTD binding to RAW264.7 mouse macrophage-like cells. This suggested that GRP94.NTD-HSPG cell surface interactions may require the expression of a specific type of cell surface HSPG that is not expressed by RAW264.7 cells. However, additional studies strongly suggested that GRP94.NTD-HSPG cell surface interactions were mediated by the heparan sulfate-containing side chains rather than the presence of a specific cell surface HSPG core protein.

This dissertation focuses on the critical re-examination of CD91 functions in GRP94 surface binding, uptake, and cross-presentation. Together, these results clarify conflicting data on CD91 function in GRP94 surface binding and endocytosis. This dissertation also describes the identification of cell surface HSPGs as GRP94 binding

sites on MEF cells. These studies extend the diversity of surface receptors that recognize of GRP94, and suggest that cell surface HSPG-dependent interactions may contribute to the biology of GRP94-elicited immune responses.

Dedication

To my family: your continuous love and support have meant the world to me. You've always been there to help me keep my focus and my sanity, and to "walk" me to my car at night. Words can never express my gratitude.

To my husband James: your companionship has kept me alive in so many ways. You've stood by me through good days and bad, and have always made sure that I remembered the important things in life, other than research. I love you.

To Chris: it has been amazing to work for someone who has such an endless and contagious enthusiasm for science. Your encouragement has contributed a large part to my success, and has helped me develop into a more confident researcher. Thank you for being such a wonderful mentor and for directing me through these studies.

Contents

List of Tables

List of Figures

List of Abbreviations

Ad5	adenovirus type 5
ADP	adenosine diphosphate
APC	antigen presenting cell
apoE	apolipoprotein E
ATP	adenosine triphosphate
BSA	bovine serum albumin
ConA	concavalin A
CR	complement-type repeats
CTL	cytotoxic T-lymphocyte
Da	dalton
DC	dendritic cell
DC2.4	mouse dendritic cell line
DEAE	diethylaminoetyl (anion exchange media)
DMEM	Dulbecco's Modified Eagle Medium
EDTA	ethylenediaminetetraacetic acid
EGF	epidermal growth factor
ELISA	enzyme-linked immunosorbent assay
Endog.	endogenous

ER	endoplasmic reticulum
ERK	extracellular-signal-regulated kinase
ERP99	endoplasmic reticulum protein of 99 kDa
FBS	fetal bovine serum
FcγR1	Fcγ receptor 1 (CD64)
Fluor	fluorophore
fVIII-vWF	coagulation factor VIII complexed to von Willebrand factor
GAG	glycosaminoglycan
gp96	GRP94
Gpc	glypican
GPI	glycosylphosphatidylinisotol
GRP94	glucose-regulated protein of 94 kDa
GRP94.LREK	N-terminal domain of GRP94 encoding residues 69-337
GRP94.NTD	N-terminal domain of GRP94 encoding residues 22-337
GRP94.NTD-HS	heat-shocked GRP94.NTD
GRP94.NTDΔKDEL	GRP94 construct encoding the GRP94 N-terminal domain without the KDEL retention signal
GRP94ΔKDEL	GRP94 construct encoding full length GRP94 without the KDEL retention signal
Hsp	heat shock protein
HSPG	heparan sulfate proteoglycan

IFN-γ	interferon gamma
IL	interleukin
kDa	kilodalton
LAL	Limulus amoebocyte lysate
LDL	low density lipoprotein
LRP1	low density lipoprotein-related protein 1
M	molar
MDC	monodansyl cadaverine
MEF	mouse embryonic fibroblast
MEF-1	mouse embryonic fibroblast cell line
MethA	methylcholanthrene
MHCI	class I major histocompatibility complex
MHCII	class II major histocompatibility complex
min	minutes
mRNA	messenger ribonucleic acid
M.W.	molecular weight
NaCl	sodium chloride
NTD	amino terminal domain
N-terminal	amino terminal
p80	protein fragment of 80 kDa

PAGE	polyacrylamide gel electrophoresis
pAPC	professional antigen presenting cell
PAPS	3'-phosphoadenosine 5'-phosphosulfate
PBS	phosphate buffered saline
PBS^{++}	phosphate buffered saline containing 1% BSA and supplemented with CaCl2 and MgCl2
PCR	polymerase chain reaction
PDGF	platelet-derived growth factor
PDGFR	platelet-derived growth factor receptor
PEA-13	$CD91^{-/-}$ mouse embryonic fibroblast cell line
PI	propidium iodide
PI-PLC	phosphatidylinositol-specific phospholipase C
PMN	polymorphonuclear neutrophil
PMSF	phenylmethylsulfonyl fluoride
RAP	receptor associated protein
RAW264.7	mouse macrophage-like cell line
RME	receptor-mediated endocytosis
RT-PCR	reverse transcriptase polymerase chain reaction
SASD	sulfosuccinimidyl 2-(p-azidosalicylamido)ethyl-1,3'-dithiopropionate
SD	standard deviation

Sdc	syndecan
SDS-PAGE	sodium dodecyl sulfate-polyacrylamide gel electrophoresis
siRNA	small interfering ribonucleic acid
SR-A	class A macrophage scavenger receptor
SREC-I	type F scavenger receptor expressed by endothelial cells-I
TCA	trichloroacetic acid
TCR	T-cell receptor
TLR	Toll-like receptor
TNF-α	tumor necrosis factor alpha
TRA	tumor-rejection antigen
VSV	vesicular stomatitis virus
α_2M*	activated α_2-macroglobulin
α_2M	native α_2-macroglobulin

Acknowledgements

There are so many people who have guided and supported me along this journey. I wish to thank you all for being part of my life and for helping me to grow both as a scientist and a person. That being said, there are a handful of people who especially deserve to be mentioned here.

I would like to give heartfelt thanks to my friends and labmates. They have made the past several years truly enjoyable, and have counseled me through some of the most challenging experiences of my graduate school career. I have learned about as much from them as from my work. You all have a special place in my heart, and I wish you the best.

I would like to acknowledge the collaborators who directly contributed to this work. Edith Bower and the laboratory of Salvatore Pizzo have been very generous with their time and reagents. Without their help, the OT-1 studies would have never come to fruition. Mariam Totonchy put in numerous hours on the confocal microscopy to acquire the beautiful MEF images displayed in this dissertation, and Julie Neubauer assessed the *in vitro* effects of trypsin digestion on the fluorescence of Alexa Fluor®-conjugated GRP94.NTD.

I would like to thank my committee members, Dr. Marc Caron, Dr. Soman Abraham, Dr. Alejandro Aballay, and Dr. Michael Ehlers for their input throughout the development of of my dissertation, Dr. Zachary Hartman, Dr. Qi-Quan Huang, and Dr. Richard Pope for their assistance with determination of endotoxin levels, Dr. Harvey Sage for his assistance with analytical ultracentrifugation, and Dr. Jason Maynard, Joshua Lacsina, and Sujatha Jagannathan for their critical comments. The GRP94.NTD (69-337) plasmid was a kind gift from the laboratory of Dr. Daniel T. Gewirth.

Confocal imaging was conducted at the Duke Cell Biology confocal facilities with the aid of Tim Oliver. Flow cytometry was performed in the Duke Human Vaccine Institute Flow Cytometry Core Facility, which is supported by the National Institutes of Health award AI-51445.

Chapter 1: Introduction

A. Overview

Glucose-regulated protein 94 (GRP94, gp96, HSP90B1) is a ubiquitously expressed heat shock protein 90 (Hsp90) homolog that is localized to the cell's endoplasmic reticulum (ER), where it comprises 5-10% of the ER luminal content (Koch et al., 1986). GRP94 is believed to function as a molecular chaperone, and is necessary for the functional expression of Toll-like receptors (TLRs) and a subset of integrins (Randow and Seed, 2001). However, the GRP94 proteome – the proteins that require GRP94 for structural maturation – remains largely undefined. GRP94 expression is essential in both mice and *Drosophila*, although loss of GRP94 does not result in the death of individual cells grown in culture (Chen et al., 2006; Maynard et al.; Randow and Seed, 2001; Wanderling et al., 2007). *GRP94* expression is up-regulated in response to the unfolded protein response and a variety of other stresses, including low glucose and low extracellular pH (reviewed in Argon and Simen, 1999). However, unlike its cytosolic paralog, *GRP94* does not contain a heat shock response element in its promoter region, and its expression is not altered in response to elevated temperatures.

Interestingly, GRP94 also has the capacity to stimulate adaptive and innate immune responses when present in the extracellular space (reviewed in Nicchitta, 2003; Nicchitta et al., 2004; Srivastava, 2002). This immunostimulatory capacity was first

characterized following the identification of GRP94 as a putative tumor-rejection antigen (Srivastava et al., 1986). This discovery launched an era of investigations into the immunological functions of extracellular GRP94, as well as several other stress proteins including Hsp90, Hsp70, and Hsp60. These stress proteins have been shown to play significant roles in viral infections, tumor rejection, and generation of tolerance to autoimmune diseases such as lupus, cancer, and autoimmune diabetes.

To date, there has been a substantial body of research dedicated to understanding how GRP94 and other stress proteins elicit immune responses. However, the molecular mechanism(s) by which stress proteins regulate immune effector cells remains poorly understood. It is well established that GRP94-mediated immune responses require the interaction between GRP94 and cell surface receptors expressed by immune effector cells. In particular, GRP94 is recognized by a variety of receptors on professional antigen presenting cells (pAPCs), including CD91, SR-A, SREC-I, TLR2, and TLR4 (Berwin et al., 2004; Berwin et al., 2003; Binder et al., 2000; Vabulas et al., 2002). Additionally, I have discovered that cell surface heparan sulfate proteoglycans (HSPGs) facilitate GRP94 binding to non-immune cells.

The work presented in this dissertation will examine the ability of two different receptors to facilitate GRP94 recognition and clearance: CD91 and cell surface HSPGs.

CD91 has been called the universal Hsp receptor and has been shown to influence GRP94-mediated peptide cross-presentation, during which a GRP94-associated peptide is processed and presented on a class I MHC receptor (Basu et al., 2001; Binder et al., 2000; Binder and Srivastava, 2004). However, there is evidence that CD91 may not directly interact with GRP94 at the cell surface (Berwin et al., 2002a; Binder and Srivastava, 2004). While this has raised questions about the ability of CD91 to function as a GRP94 endocytic, it is important to consider that cross-presentation is a complex process that also involves ligand internalization and processing. Chapter 3 of this dissertation thoroughly investigates the ability of CD91 to influence GRP94 surface binding, GRP94 internalization/processing, and GRP94-mediated peptide cross-presentation. Chapter 4 is dedicated to the discovery that GRP94 can interact with cell surface HSPGs on MEF-1 cells. Interestingly, these are the first GRP94 binding sites identified using a non-immune cell line. Finally, chapter 5 will re-evaluate the role of CD91 in GRP94-mediated peptide cross-presentation and propose a mechanism whereby GRP94 interacts with cell surface HSPGs on non-immune cells to facilitate pAPC migration to a site of injury.

B. The discovery of GRP94 extracellular functions: the search for tumor-rejection antigens

During the 1950's it was established that vaccination with irradiated tumor cells could protect syngeneic mice against a subsequent challenge with the identical chemically-induced sarcoma (Figure 1). Interestingly, these anti-tumor immune responses were highly specific against the tumor of origin (Foley, 1953; Klein et al., 1960; Prehn and Main, 1957). Immunization with irradiated tumor cells did not protect syngeneic mice against transplantation of different sarcomas, even when that sarcoma was isolated from the same mouse. This lack of cross-reactivity led to the hypothesis that tumors were antigenically distinct, expressing a unique repertoire of antigens. It was subsequently hypothesized that these antigens could be recognized by the immune system, and utilized as tumor rejection antigens (TRAs) in both prophylactic and therapeutic immunotherapies.

In an attempt to identify putative TRAs, the laboratory of Pramod Srivastava fractionated the homogenates of two distinct chemically-induced sarcomas via ConA and DEAE columns, and then assayed each fraction for their ability to protect syngeneic mice against subsequent tumor challenge (Srivastava et al., 1986). Interestingly, a 96 kDa glycoprotein was identified in the active fractions of both the methylcholanthrene (MethA)- and CMS5-induced sarcomas. Consistent with the description of a bona fide TRA, immunization with the MethA-derived 96 kDa protein protected mice against the

identical sarcoma, but could not suppress growth of transplanted CMS5-induced sarcomas. Conversely, the CMS5-derived 96 kDa protein could not protect mice against MethA-induced sarcomas.

Although the existing model for TRAs predicted that the two 96 kDa glycoproteins would be antigenically distinct, rabbit serum prepared against the MethA-derived 96 kDa protein cross-reacted with the CMS5-derived 96 kDa protein on Western blots. This unexpected finding suggested that these two proteins were "structurally related but distinct" (Srivastava et al., 1986). However, it was later discovered that these two 'distinct' 96 kDa proteins had no detectable structural differences (Srivastava et al., 1987). The amino-terminal (N-terminal) amino acid sequences were identical, and cDNA probes designed against the N-terminal region hybridized to transcripts found in both MethA- and CMS5-induced tumor cells. Furthermore, the protein transcript was readily detected in all normal tissues examined, including the thymus, spleen, and cerebellum. These observations lead to a conundrum: the ubiquitous expression of the 96 kDa protein and its lack of distinguishable modifications argued against its role as a TRA. However, when the protein was isolated from chemically-induced sarcomas, it displayed a stringent tissue restriction.

A vital insight into this puzzle arose when it was discovered that the 96 kDa protein was highly homologous to the cytosolic 90 kDa heat shock protein (Hsp90), and identical to the independently-characterized GRP94 and ERP99 (Maki et al., 1990; Mazzarella and Green, 1987). Because Hsp90 was known to chaperone a diverse range of proteins and because GRP94 expression was up-regulated in response to the accumulation of misfolded proteins in the ER, it was suggested that GRP94 could function as a molecular chaperone (Kozutsumi et al., 1988; Shaknovich et al., 1992; Wiech et al., 1992). Based on these observations, it was hypothesized that GRP94 could bind peptides unique to its tissue of origin and through these peptides, convey a tissue-specific immune response (Figure 1) (Srivastava, 1993; Srivastava and Maki, 1991).

In support of this hypothesis, Li and Srivastava demonstrated that a variety of peptides could be co-purified with GRP94 (Li and Srivastava, 1993). After separating nascent peptides from purified GRP94 by acid stripping, it was observed that GRP94 interacted with a highly heterogeneous peptide pool that varied from 400-2000 Da. Additionally, because the GRP94-peptide interactions were extremely stable (resistant to elution buffers containing 0.5 M NaCl), these results suggested that the GRP94-peptide interaction could remain intact in the extracellular environment. However, these isolated peptides were not present in high enough concentrations to sequence, and the potentially tumor-specific antigens were never directly analyzed. Although numerous

studies later confirmed that GRP94 can interact with a variety of peptides, it is important to note that the ability of GRP94 to bind peptides *in vivo* is still under debate (see section D: Endogenous vs. exogenous peptide binding activities).

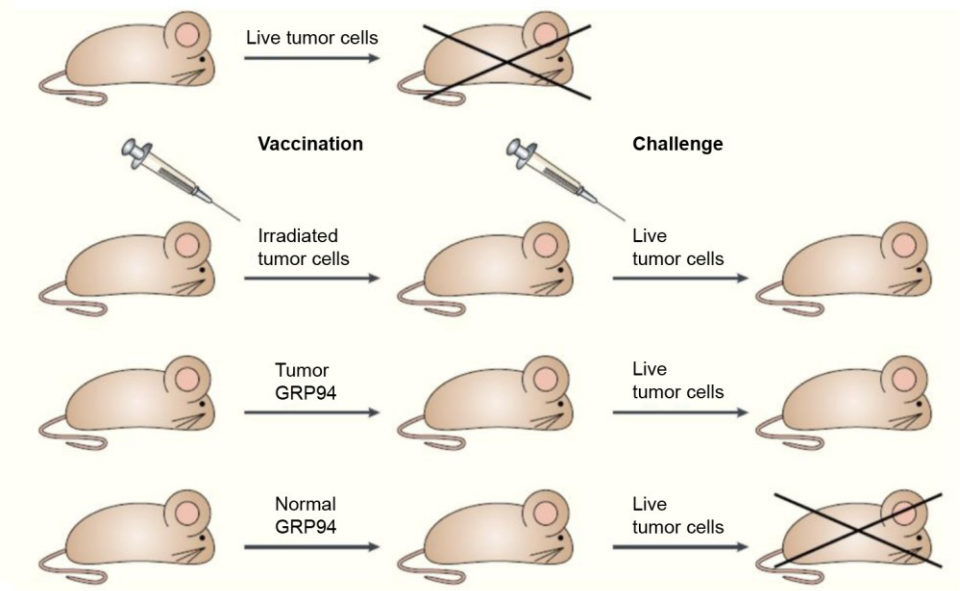

Figure 1: Experiments that established GRP94 as a tumor-rejection antigen.

Prophylactic vaccination with irradiated tumor cells has been shown to protect syngeneic mice against challenge with the identical chemically-induced sarcoma. Studies by Srivastava and colleagues later identified GRP94 as a putative tumor-rejection antigen (TRA). In these experiments, GRP94 isolated from chemically-induced tumor cells induced protective immunity against the identical tumor. GRP94 isolated from other chemically-induced sarcomas, or from non-tumor sources, could not induce immunity. These studies established GRP94 as a potential TRA. Image adapted from Nicchitta, 2003.

C. GRP94 escorts peptides into the class I MHC cross-presentation pathway

While GRP94 had been identified as a carrier of antigenic peptides, the mechanism of GRP94-mediated anti-tumor responses remained a mystery. To help elucidate this pathway, Udono et al. depleted BALB/cJ mice of three types of immune effector cells that are known to play essential roles in the immune surveillance system: antigen presenting cells (APCs), $CD8^+$ T-cells, and $CD4^+$ T-cells (Udono et al., 1994). Mice were then vaccinated with MethA-derived GRP94, challenged with the identical tumor, and monitored for tumor growth. Mice depleted of either phagocytic APCs or $CD8^+$ lymphocytes showed normal tumor growth during the priming phase, demonstrating that these cell types are essential for GRP94 anti-tumor activity. While $CD4^+$ lymphocyte depletion had no effect during the priming phase, both $CD4^+$ and $CD8^+$ lymphocytes were required during the effector phase. Cumulatively, these experiments established that the initiation of GRP94-mediated anti-tumor responses hinges on both phagocytic APCs and $CD8^+$ lymphocytes. Although it was not noted at the time of publication, this finding suggested that GRP94 could escort tumor peptides into the cross-presentation pathway.

Professional APCs (pAPCs), such as macrophages and dendritic cells (DCs), are highly phagocytic cells that constitutively sample the extracellular environment. Once extracellular antigens are internalized, they are processed and loaded onto major

histocompatibility (MHC) receptors. Although pAPCs express two classes of MHC receptors, it was originally believed that processed extracellular antigens were presented exclusively by class II MHC (MHCII) receptors. These MHCII-peptide complexes were then trafficked to the cell surface and surveyed by $CD4^+$ T-cells. However, studies in the 1970s demonstrated that pAPCs could also present exogenous peptides on class I MHC (MHCI) receptors using a specialized mechanism of antigen processing called cross-presentation (Figure 2) (Bevan, 1976a; Bevan, 1976b). The MHCI-peptide complexes are presented at the cell surface, where they are surveyed by $CD8^+$ T-cells. Recognition of a specific MHCI-peptide complex results in $CD8^+$ T cell activation and generation of cytotoxic T lymphocytes (CTLs), which are capable of lysing cells that present the specific MHCI-peptide complexes. Antigen cross-presentation is now a well-established process and is considered a major mechanism for the detection of tumors and virally infected cells.

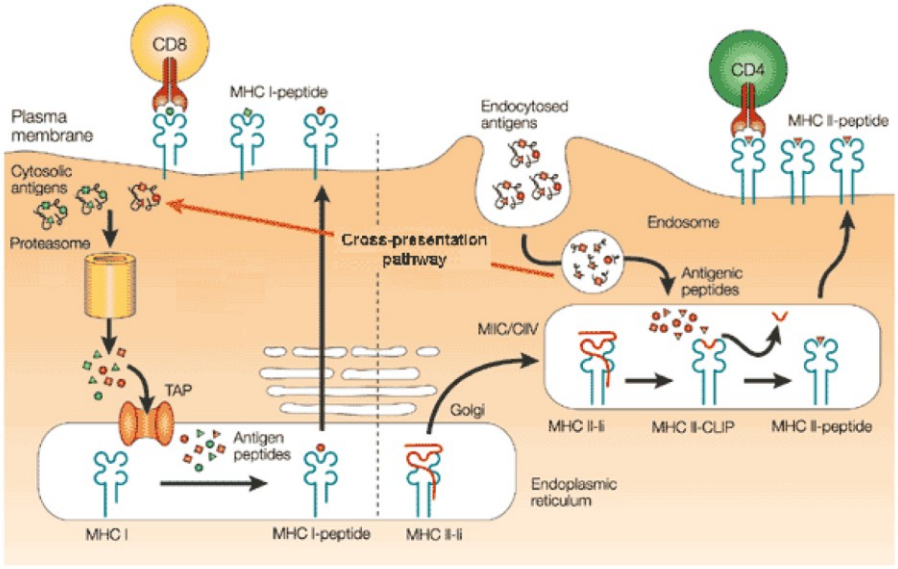

Figure 2: Schematic representation of peptide cross-presentation

Left: Endogenous peptides (indicated in green) are presented on class I MHC (MHCI) receptors. Antigens originating from endogenous sources are processed via the proteosome, transported into the ER through the transporter associated with antigen processing (TAP), and loaded onto empty MHCI receptors. MHCI-peptide complexes are then transported to the cell surface, where they are surveyed by $CD8^+$ T-cells (yellow). Right: Exogenous peptides (indicated in red) are presented on class II MHC (MHCII) receptors of professional antigen-presenting cells (pAPC). Exogenous antigens are internalized by pAPCs through either fluid-phase uptake or receptor-mediated endocytosis. These peptides are then processed and loaded onto empty MHCII receptors in a post-ER compartment. MHCII-peptide complexes are then transported to the cell surface, where they are surveyed by $CD4^+$ T-cells (green). Middle: Exogenous peptides are presented on MHCI receptors of pAPCs. During a specialized process called cross-presentation, exogenous antigens are internalized, processed, and loaded onto empty MHCI molecules. These MHCI-peptide complexes are then transported to the cell surface, where they can elicit a $CD8^+$ T-cell response against the exogenous antigen. Image adapted from Heath and Carbone, 2001.

Since this initial discovery, there have been numerous reports of GRP94 escorting peptides into the cross-presentation pathway using both *in vitro* and *in vivo* experimental systems (Nair et al., 1999; Nieland et al., 1996; Singh-Jasuja et al., 2000b; Suto and Srivastava, 1995). This phenomenon was first demonstrated *in vitro* by Suto and Srivastava. GRP94 was first isolated from N1 cells that had been transfected with a gene encoding the vesicular stomatitis virus (VSV) nucleocapsid protein (Suto and Srivastava, 1995). Macrophage pulsed with N1-derived GRP94 stimulated VSV-specific CTLs, which secreted the pro-inflammatory cytokine TNF-α and targeted the pulsed macrophages for lysis. GRP94 isolated from untransfected cells did not simulate the CTLs in either assay. Later studies recapitulated this observation using a variety of different CTLs systems, as well as demonstrated the ability of purified GRP94 to generate peptide-specific CTL responses *in vivo*. For example, Singh-Jasuja et al. utilized RMA-S SigE1B cells, which express the Ad5-E1B epitope (VNIRNCCYI) in the context of H-2D^b (Singh-Jasuja et al., 2000b). Mice injected with RMA-S SigE1B-derived GRP94 generated CTLs that specifically recognized both RMA-S SigE1B cells and RMA-S that had been pulsed with Ad5-E1B peptide. The CTLs were not simulated by RMA-S cells themselves. Furthermore, tissue culture DCs pulsed with RMA-S SigE1B-derived GRP94 stimulated two CTL clones that specifically recognized the Ad5-E1B epitope.

Also consistent with a role in mediating peptide-cross presentation, GRP94 is endocytosed and trafficked through a non-traditional intracellular pathway. Following receptor-mediated endocytosis (RME), GRP94 is rapidly trafficked into a Rab5a-, transferrin-, CD1-negative, MHCI-positive compartment, and was shown to co-localize with recycling MHCI molecules (Berwin et al., 2002b; Singh-Jasuja et al., 2000b). Internalized GRP94 also avoids trafficking to the lysosomes and retrograde targeting to the ER (Berwin et al., 2002b; Wassenberg et al., 1999). Interestingly, this endocytic pathway shares several characteristics with that of FcγRI, which has an established role in directing antigen cargo into MHCI cross-presentation compartments (Berwin et al., 2003; Berwin et al., 2002b; Gromme et al., 1999; Guyre et al., 2001; Kleijmeer et al., 2001). It is also important to note that GRP94-peptide complexes internalized via RME and fluid-phase endocytosis differ in their subcellular trafficking itineraries. GRP94 internalized via RME was retained by macrophage cells for upwards of 30 min, whereas GRP94 internalized through fluid-phase endocytosis quickly recycled back to the extracellular space ($t_{1/2}$ <15 min) (Berwin and Nicchitta, 2001).

Together, these studies paint a picture of how GRP94 could stimulate the adaptive arm of the immune system (Figure 3). Under physiological conditions, GRP94 associates with tissue-specific peptides. However, during pathological cell death, GRP94-peptide complexes would be released into the extracellular environment (Basu et

al., 2000; Berwin et al., 2001). The GRP94-peptide complexes would then be recognized by circulating pAPCs and internalized either by RME or fluid-phase endocytosis. The associated peptide would then be processed and be loaded onto MHCI receptors for subsequent detection by $CD8^+$ T-cells. This would finally culminate in the generation of peptide-specific CTL response that would mediate $CD8^+$ T-cell immunity against GRP94-bound peptides.

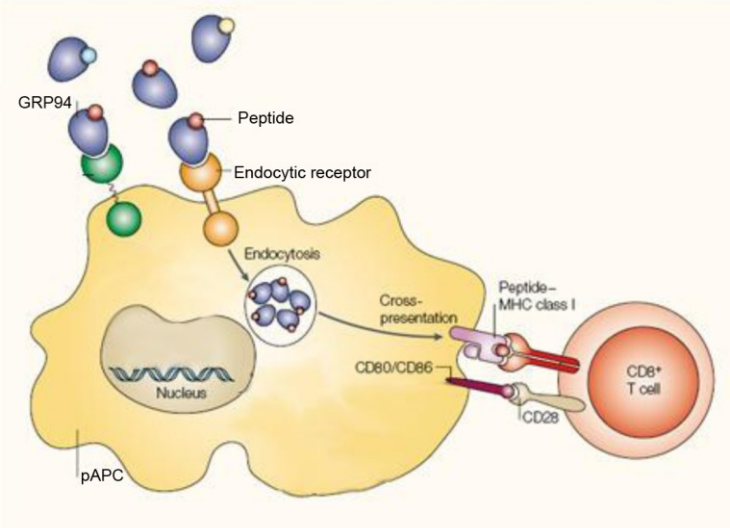

Figure 3: Model of GRP94-mediated peptide cross-presentation.

Extracellular GRP94/peptide complexes are internalized by pAPCs and processed through the cross-presentation pathway. The associated peptides are then loaded onto empty MHCI receptors, and presented at the cell surface. Detection of these MHCI-peptide complexes by $CD8^+$ T-cells generates CTL activity, and an adaptive immune response against that specific MHCI-peptide complex. Image adapted from Nicchitta, 2003.

D. Endogenous vs. exogenous peptide binding activities

The tissue-restricted immunogenicity of GRP94 suggested that it has the capacity to bind peptides *in vivo*. Additionally, numerous studies have demonstrated that GRP94-associated peptides can stimulate peptide-specific CTL responses both *in vitro* and *in vivo*. While these studies suggest that GRP94 has endogenous peptide binding activities, the ability of GRP94 to directly bind peptides *in vivo* has been the subject of debate.

There have been several attempts to isolate peptides from endogenous GRP94. However, the expected diverse selection of GRP94 peptides has never been observed (reviewed in Nicchitta et al., 2004). Similar to what was seen by Srivastava and colleagues, Demine and Walden reported that MyLa-derived GRP94 bound a complex array of peptides that varied from 800-2600 Da (7-24 residues) (Demine and Walden, 2005). However, peptide sequencing revealed that the peptide pool contained a mixture of hydrophobic and hydrophilic peptides, and encoded proteins from a variety of subcellular localizations, including the nucleus, the cytosol, and the lysosome. Mass spectral analysis of these peptides revealed no recurring peptide binding motif, aside from the observation that all of the isolated peptide fragments contained at least one aromatic amino acid. Furthermore, it was calculated that only 0.1-0.4% of the isolated GRP94 molecules were associated with peptides, strongly suggesting that GRP94 does not function as a peptide chaperone involved in antigen processing. Interestingly, this

low binding stoichiometry has been observed in several independent studies (Blachere et al., 1997; Ying and Flatmark, 2006).

In other studies, Ying and Flatmark concluded that VSV8 bound multiple sites on both native and recombinant GRP94 by an adsorptive, rather than bioselective, mechanism (Ying and Flatmark, 2006). Although GRP94 isolated from VSV-expressing cells could elicit anti-VSV CTL responses, VSV8 bound to GRP94 with a low affinity at 25°C and 37°C, and was partially inhibited by physiological ER concentrations of ATP and Ca^{2+}. The kinetics of association between GRP94 and radiolabeled peptides was also very slow, requiring more than five hours to reach detectible levels (Vogen et al., 2002).

In an attempt to validate the putative *in vivo* peptide-binding activity of GRP94, Suto and Srivastava generated GRP94-peptide complexes by heating GRP94 with synthetic VSV peptide A (KRQIYTDLEMNRLGK) at 50°C for 10 min (Suto and Srivastava, 1995). Following this heat shock, the GRP94/peptide A complex was purified and examined for antigenic activity. Surprisingly, the synthetic GRP94/peptide A complexes efficiently elicited peptide-specific CTL responses *in vivo*, and could effectively immunize mice against subsequent tumor challenge (Blachere et al., 1997; Suto and Srivastava, 1995). Even more surprisingly, this unorthodox method could reproducibly create immunologically-active GRP94/peptide complexes with a wide

variety of different peptides (Blachere et al., 1997; Suto and Srivastava, 1995). Further characterization of these complexes revealed that the association of GRP94 with radio-iodinated peptide A could be competed using several different unlabeled VSV peptides, but not albumin or ovalbumin, suggesting a specific interaction between GRP94 and peptide A (Blachere et al., 1997; Wearsch and Nicchitta, 1997).

Interestingly, the GRP94/peptide association was temperature sensitive and optimal GRP94/peptide A association could be visualized by SDS-PAGE after incubation at 60°C for 10 min. Association could also occur at lower temperatures when 2 M NaCl was included in the reaction (Blachere et al., 1997). It was initially suggested that heat/chemical treatment was necessary to either overcome the kinetic barrier of peptide binding, or to help dissociate endogenous peptides from purified GRP94 molecules (Blachere et al., 1997; Wearsch and Nicchitta, 1997). However, detailed studies from the Nicchitta lab demonstrated that GRP94 undergoes an irreversible conformational change when incubated at 37°C for extended periods of time, or at elevated temperatures (>50°C) for short periods of time (Wearsch and Nicchitta, 1997; Wearsch et al., 1998). Using environment-sensitive dyes such as acrylodan and Nile Red, Wearsch et al. demonstrated that 'activation of peptide binding' by heating created GRP94 tetramers and higher order oligomers. Significantly, no changes in GRP94 secondary structure were observed, and the formation of higher order oligomers was not necessary for the

formation of GRP94/peptide complexes (Wearsch et al., 1998). The GRP94/peptide complexes also formed independently of ATP or ADP, suggesting that the association between GRP94 and peptides was energy-independent (Blachere et al., 1997; Vogen et al., 2002; Wearsch and Nicchitta, 1997).

The proof-of-principle binding studies established that GRP94 can associate with a variety of peptides when exposed to elevated temperatures, and suggested that these interactions were specific. However, several characteristics of GRP94-peptide complexes argue against a model where GRP94 binds peptides *in vivo*. First, if GRP94 functions as a molecular chaperone, it would be expected to interact with peptides in a reversible manner. However, peptides purified from endogenous GRP94 are tightly associated with GRP94 and are resistant to buffers containing up to 0.5 M NaCl (Li and Srivastava, 1993). Additionally, synthetic GRP94/peptide complexes generated by heat shock are incredibly stable and remain intact under conditions that normally disrupt protein-protein interactions, including 1 M urea, buffers adjusted to pH 2.0 or 9.0, 2 M NaCl, and SDS-PAGE (Blachere et al., 1997; Suto and Srivastava, 1995; Vogen et al., 2002; Wearsch and Nicchitta, 1997).

Secondly, if GRP94 functioned as a carrier for tumor-specific peptides, it would also be expected to interact with a diverse selection of peptides. However, studies by

Demine and Walden, Ying and Flatmark, and Blachere et al. suggest that GRP94-peptide binding is a rare event both *in vivo* and *in vitro*. It is well established that Hsp90 cellular functions are facilitated by various co-chaperones. Because GRP94 and Hsp90 share a high degree of homology, it is possible that GRP94-peptide interactions depend on the presence of various co-chaperones. However, no such interactions have been identified to date. It remains to be determined whether the GRP94 peptide binding activity observed *in vitro* reflects its putative *in vivo* peptide binding function.

E. Peptide-independent immune stimulation: GRP94 stimulates the innate immune system

In addition to mediating peptide cross-presentation, GRP94 has peptide-independent immunostimulatory activities. It is now well established that GRP94 can directly elicit pAPC maturation/activation irrespective of its tissue source. In response to extracellular GRP94, both mouse and human dendritic cells up-regulate co-stimulatory molecules (CD86, CD83, and MHCII molecules), secrete pro-inflammatory cytokines (IL-6, IL-12, TNF-α, and IFN-γ), and elicit strong proliferation of alloreactive T cells (Baker-LePain et al., 2004; Basu et al., 2000; Reed et al., 2003; Singh-Jasuja et al., 2000a; Singh-Jasuja et al., 2000b; Warger et al., 2006). Furthermore, transgenic mice expressing a cell surface form of GRP94 display systemic, MyD88-dependent dendritic cell activation and developed a lupus-like autoimmune disease (Liu et al., 2003).

In a set of pivotal experiments, Baker-LePain et al. demonstrated that GRP94 can induce tumor rejection independently of it tissue source *in vivo*, and suggested that this response could be elicited in the absence of bound peptides (Baker-LePain et al., 2002; Baker-LePain et al., 2004). For these experiments, Baker-LePain et al. constructed two non-tumor cell lines capable of secreting either full length GRP94 (GRP94ΔKDEL) or an N-terminal region of GRP94 (GRP94.NTDΔKDEL) that lacks a canonical peptide binding motif. GRP94.NTD was found to have nearly identical biological activity to full length GRP94 in several *in vitro* assays, including APC maturation, APC surface binding and internalization, and maturation (Baker-LePain et al., 2002). When irradiated and injected into BALB/c mice, both GRP94-secreting cell lines enhanced tumor suppression and decreased metastatic progression of a 4T1 mammary carcinoma (Baker-LePain et al., 2002).

Using this same system, it was further demonstrated that injection of GRP94ΔKDEL- or GRP94.NTDΔKDEL-secreting fibroblasts elicited Th1 cytokine secretion from a relatively large population (>20%) of $CD4^+$ splenocytes (Baker-LePain et al., 2004). No such stimulation was observed for $CD8^+$ T-cells and no significant activation of natural killer cells was observed. However, treating with carrageenan attenuated the magnitude of the $CD4^+$ response, suggesting that this $CD4^+$ bystander response necessitated the upstream activation of pAPCs.

Cumulatively, these studies demonstrate that GRP94 can stimulate innate immune responses independently of its ability to mediate peptide cross-presentation. They also suggest that GRP94 can function as an endogenous adjuvant or "danger signal." In this capacity, GRP94 can enhance the immunogenicity of various antigens, including small peptides and lipopolysaccharide, and may alert the immune system of pathological cell death (reviewed in Matzinger, 1994; Nicchitta, 2003). Consistent with this hypothesis, *in vitro* studies have demonstrated that GRP94 is found in the extracellular space following necrotic cell death (virally-induced cell death, mechanical cell death), but not apoptotic cell death (Basu et al., 2000; Berwin et al., 2001).

F. CD91: the first identified GRP94 receptor

It has been firmly established that the ability of GRP94 to stimulate innate and adaptive immune responses hinges on its interaction with phagocytic immune effector cells such as macrophages and DCs (Baker-LePain et al., 2004; Udono et al., 1994). Additionally, these interactions were shown to be saturable and specific, suggesting that GRP94 binds high-affinity cell surface receptors on pAPC lines (Arnold-Schild et al., 1999; Singh-Jasuja et al., 2000b). Together, these works suggested that GRP94 was recognized by pAPC surface receptors, and that these interactions could be necessary GRP94-mediated immune responses.

The existence of GRP94 endocytic receptors was first established by Arnold-Schild et al., who observed that gold-labeled GRP94 molecules localized to clathrin-coated pits, and that excess unlabled GRP94 could reduce the amount of gold-labeled GR94 found in these pits (Arnold-Schild et al., 1999). Later studies confirmed that GRP94 could be internalized through RME using monodansyl cadaverine (MDC), a pharmacological agent that interferes with clathrin-mediated receptor trafficking. In these studies, MDC treatment of human monocyte-derived immature DCs prevented the internalization of fluorescently-labeled GRP94, as well as abrogated the ability of GRP94 to induce DC maturation and cytokine secretion (Vabulas et al., 2002). This suggested that the ability of GRP94 to mediate peptide-independent responses required RME.

It has also been established that that GRP94-mediated peptide cross-presentation is mediated through GRP94 endocytic receptors. Numerous *in vitro* and *in vivo* studies have demonstrated that GRP94-mediated peptide cross-presentation could be competed with excess "peptide-deficient" GRP94 (i.e., GRP94 that had not complexed with the peptide of interest, or GRP94 that had been isolated from a tissue source that did not express the peptide of interest). Additionally, pharmacological inhibition of RME significantly reduced the ability of elicited peritoneal macrophages to cross-present synthetic GRP94/SIINFEKL complexes (Berwin et al., 2002b). Further support for the

RME of GRP94-peptide complexes was obtained with the identification of individual GRP94 endocytic receptors.

CD91 (low density lipoprotein receptor-related protein 1, LRP1) was the first receptor proposed to function in GRP94 binding and endocytosis. It is one of the largest members of the low density lipoprotein (LDL) receptor family, and consists of two non-covalently associated subunits of 515 and 85 kDa (Figure 4). The complex ectodomain of CD91 contains β-propeller domains, EGF repeats that are necessary for ligand dissociation in the endosomes, and four clusters of cysteine-rich complement-type repeats (CRs) that are attributed with the ligand-binding activity of CD91 (reviewed in Herz and Strickland, 2001; Krieger and Herz, 1994; Lillis et al., 2008). Through these domains, CD91 can recognize and internalize over 30 structurally distinct, functionally divergent ligands, including activated α_2-macroglobulin (α_2M*), thrombospondin-1, apoE, PDGF, and lactoferrin. Meanwhile, the relatively short intracellular domain contains two dileucine motifs, two NPxY internalization motifs, and can interact with a variety of adaptor molecules to influence cellular signaling pathways. CD91 is widely expressed and can participate in a variety of physiological responses, including lipoprotein metabolism, proteinase homeostasis, cell migration, and modulation of the blood-brain barrier (reviewed in Herz and Strickland, 2001; Krieger and Herz, 1994; Lillis et al., 2008).

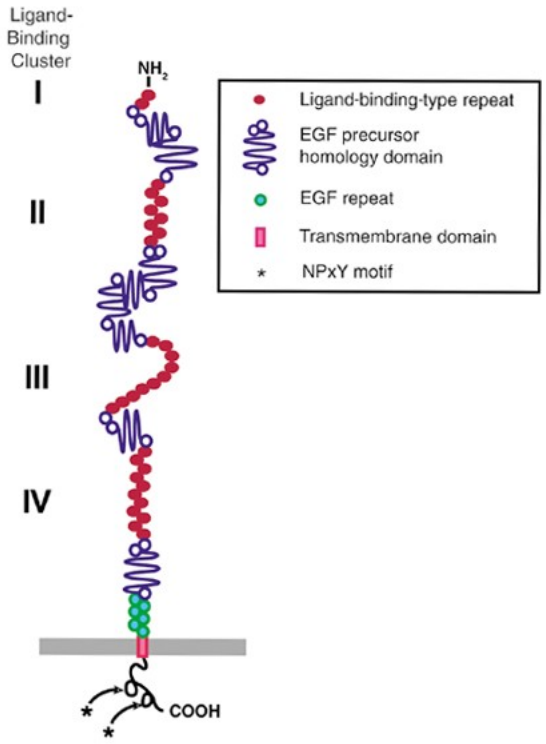

Figure 4: Structure of CD91.

CD91 is a 600 kDa member of the LDL receptor family. The ectodomain (515 kDa) consists of four distinct cysteine-rich (CR) complement-type ligand binding clusters. Each of these domains is separated by one or more EGF repeats. The intracellular domain (85 kDa) contains two NPxY domains and is known to interact with a variety of adaptor molecules. Image adapted from Herz and Strickland, 2001.

The original studies that identified CD91 as a GRP94 endocytic receptor utilized two different techniques to search for GRP94 surface receptors (Binder et al., 2000). In the first approach, Binder et al. used an agarose-GRP94 column to affinity purify proteins derived from detergent-solubilized membranes of surface-biotinylated RAW264.7 cells. In the second approach, ^{125}I-SASD-GRP94 was cross-linked to peritoneal

macrophages, and subsequently treated with 2-βME to transfer ^{125}I to putative surface receptors. An 80 kDa molecule (p80) was identified in both the affinity column eluant and in the iodinated membrane preparation. Importantly, this p80 was not isolated from P815 cells, which are incapable of cross-presentation. Sequencing of this p80 fragment revealed that it corresponded to the N-terminal extracellular region of CD91 (residues 338-518). This region does not correspond to any of the CR domains that are attributed with CD91 ligand binding and is not known to bind any established CD91 ligands (Binder and Srivastava, 2004). Nonetheless, an antibody raised against p80 could inhibit GRP94-mediated cross-presentation of the AH1-19 peptide. Additionally, it was shown that GRP94-mediated cross-presentation could be almost completely suppressed using either a monoclonal CD91 blocking antibody (5A6) or excess α_2-macroglobulin (α_2M). α_2M is a broad-spectrum protease inhibitor that binds CD91 when activated (α_2M*). Although this initial discovery paper does not report the use of α_2M*, later studies mention that the α_2M samples contain some α_2M*. The relative quantities of the native and activated forms are never specified.

Since this discovery, several studies have confirmed that various CD91 ligands can inhibit GRP94-mediated peptide cross-presentation both *in vitro* and *in vivo*. Commercially available anti-CD91 antibodies, α_2M*, and the pan-CD91 ligand inhibitor receptor-associated protein (RAP) were shown to inhibit GRP94/AH-19 cross-

presentation by RAW264.7 cells (Basu et al., 2001; Binder et al., 2000; Binder and Srivastava, 2004). Ablation of CD91 expression via CD91-directed siRNA also severely blunted the ability of these cells to cross-present GRP94-associated peptides (Binder and Srivastava, 2004). Furthermore, co-injection of GRP94/AH1-19 complexes and either α_2M* or anti-CD91 antibodies significantly reduced the ability of two different BALB/c mice to generate AH1-19 specific lymphocytes (Binder and Srivastava, 2004). Subsequent works extended these observations to demonstrate that CD91 ligands could influence the cross-presentation of peptides associated with other immunologically-relevant stress proteins (Basu et al., 2001). Both α_2M and an anti-CD91 antibody inhibited the cross-presentation of AH1-19 associated with GRP94, Hsp90, Hsp70, and calreticulin in a titratable manner. Additionally, un-complexed GRP94, Hsp60, Hsp70, and calreticulin inhibited the cross-presentation of GRP94/AH1-19 peptide complexes by RAW264.7 mouse macrophage-like cells (Basu et al., 2001). For these reasons, it was suggested that CD91 functioned as the common Hsp receptor.

These studies establish a role for CD91 in GRP94-mediated peptide cross-presentation and are consistent with a function in GRP94 endocytosis. However, none of the initial studies directly tested the ability of CD91 to bind GRP94 at the cell surface. To date, two reports have specifically examined this interaction. Both demonstrate that GRP94 surface binding to unfixed macrophage cells is not inhibited by excess CD91

ligands, suggesting that CD91 does not directly bind GRP94 (Berwin et al., 2002a; Binder and Srivastava, 2004). However, there is some debate as to the appropriate conditions utilized for the assay, and reports arrive at conflicting conclusions. Therefore, the ability of CD91 to directly bind GRP94 remains unresolved. Chapter 3 contains a detailed examination of the mechanism of CD91-mediated GRP94/peptide cross-presentation.

G. Cell surface heparan sulfate proteoglycans (HSPGs) and other GRP94 surface receptors

Although CD91 was reported to be the common Hsp receptor, it was soon discovered that GRP94 and other stress proteins could bind immune cells independently of CD91 (Berwin et al., 2004; Berwin et al., 2003; Calderwood et al., 2007; Delneste et al., 2002; Theriault et al., 2006). This was visualized by Berwin et al., who utilized confocal microscopy to follow the trafficking itineraries of GRP94 and various CD91 ligands by elicited peritoneal macrophages (Berwin et al., 2002a). At discrete time points, no co-localization was observed between GRP94 and an anti-CD91 antibody, or between GRP94 and the CD91 ligand *Pseudomonas* exotoxin A. This suggested that GRP94 could be internalized by surface receptors other than CD91. Furthermore, GRP94-mediated peptide cross-presentation could be inhibited by the scavenger receptor ligand fucoidan, whereas fucoidan did not affect α_2M* surface binding or endocytosis (Berwin et al., 2003). Cumulatively, these studies demonstrated that GRP94 could bind cells independently of CD91. Subsequent work identified several GRP94 surface receptors,

including SR-A, SREC-I, TLR2, TLR4, and cell surface heparan sulfate proteoglycans (HSPGs) (Berwin et al., 2004; Berwin et al., 2003; Vabulas et al., 2002).

HSPGs are ubiquitously expressed, structurally diverse group of proteoglycans that contain highly heterogeneous, sulfated polysaccharide side chains (Figure 5). Their cell surface expression patterns vary by cell/tissue type, by developmental stage, and can be altered in response to extracellular stimuli such as tissue injury. Additionally, the HSPG structure itself can be modified during its biosynthesis and through interactions with extracellular proteases. These characteristics make cell surface HSPGs uniquely poised to play a broad variety of physiological roles in ligand binding, processing, and signal transduction (Conrad, 1998).

Because pAPCs are necessary for GRP94-mediated immune stimulation, the search for GRP94 surface receptors has been primarily focused on those receptors expressed by pAPC. However, GRP94 is known to interact with receptors on a variety of non-pAPC cell types, including B cells, neutrophils, and platelets (Hilf et al., 2002; Radsak et al., 2003; Singh-Jasuja et al., 2000b). Additionally, it is important to note that CD91, TLR2, TLR4, and SCREC-I are expressed by a variety of non-immune cell types, suggesting that numerous tissues express high-affinity GRP94 receptors. Recently, I have observed that GRP94 binds mouse embryonic fibroblast (MEF) in a low-

affinity/high-capacity manner. Investigations into the identity of these receptors lead to the discovery that GRP94 can interact with cell surface HSPGs on a variety of non-immune cells. These data will be discussed further in chapter 4. Additionally, because the study of GRP94-HSPG interactions is still in its infancy, chapter 5 will speculate on the potential biological relevance of this low-affinity/high-capacity interaction.

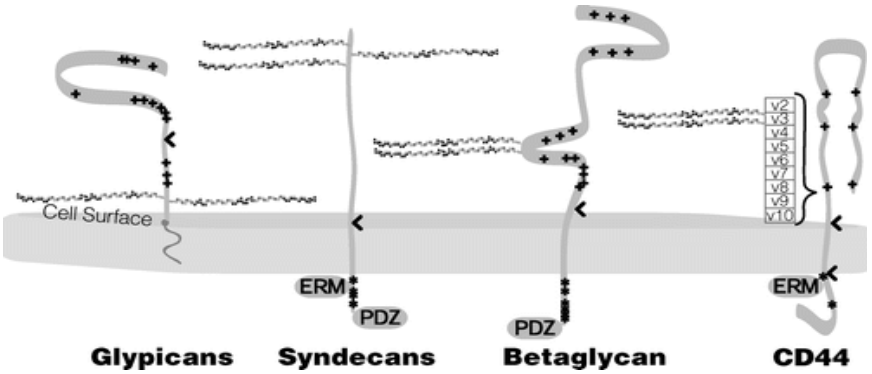

Figure 5: Structure of cell surface heparan sulfate proteoglycans (HSPGs).

Cell surface HSPGs are a structurally diverse family of proteoglycans. They consist of a protein core to which highly heterogeneous, sulfated polysaccharide side chains are attached. Of the four classes of cell surface HSPGs, only syndecans and glypicans are considered "full time" HSPGs; betaglycan and CD44 are occasionally decorated with heparan sulfate-containing side chains. Only glypicans are attached to the cell surface with a GPI-anchor. Image adapted from Kramer and Yost, 2003.

H. Overview of results

The following sections will examine the interaction of GRP94 with two different cell surface receptors: CD91 and HSPGs. First, chapter 2 will encompass the expression, purification, depyrogenation, and characterization of the N-terminal GRP94 (GRP94.NTD) constructs utilized in these studies. In chapter 3, I will thoroughly examine the putative role of CD91 as a GRP94 endocytic receptor. To this end, I will specifically examine three distinct processes that are necessary for GRP94-mediated peptide cross-presentation: surface binding, internalization, and processing. By individually examining each of these processes, I will demonstrate that CD91 does not directly function in 1) GRP94.NTD binding, 2) GRP94.NTD endocytosis, or 3) GRP94.NTD processing. I will also provide evidence that CD91 may facilitate GRP94.NTD internalization/processing by the pAPC cell line DC2.4, but does not significantly contribute to GRP94-mediated peptide cross-presentation by these cells. In chapter 4, I will present data that identify cell surface HSPGs as a novel class of GRP94 binding sites, and characterize this interaction using well established biochemical techniques. Lastly, I will suggest a model of GRP94-mediated immune activation that involves the interaction of GRP94 with non-immune cells. Taken together, this work clarifies the existing controversy over the role of CD91 in GRP94 binding and endocytosis, as well as identifies a novel interaction between GRP94 and cell surface HSPGs.

Chapter 2: Materials and methods

Reagents: Molecular biology reagents were acquired from Sigma, Invitrogen, Pierce and Bio-Rad. Tissue culture reagents were acquired from Cellgro, Gibco, and Invitrogen. All PCR primers were synthesized through Integrated DNA Technologies. Endotoxin content was determined using the QCL-1000 chromogenic limulus amoebocyte lysate (LAL) assay from Lonza, unless otherwise noted. SIINFEKL was purchased from GenScript and ova20 (SGLEQLESIINFEKLTEWTS) was synthesized by NeoBioScience. The sources of any other reagents are noted.

Cell culture: MEF-1, PEA-13, and RAW264.7 cells were maintained in Dulbecco's Modified Eagle Medium (DMEM) with glucose, L-glutamine, and sodium pyruvate supplemented with 10% fetal bovine serum (FBS), and grown according to ATCC specifications. DC2.4 cells were maintained in RPMI 1640 with L-glutamine supplemented with 10% FBS, and grown according to ATCC specifications.

siRNA transfection: MEF-1 and PEA-13 cells were transfected with 200 nM CD91-directed siRNA (Qiagen) using Lipofectamine2000 and OPTI-MEM serum-free media, according to the manufacturer's protocol. Cells were maintained in DMEM/10% FBS after transfection. Cells were examined for optimal knock-down of CD91 at 24, 48, and 72 hours post-transfection using reverse-transcriptase PCR. LRP1_1 (target sequence

CAC GTT GGT TAT GCA CAT GAA) and LRP1_2 (target sequence CTG CCG GGT GTA CAA ATG TAA) were directed against mouse LRP1 (NM_008512).

Mice: OVA-specific TCR transgenic mice [C57BL/6-Tg(TcraTcrb)1100Mjb/J, commonly called OT-1 mice] were purchased from Jackson Laboratories (Bar Harbor, ME, USA). All mice were housed in the Duke University Animal Facility (Durham, NC, USA), an Association for Assessment and Accreditation of Laboratory Animal Care International-approved facility. All experiments were conducted under an Institutional Animal Care and Use Committee-approved protocol.

Protein purification:

It has been previously demonstrated that *in vivo* expression of a secretable form of the GRP94 N-terminal domain (NTD) (residues 22-337) is sufficient to elicit anti-tumor immunity, and that GRP94.NTD can mediate APC activation (Baker-LePain et al., 2002; Huang Q, 2009; Warger et al., 2006). Additionally, Biswas et al. reported that GRP94.NTD-synthetic peptide complexes could elicit both cross-presentation of bound peptides on MHC class I molecules in vitro, and peptide-specific cytotoxic T cell responses in vivo (Biswas et al., 2006). For these reasons, I have chosen to conduct the following studies using recombinant GRP94.NTD. All the surface binding and kinetics of internalization studies were conducted with both GRP94.LREK and GRP94.NTD.

Because GRP94.LREK and GRP94.NTD behaved comparably in these assays, the term GRP94.NTD will be used interchangeably to describe both GRP94 constructs.

The N-terminal domain (NTD) of canine GRP94 (residues 69-337) (GRP94.LREK) was expressed in E. coli strain BL21 as an N-terminal glutathione S-transferase fusion (pGEX-NB modified pGEX-2T vector). All protein expressions were conducted using freshly-transformed BL21 cells. GRP94.LREK was purified as previously described (Soldano et al., 2003), with minor modifications. Following elution from Sepharose 4B glutathione agarose resin (GE Healthcare), the GST-tag was cleaved using thrombin (Haematologic Technologies). Thrombin cleavage was arrested by addition of 1 mM phenylmethylsulfonyl fluoride (PMSF) and the protein pool was re-chromatographed on a Sepharose 4B glutathione-agarose column. Peak fractions were pooled, loaded on a HiTrap QHP column (GE Healthcare), and washed with 150 column volumes of cold, sterile depyrogenation buffer (1% Triton X-114, 20 mM Tris, pH 8.0). All materials used during and after depyrogenation were decontaminated by either baking for 4 hours at 300°C or by extensive washing with 0.2 M NaOH. Detergent was removed by washing the column with sterile 150 mM NaCl, 20 mM HEPES, pH 7.9 until the A_{230} returned to baseline. This step was essential to ensure that Triton X-114 was completely removed. Recombinant protein was then eluted with sterile 750 mM NaCl, 20 mM HEPES, pH 8.0 (Figure 6). Peak fractions were pooled and subjected to sequential concentration in a

YM-10 spin column (Millipore). Salt concentrations were reduced to <300 mM NaCl. GRP94.LREK aggregation was assessed by native polyacrylamide gel electrophoresis (PAGE) (3% native stacking gel; 6% native resolving gel; 15mM Tris, 50 mM Tricine, pH 7.0) (Figure 6). GRP94.LREK endotoxin content was determined to be 14.7 EU/mg using a commercial LAL kit, performed according to the manufacturer's protocol.

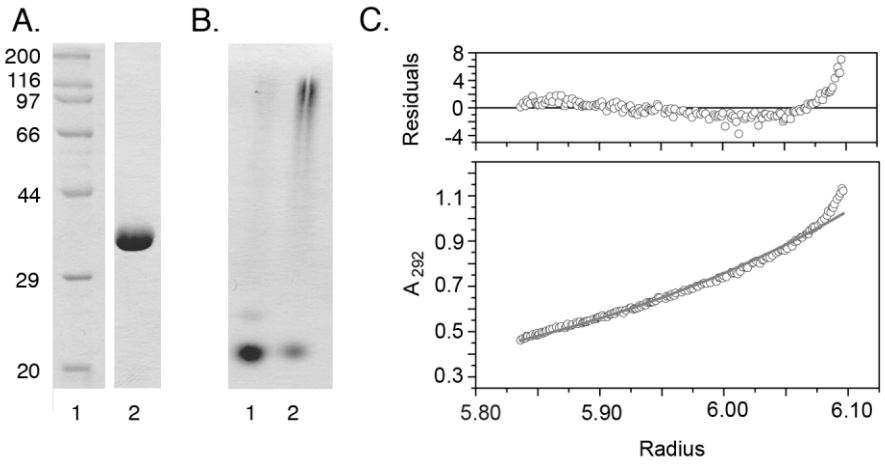

Figure 6: Purification and biophysical characterization of GRP94.LREK.

Recombinant GRP94.LREK was expressed, purified, and depyrogenated. A. 5 μg GRP94.LREK (lane 2) was resolved by 12.5% SDS-PAGE and detected by Coomassie Blue staining. M.W. marker is shown in lane 1.
B. To examine the oligomeric state of purified GRP94.LREK, 7.5 μg GRP94.LREK was resolved by 6% native PAGE and detected by Coomassie Blue staining (lane 1). Incubation at 42°C for 30 min promotes formation of higher-order oligomers (lane 2). C. Analytical ultracentrifugation was performed on 2.3 mg/mL GRP94.LREK at 4°C. The protein displayed a high degree of homogeneity, and mass average calculations yielded a molecular mass estimation of 41 kDa.

The protocol for GRP94.LREK purification has since been modified to include an on-column thrombin cleavage step. This increased the overall yield of the purification two- to three-fold. After loading GRP94.LREK on the Sepharose 4B glutathione resin, the column was rinsed with PBS and depyrogenated overnight. Following depyrogenation, detergent was removed as previously described. The beads were then placed in PBS containing approximately 20 NIH units endotoxin-free thrombin per 1 mL bed volume, and incubated at 4°C for 1 hour with rotation. Thrombin was subsequently inactivated with 1 mM PMSF.

Recombinant rat RAP was expressed in E. coli strain BL21 as a His-tagged fusion (pLE1 modified pET24a vector) (Laskowitz et al., 2001). Cells were induced with 0.1mM isopropyl-β-D-galactopyranoside for three hours and the bacteria were recovered by centrifugation. Bacterial pellets were resuspended in cold buffer A (50 mM dextrose, 50 mM Tris, pH 8.0, 10 mM imidazole, 300 mM NaCl), and homogenates prepared by French press. Homogenates were incubated with an equal volume of buffer B (10 mM Tris, pH 8.0, 50 mM KCl, 0.5% (v/v) Tween 20, 0.5% (v/v) Triton X-100, 300 mM NaCl, and 10 mM imidazole) for 30 min on ice. Insoluble debris was subsequently removed by centrifugation at 40,000 x g for 30 min at 4°C. The supernatant fraction was applied to nickel-Sepharose resin (GE Healthcare), washed with 30 column volumes of wash buffer (PBS with 0.2% (v/v) Tween 20, 0.2% (v/v) Triton X-100, and 40 mM imidazole, pH 8.0),

and washed overnight in sterile depyrogenation buffer (1% Triton X-114 in PBS, pH 7.5). Recombinant protein was eluted using sterile 150 mM imidazole in PBS, pH 7.9, and dialyzed against sterile PBS. To remove excess detergent, protein was incubated with sterilized, depyrogenated Bio-Beads (Bio-Rad) for 1 hour at 4°C, and then dialyzed against PBS. RAP endotoxin content was determined to be <1 EU/mg using a commercial LAL kit, performed according to the manufacturer's protocol.

Recombinant canine GRP94.NTD (residues 22-337) was also utilized in these studies. Canine GRP94.NTD was expressed in E. coli strain BL21 as a His-tagged fusion (pET15b vector; Novagen), and was purified as described above for RAP. Following depyrogenation, detergent was removed by washing the column with sterile PBS, as described for GRP94.LREK. Recombinant protein was then eluted with sterile 150 mM imidazole in PBS, pH 7.4. Higher imidazole concentrations were found to elute higher-order oligomer forms of GRP94.NTD (Figure 7). Peak fractions were pooled and dialyzed against sterile PBS. GRP94.NTD aggregation was assessed by native PAGE as previously described (Figure 7). GRP94.NTD samples were subsequently analyzed using analytical ultracentrifugation. GRP94.NTD endotoxin content was determined to be 19.5 EU/mg using a commercial LAL kit, performed according to the manufacturer's protocol.

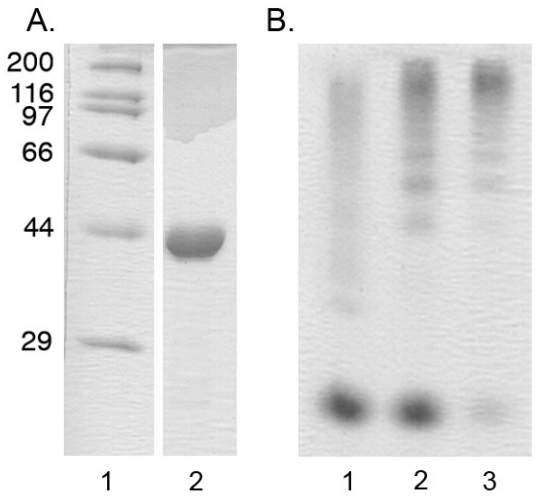

Figure 7: Purification and analysis of GRP94.NTD.

Recombinant GRP94.NTD was expressed, purified, and depyrogenated. A. 5 μg GRP94.NTD (lane 2) was resolved by 12.5% SDS-PAGE and detected by Coomassie Blue staining. M.W. marker is shown in lane 1. B. To examine the oligomeric state of purified GRP94.NTD, 7.5 μg GRP94.NTD was resolved by 6% native PAGE and detected by Coomassie Blue staining (lane 1). Incubation at 42°C for 20 and 60 min promotes formation of higher-order oligomers (lanes 2 and 3, respectively).

Endogenous GRP94 was purified as previously described (Wearsch and Nicchitta, 1996). Total luminal extract was applied to a HiTrap Q HP column (GE Healthcare), rinsed with sterile PBS, and eluted with increasing concentrations of sterile NaCl in PBS. GRP94 eluted from the column with 400 mM NaCl in sterile PBS. GRP94 was purified to >95%, as determined by SDS-PAGE (Figure 8). GRP94 endotoxin content was determined to be <0.1 EU/mg using the QCL-1000 chromogenic LAL assay, performed according to the manufacturer's protocol.

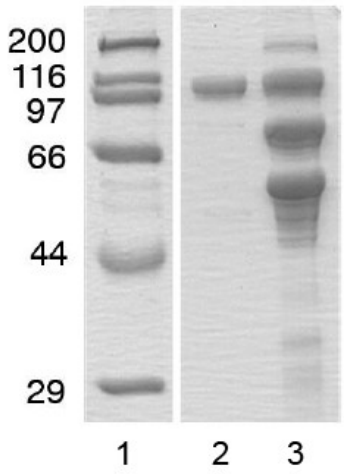

Figure 8: Purification and analysis of endogenous GRP94.

Endogenous GRP94 was purified from whole luminal protein extract. 1.2 μg purified endogenous GRP94 (lane 2) and 3 μL total luminal extract (lane 3) were resolved by 12.5% SDS-PAGE and detected by Coomassie Blue staining. M.W. marker is shown in lane 1.

Purification of α_2M was performed using endotoxin-free plasma, columns, and buffers and followed a protocol modified from that described previously (Bowers et al., 2009). α_2M was separated from mouse plasma (Harlan) by consecutive precipitation at 4% and 16% polyethylene glycol (Fluka), followed by DEAE Sephacel fractionation (Sigma-Aldrich) and purified further over a Sephacryl S-300 sizing column (Amersham Biosciences). Native α_2M was converted to the activated form (α_2M*) by incubation in 200 mM ammonium bicarbonate at 37°C overnight. Activated protein was then dialyzed for 4 hours into PBS and stored at 4°C. Purified protein contained <10 pg endotoxin/mg protein, as determined by a commercial assay kit (LAL kinetic-quantitative chromogenic

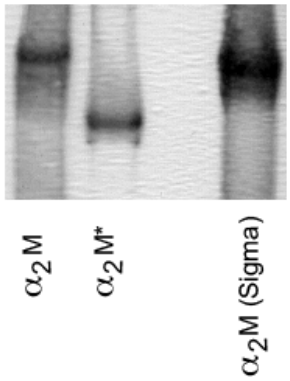

Figure 9: Analysis of native α_2M, α_2M*, and α_2M (Sigma).

Native α_2M was purified from human plasma and activated as described. 1 μg native α_2M (slow form) and 1 μg α_2M* (fast form) were resolved by 6% native TBE gel electrophoresis. 2 μg human α_2M (Sigma) was also examined to determine its activation state.

by Cambrex). Samples were analyzed by 6% native Tris-borate EDTA gel electrophoresis (Figure 9).

Analytical ultracentrifugation: The molecular weight of GRP94.LREK preparations were determined by sedimentation equilibrium ultracentrifugation in a Beckman XL-A analytical ultracentrifuge. GRP94.LREK, at concentrations of 0.9, 1.7, and 2.3 mg/mL in 50 mM Tris, pH 8.0, 100 mM NaCl, 1 mM DTT was analyzed at 10,000 rpm. The partial specific volumes (0.7278) and solvent densities (1.015) were calculated from the amino acid and solvent compositions using SEDENTERP (Figure 6).

Protein labeling: Proteins were conjugated to Alexa Fluor® carboxylic acid succinimidyl esters (Molecular Probes) according to the manufacturer's protocol. Briefly, purified protein samples were diluted with sterile 0.15 M sodium bicarbonate, pH 9.0, and incubated with Alexa Fluor® dye (dissolved in sterile DMSO) for 60 min at room temperature in the dark. Free dye was removed using a depyrogenated, PBS-equilibrated Sephadex G-25 column (Sigma). Proteins were concentrated in a YM-10 or YM-30 spin column (Millipore).

Reverse-transcriptase PCR: Total RNA was extracted from tissue culture cells using TRIzol Reagent, according to manufacturer's specifications, and dissolved in nuclease-free water (Ambion). RNA concentrations were determined spectrophotometrically and RNA integrity was assessed using a 1% formaldehyde gel. Samples were then treated with RNase-free DNase I (Ambion) at 37 °C for 30 min prior to heat-inactivation. cDNA was synthesized from 7.2 μg DNase-treated RNA using Superscript, according to the manufacturer's protocol. The optional RNase OUT and RNase H treatments were not included. cDNA was recovered by phenol/chloroform/isoamyl alcohol (25:24:1) extraction and sodium acetate/ethanol precipitation, and resuspended in 75 μL 10 mM Tris-Cl, pH 8.5.

PCR was carried out according to manufacturer's specifications using Taq polymerase (Qiagen). The following primer sequences were used: CD91 sense: 5'-ATC ACC CTT CCC GGC AGC CCA-3'; CD91 antisense: 5'-ACC CAG AGC CAT CGG CTT TGT-3'; 18S sense: 5'-TCA AGA ACG AAA GTC GGA GG-3'; 18S antisense: 5'-GGA CAT CTA AGG GCA TCA CA-3'. Thermocycling was performed in a PTC-200 Thermal Cycler (MJ Research, Watertown, MA) using the following parameters: denaturation at 94°C for 3 min; 33 cycles of 94°C for 30 seconds, 62°C for 1 min, 72°C for 1 min; final extension at 72°C for 10 min. PCR products were separated on a 1% agarose gel and visualized using ethidium bromide. Quantification of band intensities was measured using Image J version 1.38x (NIH).

Surface binding and internalization assays: Adherent MEF-1 and PEA-13 cultures were rinsed and incubated with pre-warmed PBS^{++} (PBS with 1% BSA (Gibco), supplemented with 0.22 μm filter-sterilized 0.9 mM CaCl2 and 0.5 mM MgCl2) for 30 min at 37°C. Cells were then rinsed with room temperature PBS without calcium or magnesium, lifted with Verseen, and diluted with an equal volume of cold PBS^{++}. In all experiments conducted with RAW264.7 and DC2.4, cells were rinsed with room temperature PBS without calcium or magnesium, lifted with Verseen, and diluted with an equal volume of PBS with calcium and magnesium, supplemented with 1% BSA (fraction VII; tissue culture tested). All staining steps were conducted using pre-conditioned media.

Surface binding and uptake experiments were conducted as previously described (Wassenberg et al., 1999). For surface binding studies, cells were incubated with 10 μg/mL RAP, 300 μg/mL native α_2M, 300 μg/mL α_2M*, 250 μg/mL GRP94.NTD, or 250 μg/mL heat shocked GRP94.NTD for 30 min on ice, washed, and then incubated with the specified ligand. All samples were stained with propidium iodide (PI) for 30 min on ice and immediately analyzed using an LSRII flow cytometer (BD). PI-positive cells were excluded from final analyses, and cell autofluorescence was subtracted from the total fluorescence at each data point. All flow cytometry data was analyzed using FlowJo version 8.6.1. All data represents mean fluorescence intensity, and is depicted using biexponential scaling.

To measure a single round of endocytosis, internalization experiments were conducted as previously described, with minor modifications (Wassenberg et al., 1999). Briefly, cells were prepared as described above. Cell suspensions were then supplemented with ligands and incubated at 37°C with 5% CO_2. Where indicated 50 μg/mL unlabeled RAP, 300 μg/mL native α_2M, or 300 μg/mL α_2M*, 250 μg/mL GRP94.NTD, or 250 μg/mL heat shocked GRP94.NTD was included in the internalization buffer. Endocytosis was arrested by the addition of ice cold PBS^{++} at the specified time points. Cells were then washed with additional cold buffer. To remove residual surface-bound ligand, cells were treated with 0.25% trypsin-EDTA for 15 min

on ice and proteolysis was arrested with 50 μg/mL soybean trypsin inhibitor. The amount of time utilized for these digestions was determined experimentally (Figure 10). Cells were then washed and resuspended in cold PBS^{++}. All samples were stained with propidium iodide (PI) for 30 min on ice and immediately analyzed using an LSRII flow cytometer (BD). PI-positive cells were excluded from final analyses, and cell autofluorescence was subtracted from the total fluorescence at each data point. All flow cytometry data was analyzed using FlowJo version 8.6.1. All data represents mean fluorescence intensity, and is depicted using biexponential scaling.

No pre-incubation step was included for those experiments comparing fluid phase and receptor-mediated endocytosis.

For protease inhibition studies, cells were incubated with pre-warmed PBS^{++} containing 100 μg/mL leupeptin (Sigma) for 30 min. 100 μg/mL leupeptin was also included during surface binding and internalization steps.

All samples analyzed by confocal analysis were fixed with 4% paraformaldehyde following internalization, mounted using FluorSave Reagent (Calbiochem), and imaged on a Zeiss LSM510 laser scanning confocal microscope. Only labeled GRP94.NTD (22-337) was used for these experiments.

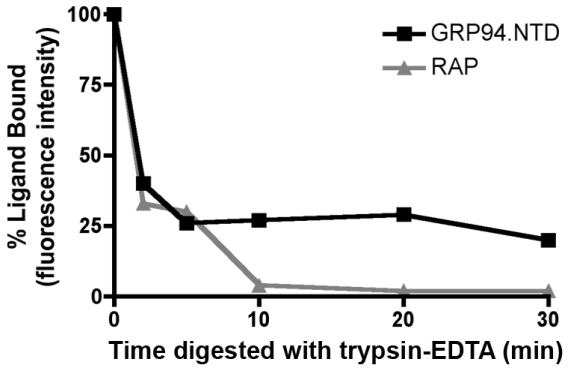

Figure 10: Optimization of surface proteolysis.

Optimal conditions for trypsin-EDTA surface proteolysis were determined using RAW264.7 cells. Following surface binding of either GRP94.NTD or RAP, cells were rinsed with buffer, and incubated with 0.25% trypsin-EDTA on ice. After a given period of time, digestion was arrested with 50 μg/mL soybean trypsin inhibitor. Cells were then rinsed and analyzed by flow cytometry. Samples were normalized to the total GRP94.NTD or RAP bound by undigested cells.

Sodium chlorate and heparinase II treatments: MEF-1 and PEA-13 cells were exchanged into media containing 20 mM sodium chlorate (cell culture tested), and cells were grown for an additional 24 hours. Cells were rinsed and incubated with pre-warmed PBS^{++} supplemented with 20 mM sodium chlorate for 30 min at 37°C. Cells were then rinsed, lifted, and stained as described above.

To examine the effects of heparinase II treatment of cells on GRP94 binding and internalization, MEF-1 and PEA-13 cells were rinsed with PBS^{++} and incubated with 0.01 IU/mL heparinase II in PBS^{++} for 90 min at 37°C. Cells were then rinsed, lifted, and

stained as described above. Heparinase II enzymatic activity was assayed at the onset of each experiment (Sigma SSHEPA02).

Where indicated, desulfation of surface HSPGs was confirmed using monoclonal anti-heparan sulfate antibody 10E4 (Seikagaku) and goat anti-mouse IgG conjugated to Alexa Fluor 647 (Invitrogen). All experiments included a purified mouse IgM isotype control (Invitrogen).

Trypsin-mediated proteolysis of GRP94: Labeled GRP94.NTD was incubated with trypsin-EDTA at a 34:1 (w/w) ratio in cytosol/MES buffer (100 mM KCl, 20 mM NaCl, 2 mM Mg(OAc)2, 25 mM MES, pH 6.0). Proteolysis reactions were quenched at the indicated time points by addition of 20% trichloroacetic acid. The precipitated proteins were then analyzed by 12.5% SDS-PAGE and visualized with Coomassie Brilliant Blue-G250 staining. The relative amounts of GRP94 were normalized to the total GRP94 present before the addition of trypsin using ImageJ (NIH). To examine changes in fluorescence intensity, fluor-conjugated GRP94 was incubated in cytosol buffer until a stable baseline was acquired on a Shimadzu RF-5301 PC Spectrofluorophotometer. Trypsin was then added to the solution, and measurements were taken every 30 seconds. All readings were taken using an excitation wavelength of 647 nm and an

emission wavelength of 665 nm. Relative GRP94 fluorescence was normalized to the maximum signal acquired during each analysis.

Cross-presentation of GRP94.NTD/SIINFEKL and GRP94.NTD/ova20 complexes: GRP94.NTD/SIINFEKL and GRP94.NTD/ova20 complexes were prepared as previously described (Suto and Srivastava, 1995). Briefly, GRP94.NTD was diluted to 1 mg/mL and incubated with 50-fold molar excess peptide at 50°C for 10 min, followed by a 30 minute incubation at room temperature (Figure 11). Free peptide was removed by size exclusion spin concentration using a YM-10 Centricon column, and/or dialysis against sterile PBS at 4°C.

To assay GRP94-mediated peptide cross-presentation, DC2.4 cells (2.5 x 104 cells/well) were co-incubated with 10 μg/mL GRP94.NTD/peptide complex in the presence or absence of the following ligands: 300 μg/mL α_2M, 300 μg/mL α_2M *, 300 μg/mL commercial α_2M (Sigma), 500 μg/mL RAP, 500 μg/mL GRP94.NTD, 500 μg/mL heat-shocked GRP94.NTD, or 500 μg/mL endogenous GRP94. All samples were diluted in conditioned media. Cells were incubated for 4 hours under standard conditions, rinsed with PBS to remove unbound protein, and replenished with 100 μL complete media. OT-1 splenocytes were harvested from MHC Class I-restricted OVA-transgenic mice, and single cell suspensions were prepared by repeated subcapsular injection of

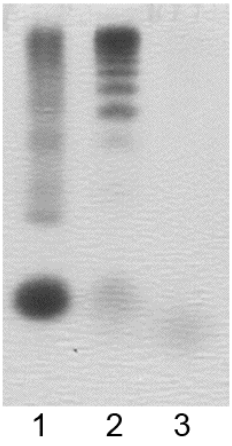

Figure 11: Analysis of GRP94.NTD/ova20 complexes.

Purified GRP94.NTD was complexed with 50-fold molar excess ova20 peptide by heat-shock. To examine the oligomeric state of complex, 7.5 μg purified GRP94.NTD (lane 1), 7.5 μg GRP94.NTD/ova20 complex (lane 2), and 25 μg ova20 (lane 3) were resolved by 6% native PAGE.

complete culture media (high glucose phenol red-free DMEM supplemented with 10% FBS, 1% penicillin-streptomycin, 1 mM sodium pyruvate, 2 mM L-glutamine, 10 mM HEPES, 0.1 mM nonessential amino acids, and 50 μM βME). The DC2.4 cells were then co-cultured with 2.5 x 105 OT-1 splenocytes. Cell supernatants were harvested after 24 hours and stored at -20°C until IFN-γ secretion was quantified using DUO-ELISA kits (R&D Systems, Minneapolis, MN, USA).

Chapter 3: Examining the role of CD91 in GRP94 surface binding, endocytosis, and processing

A. Introduction

CD91 was first identified as a putative GRP94 endocytic receptor after an 80 kDa CD91 fragment was purified from detergent-solubilized membrane extracts using a GRP94 affinity matrix (Binder et al., 2000). Subsequent studies demonstrated that GRP94-mediated peptide cross-presentation could be inhibited by various CD91 ligands, including activated α_2-macroglobulin (α_2M*), receptor associated protein (RAP), and a CD91 blocking antibody (Basu et al., 2001; Binder et al., 2000; Binder et al., 2004). siRNA-mediated knock-down of CD91 expression was also shown to have a profound effect on GRP94-mediated cross-presentation (Binder and Srivastava, 2004). Together, these studies indicate that CD91 plays a role in GRP94-mediated peptide cross-presentation and suggest that CD91 is an endocytic receptor for GRP94. However, the conclusion that CD91 functions as an endocytic receptor for GRP94 has been challenged (Berwin et al., 2002a; Berwin et al., 2003; Berwin and Nicchitta, 2001).

Extending from the observation that CD91 ligands inhibit GRP94-mediated peptide cross-presentation, two independent investigators examined the effects of CD91 ligands on GRP94 cell surface binding. Reports by both Berwin et al. and Binder and Srivastava agree that 100-fold molar excess α_2M* or RAP do not significantly compete (<15%) for GRP94 surface binding to unfixed elicited peritoneal macrophages or unfixed

RAW264.7 mouse macrophage-like cells, respectively (Berwin et al., 2002a; Binder and Srivastava, 2004). Based on these findings, Berwin et al. concluded that CD91 does not significantly contribute to GRP94 surface binding. In contrast, Binder and Srivastava contested that this lack of cross-competition was due to the rapid internalization of CD91, which they claim can occur while cells are incubated at 4°C. To prevent this rapid internalization, RAW264.7 cells were fixed with paraformaldehyde prior to ligand binding. Using these conditions, Binder and Srivastava observed that 100-fold molar excess CD91 ligand reduced GRP94 binding 60%, and concluded that CD91 is a GRP94 surface receptor.

But is pre-fixation necessary for the analysis of putative GRP94-CD91 interactions? If pre-fixation is required, one would predict that unfixed RAW264.7 cells would have less CD91 at the cell surface than pre-fixed cells. These unfixed cells should therefore bind less GRP94. However, no significant difference in GRP94 binding is observed in the comparison conducted by Binder and Srivastava (Binder and Srivastava, 2004). This study also never established if pre-fixation alters α_2M* or RAP binding to RAW264.7 cells. Hence, it remains uncertain if pre-fixation is required for the analysis of CD91-ligand interactions at the cell surface. It is also well established that RAW264.7 cells express GRP94 surface receptors other than CD91 (Berwin et al., 2004; Berwin et al., 2003; Vabulas et al., 2002). Therefore, excess RAP and α_2M* should not be able to

completely inhibit GRP94 binding to the cell surface. In agreement with this hypothesis, GRP94 surface binding to unfixed RAW264.7 cells was reduced by 50-60% using 100-fold molar excess unlabeled GRP94, whereas an equivalent molar excess RAP and α2M* reduced GRP94 surface binding by 20-30% (Binder and Srivastava, 2004). In fixed cell, however, 100-fold molar excess RAP, α_2M*, and unlabeled GRP94 compete for GRP94 surface binding with similar efficiencies. At 250-fold molar excess competitor, there is essentially no difference in the ability of RAP, α_2M*, or unlabeled GRP94 to inhibit labeled GRP94 binding to pre-fixed RAW264.7 cells. The assumption that CD91 is rapidly internalized while on ice is addressed by surface proteolysis experiments included in chapter 2 and internalization experiments included later in this chapter.

There is also a discrepancy between the ability of CD91 ligands to inhibit GRP94 surface binding, and their ability to inhibit GRP94-mediated peptide cross-presentation. Although 50-fold molar excess RAP reduced GRP94 surface binding to unfixed RAW264.7 cells by ~20%, the same molar excess reduced GRP94-mediated peptide cross-presentation by 50-75% (Binder and Srivastava, 2004). Indeed, a noticeable inhibition of GRP94-mediated peptide cross-presentation has be achieved with as little as 10-fold molar excess α_2M* or RAP (Binder et al., 2000; Binder and Srivastava, 2004). This discrepancy can be explained by one of two models. In the first, CD91 would not significantly contribute to GRP94 surface binding, but GRP94-mediated peptide cross-

presentation would be directed primarily through CD91. This model is refuted by several reports demonstrating that GRP94-mediated peptide cross-presentation can occur independently of CD91 (Berwin et al., 2002a; Berwin et al., 2003). Specifically, the scavenger receptor ligand fucoidan was shown to dramatically reduce GRP94-mediated SIINFEKL cross-presentation, but had no effect on α_2M* surface binding or endocytosis. These results strongly suggest that CD91 is not the sole portal for GRP94-mediated peptide cross-presentation.

Alternately, CD91 (or CD91 ligands) could indirectly inhibit GRP94-mediated peptide cross-presentation by modulating GRP94 receptor turnover, or by initiating an unknown inhibitory signaling pathway. In support of this second model, there is evidence that CD91 may indirectly modulate ligand-induced PDGF receptor (PDGFR) turnover through interactions with the ubiquitin ligase c-Cbl (Takayama et al., 2005). These studies demonstrated CD91-deficient cells had accelerated ligand-induced PDGFR down-regulation and attenuated ERK activation. There was also an increased association between PDGFR and c-Cbl, which is also known to associate with CD91. Based on these observations, the authors speculate that CD91 could influence PDGFR turn-over by modulating c-Cbl activity. However, there is no evidence that CD91 can modulate the expression or activity of established GRP94 receptors, or that CD91-ligand binding alters the efficiency of the MHCI cross-presentation pathway.

To re-examine the role of CD91 as a GRP94 endocytic receptor, I have focused my studies on the ability of CD91 to mediate three processes that are required for GRP94-mediated peptide cross-presentation: surface binding, endocytosis, and intracellular processing. To this end, I utilize a recombinantly-expressed N-terminal domain of GRP94 (GRP94.NTD). GRP94.NTD has been previous shown to nearly identical biological activity to full length GRP94 in several *in vitro* assays, including APC maturation, APC surface binding and internalization, and maturation (Baker-LePain et al., 2002). I demonstrate that GRP94.NTD surface binding and internalization are not reduced in CD91 knock-down/knock-out mouse embryonic fibroblast (MEF) cells. Furthermore, various CD91 ligands do not inhibit GRP94.NTD surface binding or internalization/processing by MEF cells. I also extend these studies into DC2.4 mouse dendritic cells. Although CD91 ligands do not inhibit GRP94.NTD binding to DC2.4 cells, RAP modestly reduces GRP94.NTD internalization/processing. Lastly, I show that GRP94-mediated peptide cross-presentation is not influenced by excess CD91 ligands in the DC2.4/OT-1 system. Together, these data strongly suggest that CD91 does not directly function in GRP94 surface binding, endocytosis, or processing by MEF-1 or DC2.4 cells.

B. GRP94 binds cells independently of CD91

If CD91 binds GRP94 in a specific manner, CD91 surface expression should tightly correlate with GRP94 surface binding. To test this assumption, CD91 expression was reduced via CD91-directed siRNA. CD91-expressing mouse embryonic fibroblast (MEF-1) cells were transiently transfected with either of two different CD91-directed siRNAs (LRP1_1 and LRP1_2). The efficiency of these siRNAs was monitored by reverse-transcriptase PCR (RT-PCR) at 24, 48, and 72 hours post-transfection. Amplification of the CD91 target sequence was within the linear range, with the most efficient knockdown observed 24 hours post-transfection (Figure 12a; data not shown). At this time point, cells transfected with LRP1_2 displayed a 75% reduction in CD91 mRNA levels, as compared to untransfected (UT) and vector-only (mock) transfection controls (Figure 12b). Transfection with LRP1_1 had no effect on CD91 mRNA levels and was used as a control for off-target effects. Neither siRNA affected 18S rRNA expression, and genomic DNA contamination was monitored using paired RNA samples in which reverse transcriptase was omitted (-RT).

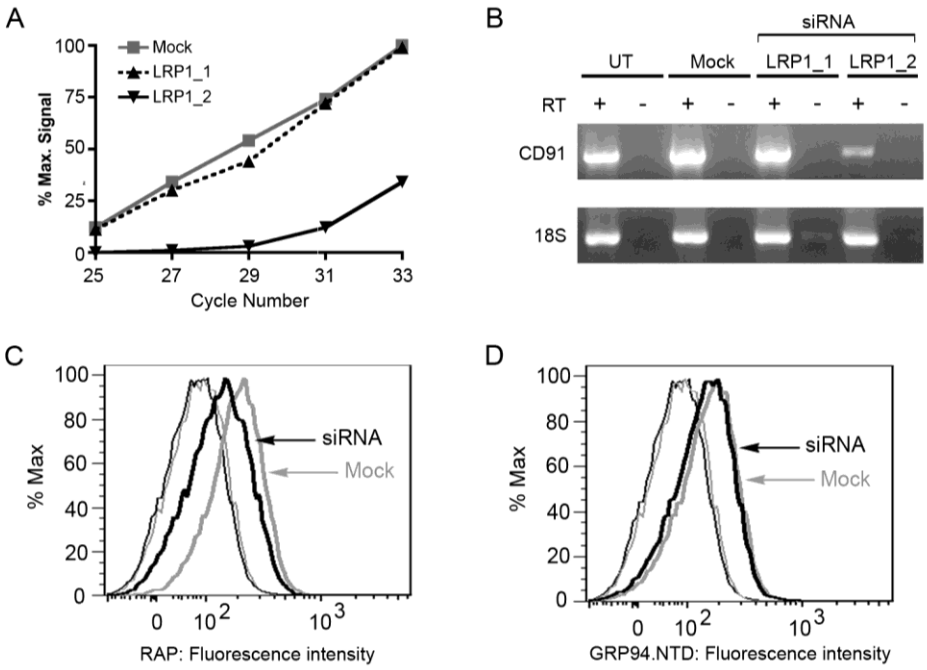

Figure 12: Suppression of CD91 expression does not affect GRP94.NTD surface binding to MEF-1 cells.

MEF-1 cells were transiently transfected with either of two CD91-targeting siRNAs (LRP1_1 and LRP1_2) or a vector only (mock) control, and examined for changes in CD91 expression 24 hours post-transfection.
A. Total RNA was isolated and CD91 mRNA knockdown efficiency was determined by RT-PCR. CD91 cDNA from mock-transfected cells displayed linear amplification between PCR cycles 25 and 33 (R^2 = 0.9974).
B. Untransfected (UT), mock-transfected, and siRNA-transfected cells were examined for changes in CD91 mRNA levels using RT-PCR. All samples were tested for DNA contamination using a paired transcriptase-deficient (RT -) reaction, and examined for off-target effects to 18S rRNA.
C & D. MEF-1 cells were transfected with LRP1_2 siRNA or a mock control and analyzed by flow cytometry. CD91 surface expression was determined using fluorescently-labeled RAP (C), and GRP94.NTD surface binding was detected using fluorescently-labeled GRP94.NTD (D): unstained cells (thin lines), stained cells (bold lines), mock-transfected cells (grey), and LRP1_2 siRNA transfected cells (black). The data presented are representative of three independent replicates.

CD91 surface expression was assessed by monitoring the surface binding of fluorescently-labeled RAP. RAP is a trafficking chaperone for newly synthesized LDL family receptors, including CD91, and prevents their premature interaction with intracellular ligands (Bu and Schwartz, 1998). While RAP is usually localized to the ER and Golgi apparatus, it has proven an invaluable tool for the study of CD91-ligand interactions at the cell surface. Because CD91 can interact with ligands through four distinct binding domains, many CD91 ligands do not cross-compete for CD91 binding. RAP, however, is bound with a high affinity (K_d ~ 3 nM) and can cross-compete with all known CD91 ligands (Bu and Schwartz, 1998; Herz et al., 1991; Iadonato et al., 1993). For this reason, the following studies utilize RAP surface binding as a measure of CD91 surface expression. Saturating levels of RAP binding to MEF-1 cells were determined experimentally, and greater-than-saturating concentrations were used in all subsequent experiments (Figure 25a, b). GRP94.NTD binding titrations were also conducted, and displayed a possible saturation point at 25 μg/mL (Figure 25c, d). This concentration was used in subsequent experiments unless otherwise noted.

Compared to mock-transfected cells, RAP binding to LRP1_2-transfected cells was reduced by 45% (Figure 12c). Transfection with LRP1_1 did not affect RAP binding, suggesting that the loss of RAP binding can be attributed to a specific decrease in CD91 surface expression (data not shown). Although these data demonstrate that CD91

expression was significantly reduced following transfection with LRP1_2, no decrease in GRP94.NTD surface binding was observed (Figure 12d). This lack of a corresponding decrease in GRP94.NTD binding indicates that GRP94.NTD binds a receptor(s) other than CD91 and suggests that CD91 does not significantly contribute to GRP94.NTD surface binding activity on MEF-1 cells. However, because RAP can associate with LDL family receptors other than CD91, alternative experimental approaches were necessary to identify CD91-dependent versus CD91-independent GRP94.NTD surface interactions. To this end, RAP and GRP94.NTD surface binding were examined the paired CD91 knock-out cell line PEA-13.

PEA-13 cells were previously generated by introducing a genetic disruption in the CD91 gene of C57BL/6 mice (Willnow and Herz, 1994). Because CD91 is an essential gene, CD91 heterozygous mice ($CD91^{+/-}$) were mated and $CD91^{-/-}$ embryonic fibroblasts were selected for further analysis. Unlike the wild-type MEF-1 cells, the $CD91^{-/-}$ PEA-13 cells were deficient for CD91 ligand binding via ligand blots and displayed defects in the ability to efficiently degrade the CD91 ligands α_2M*, uPA/PAI-1, and RAP. Furthermore, PEA-13 cells were resistant to treatment with the toxin *Pseudomona*s exotoxin A, which is only known to gain access to cells through CD91 (Kounnas et al., 1992). Although PEA-13 cells express at least one other LDL family receptor, the studies by Willnow and Herz

identify CD91 as the primary receptor for the uptake/degradation of α_2M* and RAP by MEF-1 cells.

Similar to the studies conducted with the siRNA knock-down cells, MEF-1 and PEA-13 cells were examined for CD91 expression at both the message and protein levels. Consistent with the reported genotypes, PEA-13 cells lack CD91 expression at the message level, and display very low RAP surface binding activity compared to MEF-1 cells (Figure 13a, b). In contrast, PEA-13 cells bind slightly more GRP94.NTD than MEF-1 cells (Figure 13c). To confirm these observations, ligand binding to MEF-1 and PEA-13 cells was visualized using confocal microscopy (Figure 13d, e). In agreement with the flow cytometry analyses, RAP binding was readily detectable on MEF-1 cells, but absent from PEA-13 cells. In contrast, GRP94.NTD binding was readily apparent on both cell lines. Together, these data demonstrate that CD91 expression does not correlate with GRP94.NTD surface binding, and that CD91 expression is not necessary for GRP94.NTD surface binding.

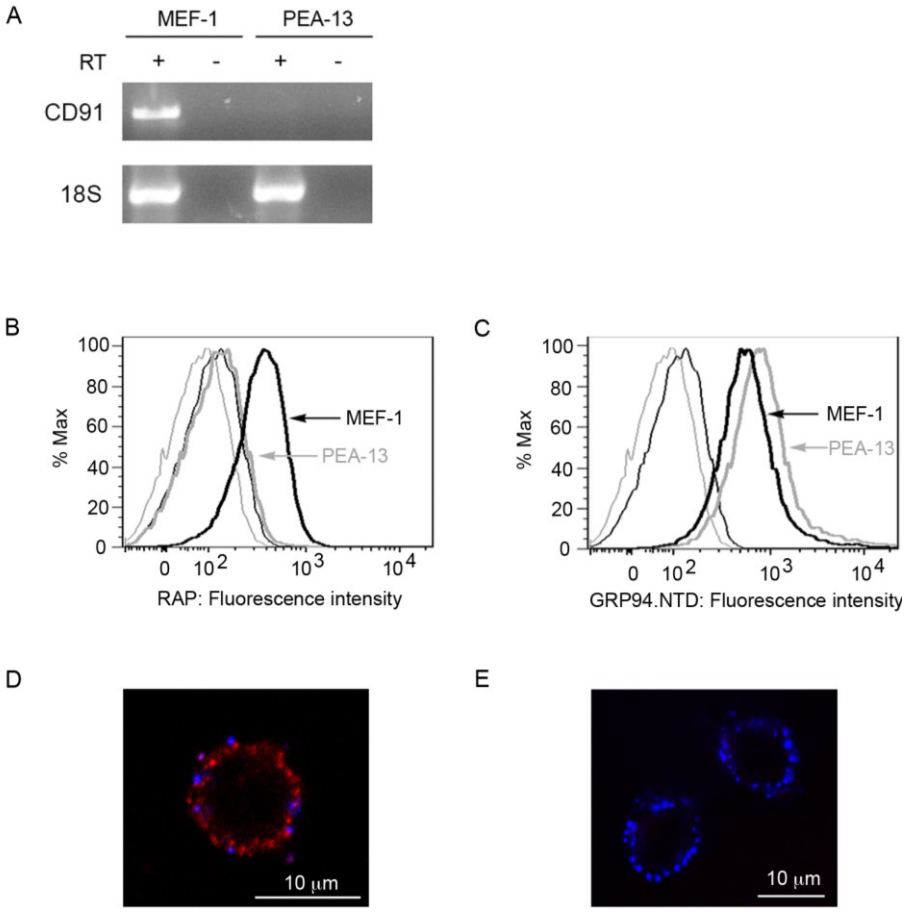

Figure 13: GRP94.NTD binds MEF-1 and PEA-13 independently of CD91 expression.

A. MEF-1 and PEA-13 cells were analyzed for CD91 expression using RT-PCR. All samples were tested for DNA contamination using a paired transcriptase-deficient (RT-) reaction, and were examined for off-target effects to 18S rRNA. B & C. MEF-1 and PEA-13 cells were incubated with RAP (B), or GRP94.NTD (C), washed, and analyzed by flow cytometry: unstained cells (thin lines), stained cells (bold lines), MEF-1 cells (black), and PEA-13 cells (grey). D & E. MEF-1 (D) and PEA-13 (E) cells were incubated with 5 μg/mL RAP (red) and 40 μg/mL GRP94.NTD (blue), washed, fixed, and processed for confocal microscopy. Images were obtained at 63X magnification on an LSM510 laser scanning confocal microscope. Scale bars: 10 μm. Data presented are representative of three independent replicates. Confocal images contributed by Mariam Totonchy.

As an alternate means of assessing the ability of CD91 to directly interact with GRP94 at the cell surface, GRP94 surface binding was cross-competed with RAP. Binding competitions were conducted with the CD91-expressing MEF-1 cell line, and analyzed using flow cytometry. Competition with 100-fold molar excess unlabeled GRP94.NTD did not significantly decrease labeled RAP surface binding to MEF-1 cells (Figure 14a). This very modest competition was also observed in the presence of 100-fold molar excess unlabeled bovine serum albumin (BSA), suggesting that this decrease was due to non-specific RAP binding. In parallel experiments, 30-fold molar excess unlabeled RAP did not significantly affect GRP94.NTD surface binding to MEF-1 cells (Figure 14b). Thirty-fold molar excess RAP was, however, sufficient to completely inhibit binding of fluorescently labeled RAP (data not shown). This lack of cross-competition demonstrates that GRP94.NTD and RAP bind MEF-1 cells independently of each other.

In summary, these studies show that CD91 expression does not correlate with GRP94.NTD surface binding to MEF tissue culture cells. While reduction/loss of CD91 expression resulted in a corresponding decrease in RAP surface binding, GRP94 surface binding was not reduced. Furthermore, RAP and GRP94.NTD do not cross-compete for surface binding. Combined, these data demonstrate that GRP94 binds cells

independently of CD91 expression and strongly suggest that CD91 does not directly interact with GRP94.NTD on MEF-1 cells.

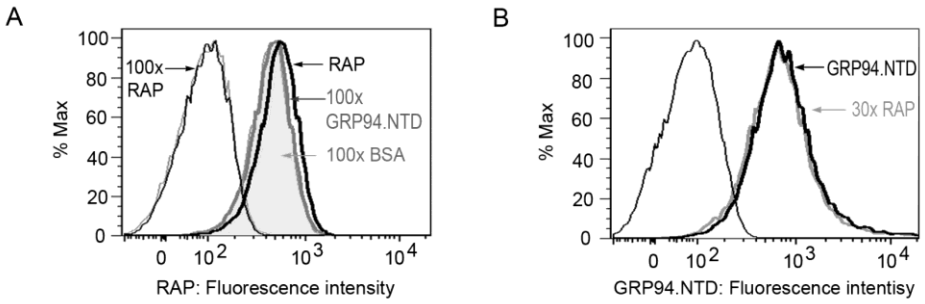

Figure 14: RAP and GRP94.NTD do not compete for surface binding to MEF-1 cells.

A. MEF-1 cells were incubated with RAP in the absence or presence of 100-fold molar excess unlabeled RAP, GRP94.NTD, or BSA. Cells were then washed and analyzed by flow cytometry: unstained cells (thin grey), RAP (bold black), unlabeled RAP (thin black), unlabeled GRP94.NTD (bold grey), and unlabeled BSA (shaded grey). B. MEF-1 cells were incubated with GRP94.NTD in the absence or presence of 30-fold molar excess unlabeled RAP. Cells were then washed and analyzed by flow cytometry: unstained cells (thin grey), GRP94.NTD (bold black), and unlabeled RAP (bold grey).

C. CD91 does not directly mediate GRP94.NTD internalization/ processing

Although CD91 does not appear to contribute to GRP94.NTD recognition at the cell surface, CD91 may influence GRP94.NTD internalization/processing independently of a direct interaction at the cell surface (Mahley and Ji, 1999; Nykjaer and Willnow, 2002; Sarafanov et al., 2001). It is well established that some surface molecules, such as heparan sulfate proteoglycans (HSPGs), can mediate ligand binding to CD91 and possibly "transfer" bound ligands to CD91 for subsequent internalization and/or processing (reviewed in Mahley and Ji, 1999). These models are of particular relevance to the conflicting data regarding the role of CD91 in GRP94 uptake, as they suggest that CD91 could function in GRP94 endocytosis without directly contributing to GRP94 recognition at the cell surface.

To determine if CD91 supports GRP94.NTD internalization, the kinetics of both RAP and GRP94.NTD internalization were examined. MEF-1 cells were incubated with either labeled RAP or labeled GRP94.NTD on ice, washed, and then warmed to 37°C to allow internalization of surface-bound proteins. At the indicated intervals, cells were rapidly cooled to arrest endocytosis and then subjected to surface proteolysis with ice-cold trypsin-EDTA. In this manner, internalized (protease resistant) ligand could be distinguished from residual surface-bound ligand. Additionally, the percent protease-

resistant signal could be calculated by comparing the protease-resistant signal to the paired un-proteolyzed sample from that same time point.

As would be predicted of a typical CD91 ligand, RAP was quickly endocytosed by MEF-1 cells, with 80-90% of the total surface-bound RAP becoming resistant to external proteases within 5 min (Figure 15a). The kinetics of GRP94.NTD internalization, however, were considerably slower, with little uptake being observed before 20 min. Because CD91 internalization rates are known to be unusually fast, the relatively sluggish rate of GRP94.NTD internalization argues against a significant role for CD91 in GRP94.NTD endocytosis (Herz and Strickland, 2001; Li et al., 2001). Furthermore, MEF-1 and PEA-13 cells internalize/process GRP94.NTD at similar rates during the first 20 min of internalization (Figure 15b). This demonstrates that CD91 expression does not enhance GRP94.NTD endocytosis, and that CD91 is not necessary for GRP94.NTD internalization.

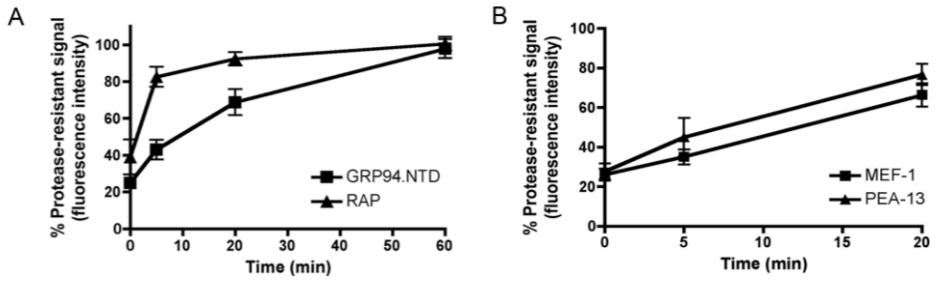

Figure 15: GRP94.NTD and RAP are internalized via kinetically distinct pathways.

A. MEF-1 cells were incubated with either 10 μg/mL RAP or 25 μg/mL GRP94.NTD, washed, and warmed to 37°C for 0, 5, 20, or 60 min. Residual surface-bound ligands were removed by proteolysis on ice. B. MEF-1 and PEA-13 cells were incubated with 25 μg/mL GRP94.NTD, and treated as in A. Percent protease resistance signal was calculated by normalizing the protease resistant signal to the total un-proteolyzed signal at each time point. Error bars represent the SD of three experiments.

These experiments also demonstrate that ~70% of RAP bound to MEF-1 cells was sensitive to protease treatment prior to internalization. Because RAP binding to MEF-1 cells is attributed to CD91 expression, this suggests that a significant percentage of CD91 remains at the cell surface during sample preparation (Figures 12 and 13; Willnow and Herz, 1994). These data argue against the hypothesis that CD91 is rapidly internalized while on ice, and therefore argue against the necessity of pre-fixation (Binder and Srivastava, 2004). The residual 20-30% of protease-insensitive RAP surface binding cannot be accounted for at this time, although this may be due to technical difficulties associated with proteolyzing MEF-1 cells. In RAW264.7 and DC2.4 cells, less than 15% of surface-bound RAP was resistant to protease treatment (Figure 10; data not shown).

While these studies demonstrate that GRP94.NTD is slowly endocytosed and that CD91 expression is not necessary for this internalization, they do not directly test the ability of CD91 to facilitate GRP94.NTD internalization. As previously mentioned, CD91 is believed to facilitate ligand internalization by accepting the transfer of surface-bound ligands. Therefore, to determine if CD91 directly functions in GRP94.NTD internalization, a competition of internalization experiment was conducted. To block surface CD91 molecules, cells were incubated on ice with saturating levels of RAP prior to GRP94.NTD surface binding. Because CD91 is constitutively internalized and recycled back to the cell surface, excess unlabeled RAP was also included in the internalization buffer. This ensured that empty, recycling CD91 molecules would be occupied with RAP instead of potentially interacting with surface-bound GRP94.NTDs. As expected, these conditions significantly inhibited both the surface binding and internalization/processing of labeled RAP (Figure 16a). However, these conditions had no effect on either the quantity or the rate of GRP94.NTD endocytosis (Figure 16b, c). Cumulatively, these data indicate that CD91 does not function as an endocytic receptor for GRP94.NTD on MEF-1 cells, either directly or via the transfer of GRP94.NTD from surface molecules such as HSPGs.

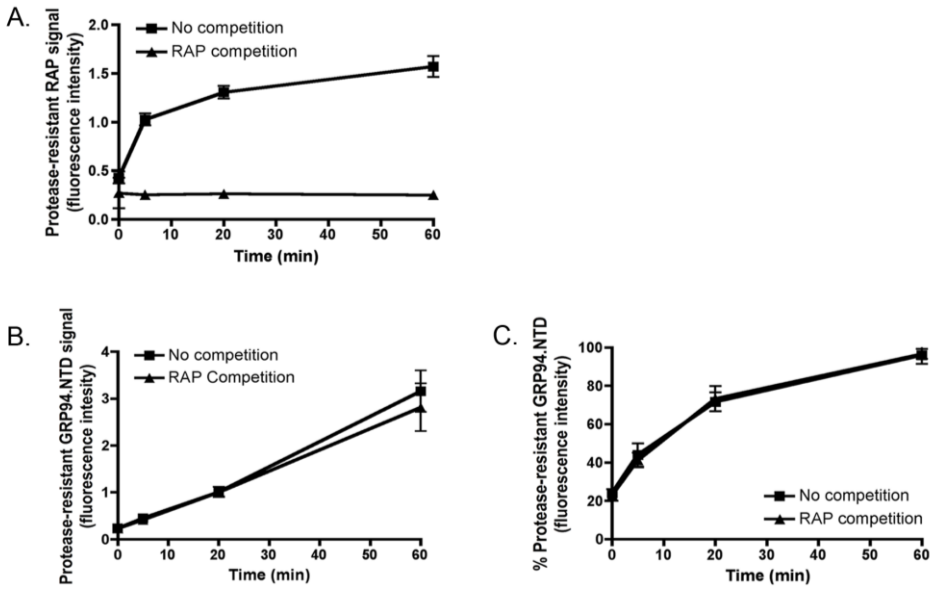

Figure 16: RAP does not inhibit GRP94.NTD internalization/processing by MEF-1 cells.

MEF-1 cells were incubated with 25 μg/mL GRP94.NTD in the absence or presence of 10 μg/mL unlabeled RAP. Cells were then washed, and incubated at 37°C in the presence of 50 μg/mL RAP for 0, 5, 20, or 60 min. Residual surface-bound ligands were removed by proteolysis on ice.
A & B. To quantify the amount of ligand internalized, the protease-resistant signal at each time point was normalized to the total amount of ligand bound to the surface of un-proteolyzed cells at time = 0 min. C. To quantify the rate of ligand internalization, the percent protease-resistant signal was calculated by normalizing the protease resistant signal to the total signal at the corresponding time point. Error bars represent the SD of three experiments.

Interestingly, GRP94.NTD that had been internalized for 60 min exhibited a level of fluorescence that greatly exceeded the initial signal from surface-associated protein (Figure 16b). In other systems, it has been reported that proteolysis of fluor-conjugated proteins can result in the loss of intramolecular quenching and a subsequent increase in fluorescence yield (Anderson and Nerurkar, 2002; Pimpaneau et al., 1989). To determine if fluor-conjugated GRP94.NTD behaves in a similar manner, GRP94.NTD integrity and fluorescence were monitored following proteolytic digestion with tryspin-EDTA. Aliquots were removed at various time points to monitor GRP94.NTD integrity, and GRP94.NTD proteolysis was visualized by SDS-PAGE (Figure 17a). Fractional loss of full length GRP94.NTD was then quantified using ImageJ. In parallel studies, GRP94.NTD fluorescence intensity was assayed in the presence of trypsin-EDTA using a spectrofluorophotometer (Figure 17b). As depicted in figure 17b, the time-dependent proteolytic degradation of fluor-conjugated GRP94.NTD was associated with an increase in total sample fluorescence. These data suggest that the increase in fluorescence observed following GRP94.NTD endocytosis is due to proteolytic processing of the internalized protein.

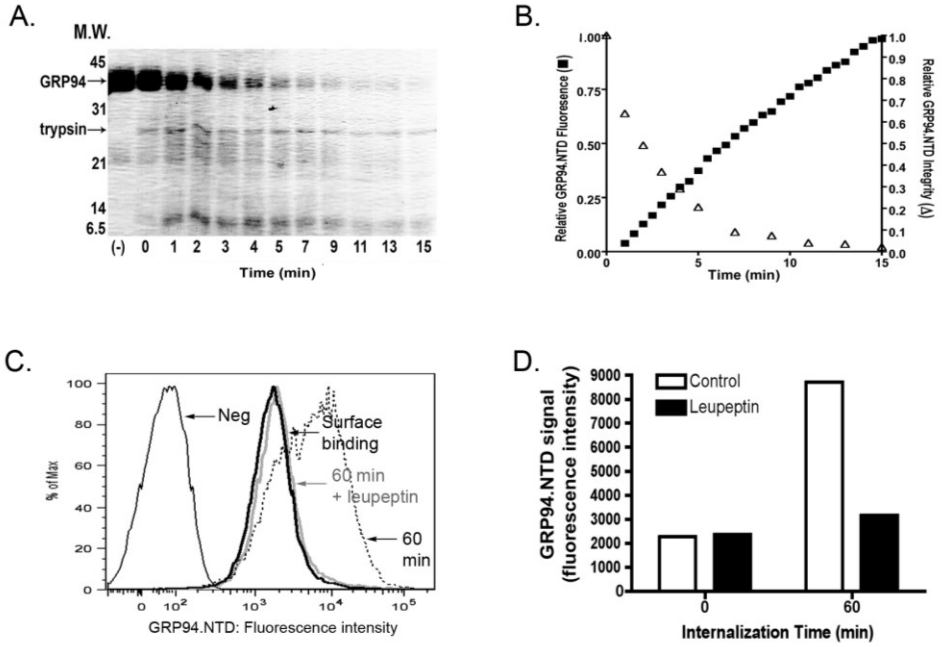

Figure 17: Proteolysis enhances the fluorescence yield of fluor-conjugated GRP94.NTD.

A & B. Fluor-conjugated GRP94.NTD was incubated with trypsin-EDTA at room temperature. A. At various time points an aliquot was removed and the reaction was quenched by the addition of TCA. Precipitated protein was then analyzed by SDS-PAGE and Coomassie Blue staining. Values were normalized to the untreated control (lane 1). B. GRP94.NTD fluorescence was determined at thirty second intervals using a spectrofluorophotometer. Relative GRP94.NTD fluorescence was normalized to the point of highest fluorescence intensity. C & D. MEF-1 cells were incubated in the absence or presence of 100 μg/mL leupeptin. Cells were then incubated with 25 μg/mL GRP94.NTD on ice, washed, and warmed to 37°C for 0 min (dashed line) or 60 (solid line) min in the absence (grey) or presence (black) of 100 μg/mL leupeptin. D. Data from C represented as a bar graph. Figures 17a and b contributed by Julie Neubauer.

To further test this hypothesis, MEF-1 cell cultures were supplemented with the serine/thiol protease inhibitor leupeptin prior to, and during GRP94.NTD uptake (Figure 17c, d). This treatment suppressed the previously observed increase in the fluorescence, reducing the total GRP94.NTD signal at 60 min to an equivalent intensity of the initial GRP94.NTD surface binding. Leupeptin treatment did not noticeably alter GRP94.NTD surface binding to MEF-1 cells (Figure 17d). Together with the *in vitro* studies, these data suggest that fluor-conjugated GRP94.NTD undergoes proteolytic processing in endosomal compartments. This finding is consistent with previous studies that demonstrated the exchange of GRP94-associated peptides onto mature MHCI molecules in endosomal compartments (Berwin et al., 2002b).

Alternately, GRP94.NTD fluorescence yield could change as it is internalized and trafficked into increasingly acidic endosomes. While Alexa Fluor® dyes themselves are relatively insensitive to changes in pH, changes in the GRP94.NTD protein conformation could result in quenching/unquenching effects. To examine this possibility, fluorescently labeled GRP94.NTD was incubated in buffers of varying pH and monitored over time. As can be seen in figure 18, GRP94.NTD fluorescence yield was increased in basic conditions and was suppressed in acidic conditions. This suggests that the observed increase in GRP94.NTD fluorescence yield is primarily due to GRP94.NTD digestion by endosomal proteases.

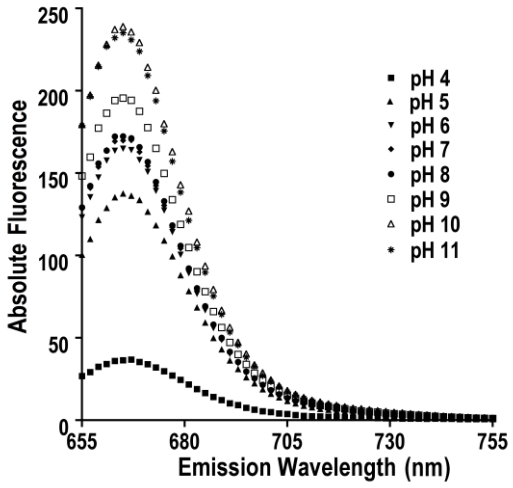

Figure 18: Alterations in pH change fluorescence yield of fluor-conjugated GRP94.NTD.

Fluor-conjugated GRP94.NTD was incubated at room temperature in cytosol buffer adjusted to the indicated pH. After the change fluorescence had equilibrated, fluorescence was measured with an excitation wavelength of 647 nm and emission wavelengths from 655 nm to 755 nm. Figure contributed by Julie Neubauer.

These studies demonstrate that internalized GRP94.NTD increases in fluorescence intensity as it is processed. Therefore, the observed time-dependent increase in fluorescence may reflect the kinetics of intracellular ligand processing rather than the kinetics of ligand uptake. To address this alternate interpretation, the kinetics of GRP94.NTD and RAP endocytosis were visualized by confocal microscopy. Similar to the other uptake experiments, MEF-1 cells were incubated with RAP and GRP94.NTD on ice, washed, and warmed to 37°C to allow internalization. Cells were then rapidly cooled at the indicated intervals to arrest endocytosis and fixed with paraformaldehyde

(Figure 19). As can be seen in figure 19b, MEF-1 completely internalized RAP within 15 min. However, GRP94.NTD remains localized to the cell periphery and is endocytosed via a substantially slower route. These data agree with the kinetic uptake analyses acquired by flow cytometry. These images also reveal that RAP and GRP94.NTD seldom co-localize at these discrete time points. Together, this demonstrates that RAP and GRP94.NTD are internalized via kinetically and spatially distinct pathways.

In summary, it stands to reason that if CD91 functioned in GRP94 internalization, both RAP and GRP94 would 1) be endocytosed with similar kinetics, 2) compete for internalization by CD91, and 3) be internalized via similar trafficking pathways. However, the data presented in this section demonstrate that GRP94.NTD and RAP are internalized via pathways that are kinetically and spatially distinct. Furthermore, excess RAP does not inhibit GR94.NTD internalization/processing by MEF-1 cells, and CD91-deficient PEA-13 cells internalize/process GRP94.NTD at a rate similar to the wild-type MEF-1 cells. Together, these data strongly suggest that CD91 does not significantly contribute to GRP94.NTD internalization/processing by MEF-1 cells, either directly or as part of a co-receptor complex.

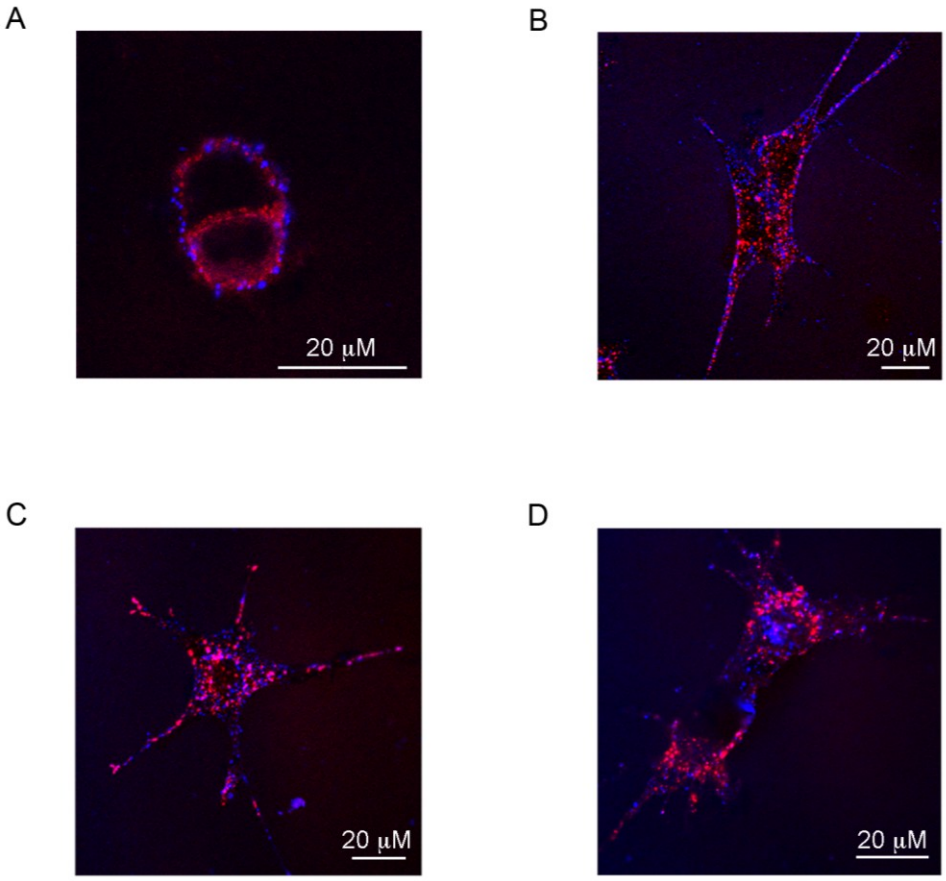

Figure 19: GRP94.NTD and RAP are internalized via spatially distinct pathways.

MEF-1 cells were incubated with 5 μg/mL RAP (red) and 40 μg/mL GRP94.NTD (blue), washed, and warmed to 37°C for 0 min (A), 5 min (B), 15 min (C), or 60 min (D) to allow internalization. Cells were then fixed and processed for confocal microscopy. Scale bars: 20 μm. All data presented are representative of three independent replicates. Confocal images contributed by Mariam Totonchy.

D. CD91 ligands do not inhibit GRP94.NTD internalization/ processing or GRP94.NTD-mediated peptide cross-presentation by DC2.4 cells

Although CD91 has been implicated in GRP94-mediated peptide cross-presentation, the data in this dissertation demonstrate that CD91 does not directly bind GRP94.NTD at the cell surface, and that CD91 does not significantly contribute to GRP94.NTD internalization/processing by MEF-1 cells. However, these experiments cannot exclude the possibility that CD91 mediates GRP94.NTD binding and endocytosis through co-receptor complexes that are not expressed by MEFs. Additionally, it is possible that CD91 (or some CD91 ligands) can suppress cross-presentation via an indirect, post-uptake mechanism. To explore these possibilities, GRP4.NTD binding, GRP94.NTD internalization/processing, and GRP94-mediated peptide cross-presentation were examined using DC2.4 mouse dendritic cells.

Working concentrations of RAP and GRP94.NTD were determined experimentally. RAP titrations reveal that DC2.4 cells bind RAP with a binding isotherm approximates the expected rectangular hyperbola (Figure 20a). In contrast, GRP94.NTD binding was linear at concentrations up to 100 μg/mL, suggesting that GRP94.NTD interacts with low-affinity/high-capacity binding sites on DC2.4 cells (Figure 20b). All experiments conducted with DC2.4 cells utilize 10 μg/mL GRP94.NTD unless otherwise stated.

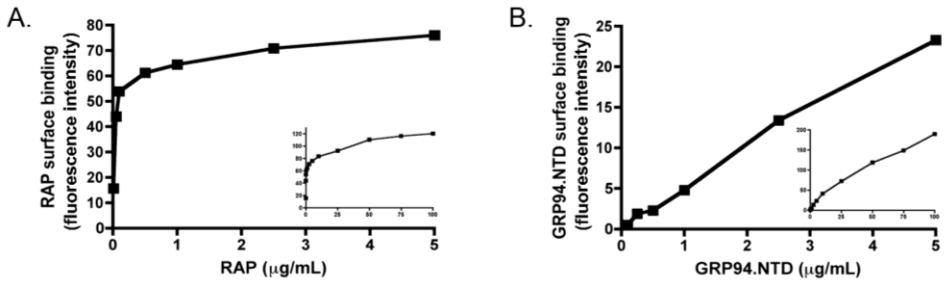

Figure 20: Binding characteristics of RAP and GRP94.NTD to DC2.4 cells.

DC2.4 cells were incubated with increasing concentrations of RAP (A) or GRP94.NTD (B). Cells were subsequently washed and analyzed by flow cytometry. Insets: extended binding titrations (0-100 μg/mL) of the respective ligand.

To examine if CD91 contributes to GRP94.NTD surface binding on DC2.4 cells, a binding competition assay was conducted. DC2.4 cells were incubated with GRP94.NTD in the absence or presence of the CD91 ligands RAP and α_2M*. As a control, GRP94.NTD surface binding was also competed with native α_2M, which is not recognized by CD91. Similar to what was observed with the MEF-1 cells, GRP94.NTD surface binding was not reduced in the presence of these ligands (Figure 21a). This further demonstrates that CD91 does not directly contribute to GRP94.NTD surface binding.

To examine if CD91 facilitates GRP94.NTD internalization/processing by DC2.4 cells, an internalization competition assay was conducted. GRP94.NTD internalization/processing was unaffected by excess α_2M* and native α_2M after 60 min of internalization (Figure 21b). However, RAP modestly reduced the overall GRP94.NTD

signal by approximately 15%. Because CD91 does not contribute to GRP94.NTD binding or internalization in MEF-1 cells, these data suggest that CD91 may influence GRP94.NTD internalization/processing through a pAPC-restricted mechanism.

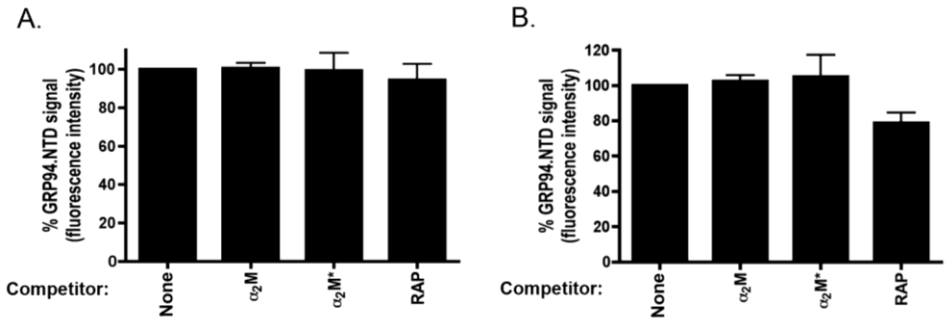

Figure 21: CD91 ligands do not repress GRP94.NTD surface binding; RAP modestly inhibits GRP94.NTD internalization/processing by DC2.4 cells.

A. DC2.4 cells were incubated with 10 μg/mL GRP94.NTD in the presence or absence of 300 μg/mL native α_2M, 300 μg/mL α_2M*, or 50 μg/mL RAP for 30 min on ice. Cells were then washed, and analyzed by flow cytometry.
B. DC2.4 cells were prepared as in A, and then incubated at 37°C in the presence or absence of 300 μg/mL native α_2M, 300 μg/mL α_2M*, or 50 μg/mL RAP for 60 min.

As specified in the introduction, there is precedence for a model whereby ligand binding to CD91 can modulate downstream signaling events without influencing ligand binding at the cell surface (Takayama et al., 2005; Takayama and Takezawa, 2006). Therefore, to determine if CD91 ligands influence GRP94-mediated peptide cross-presentation, cross-presentation studies were conducted using OT-1 splenocytes. OT-1 mice express a transgenic MHCI-restricted TCR that recognizes the $OVA_{257–264}$

(SIINFEKL) peptide in the context of an H-2K^b MHCI receptor. Therefore, to examine the ability of GRP94 to cross-present peptides, GRP94 was complexed with SIINFEKL and then incubated with DC2.4 cells, which express H-2K^b haplotype.

GRP94.NTD/SIINFEKL complexes were generated by heat-shocking GRP94.NTD in the presence of 50-fold molar excess free SIINFEKL peptide at 50°C for 10 min. After resting at room temperature for an additional 30 min, un-complexed SIINFEKL was removed by spin-concentration through a size exclusion membrane (Suto and Srivastava, 1995). To confirm the immunogenicity of the complex, DC2.4 cells were pulsed with GRP94.NTD/SIINFEKL for 4 hours at 37°C. Cells were then washed to remove any residual GPR94.NTD/SIINFEKL complex, and incubated with freshly isolated OT-1 splenocytes. CTL activity was assayed 24 hours later by monitoring IFN-γ secretion. As can be seen in figure 22a, DC2.4 cells dosed with GRP94.NTD/SIINFEKL activated OT-1 splenocytes in a dose-dependent manner.

Previous works have shown that as little as 10-fold excess CD91 ligand can profoundly inhibit GRP94/peptide cross-presentation by RAW264.7 mouse macrophage-like cells (Binder et al., 2000; Binder and Srivastava, 2004). However, neither 50 μg/mL RAP nor 300 μg/mL α_2M* inhibited GRP94.NTD/SIINFEKL cross-presentation in the

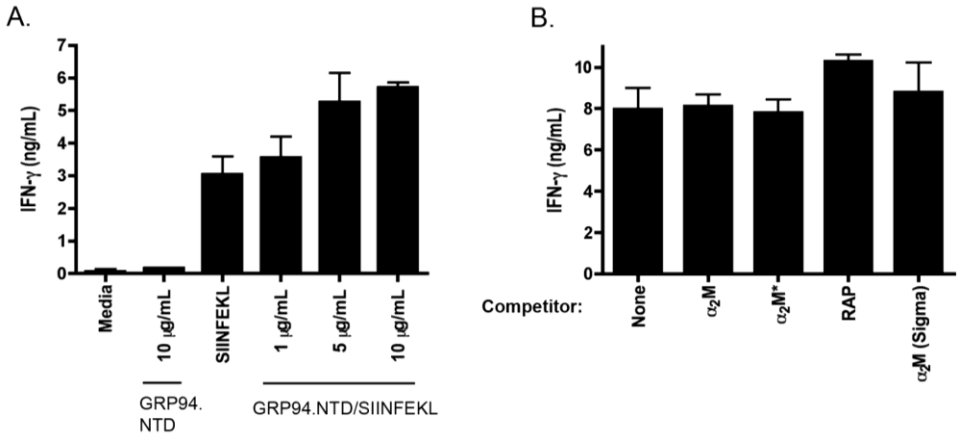

Figure 22: CD91 ligands do not reduce GRP94.NTD/SIINFEKL cross-presentation by DC2.4 cells.

A. DC2.4 cells were pulsed with media only, 10 μg/mL un-complexed GRP94.NTD, 5 μM SIINFEKL peptide, or increasing concentrations of GRP94.NTD/SIINFEKL complex for 4 hours at 37°C. Cells were then rinsed and incubated with OT-1 splenocytes for 24 hours. IFN-γ secretion was quantified by ELISA. B. DC2.4 cells were pulsed with 10 μg/mL GRP94.NTD/SIINFEKL complex in the absence or presence of 300 μg/mL native α_2M, 300 μg/mL α_2M*, 50 μg/mL RAP, or 300 μg/mL α_2M (Sigma) for 4 hours at 37°C. DC2.4 cells were then rinsed and incubated with OT-1 splenocytes for 24 hours. IFN-γ secretion was quantified by ELISA. Error bars indicate SD of triplicate measurements. Data are representative of three independent experiments.

DC2.4/OT-1 system (Figure 22b). Competition with 300 μg/mL native α_2M also had no significant effect.

These studies were also conducted using a commercial source (Sigma) of native α_2M that was shown to inhibit GRP94-mediated peptide cross-presentation in previously published works (Binder et al., 2000; Binder and Srivastava, 2004). Although

these previous works specify that Sigma α_2M contains "some activated form," no α_2M* was detected in freshly resuspended Sigma α_2M by silver staining (Figure 9). Furthermore, 300 μg/mL α_2M (Sigma) did not inhibit GRP94/SIINFEKL cross-presentation by DC2.4 cells (Figure 22b).

While these data are inconsistent with an ability of CD91 to facilitate GRP94-mediated peptide cross-presentation by DC2.4 cells, previous publications have suggested that SIINFEKL should not be utilized for cross-presentation studies (Binder and Srivastava, 2004). Because soluble SIINFEKL can be bound by empty MHCI receptors at the cell surface, there is concern that GRP94.NTD/SIINFEKL complexes could charge surface MHCI receptors independently of cross-presentation. This notion is inconsistent with the observation that GRP94.NTD/peptide complexes generated by heat-shock are remarkably stabile (Blachere et al., 1997; Suto and Srivastava, 1995; Vogen et al., 2002; Wearsch and Nicchitta, 1997). Therefore, it is unlikely that GRP94.NTD/SIINFEKL complexes can donate SIINFEKL peptide independently of intracellular processing. A more likely concern with the use of GRP94.NTD/SIINFEKL complexes is the presence of free, un-complexed SIINFEKL.

To address this concern, GRP94.NTD/SIINFEKL complexes were extensively dialyzed against PBS. Even though dialysis would have reduced any free SIINFEKL by 20,000 fold, there were no differences between the ability of pre- and post-dialyzed

samples to stimulate OT-1 splenocytes (data not shown). This lack of difference demonstrates that the ability of GRP94.NTD/SIINFEKL to stimulate OT-1 splenocytes is not due to free SIINFEKL peptide.

To further address the concern of surface-charging, cross-presentation studies were conducted with an alternate ovalbumin-based peptide: ova20 (SGLEQLESIINFEKLTEWTS). Unlike SIINFEKL, ova20 must be trimmed to an appropriate length before being loaded onto MHCI receptors. Therefore, cross-presentation of ova20 necessitates both internalization and processing. GRP94.NTD was complexed to ova20 by heat-shock and dialyzed against PBS to remove any un-complexed ova20. DC2.4 cells were pulsed with GRP94.NTD/ova20, rinsed, and incubated with OT-1 splenocytes. DC2.4 cells pulsed with GRP94.NTD/ova20 activated OT-1 splenocytes in a dose-dependent manner (Figure 23a). Despite the fact that GRP94.NTD/ova20 must be processed by DC2.4 cells in order to activate OT-1 splenocytes, GRP94.NTD-mediated ova20 cross-presentation was not significantly reduced by excess RAP, α_2M*, or native α_2M (Figure 23b). These results are identical to what was observed with the GRP94.NTD/SIINFEKL complexes, and suggest that CD91 does not significantly influence GRP94.NTD/peptide cross-presentation in the DC2.4/OT-1 system.

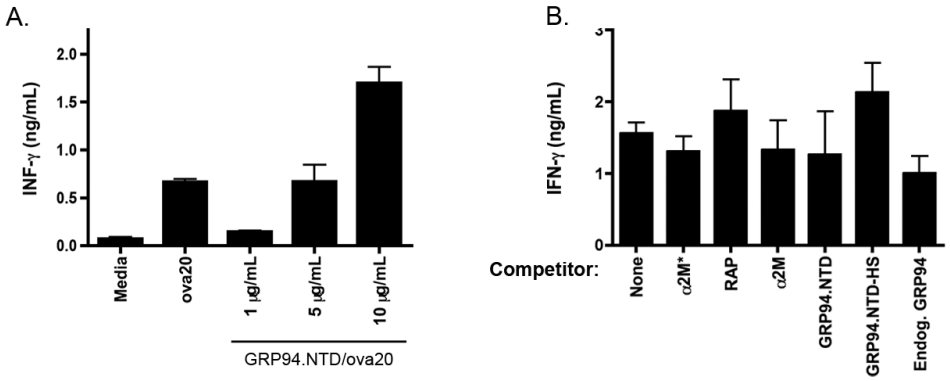

Figure 23: CD91 ligands do not inhibit GRP94.NTD/ova20 cross-presentation by DC2.4 cells.

A. DC2.4 cells were pulsed with media only, 4.6 μM ova20 peptide, or increasing concentrations of GRP94.NTD/ova20 complex for 4 hours at 37°C. Cells were then rinsed and then incubated with OT-1 splenocytes for 24 hours. IFN-γ secretion was quantified by ELISA. B. DC2.4 cells were pulsed with 10 μg/mL GRP94.NTD/ova20 complex in the absence or presence of 300 μg/mL α_2M*, 500 μg/mL RAP, 300 μg/mL native α_2M, 500 μg/mL GRP94.NTD, 500 μg/mL heat-shocked GRP94.NTD (GRP94.NTD-HS), or 500 μg/mL endogenous (Endog.) GRP94 for 4 hours at 37°C. DC2.4 cells were then rinsed and incubated with OT-1 splenocytes for 24 hours. IFN-γ secretion was quantified by ELISA. Error bars indicate mean SD of duplicate measurements. Data are representative of two independent experiments.

As an additional control, excess un-complexed GRP94.NTD and excess endogenous GRP94 were included in the cross-presentation assay. Because GRP94-mediated peptide cross-presentation has been reported to occur through receptor-mediated endocytosis (RME), it was expected that GRP94-mediated ova20 cross-presentation would be significantly diminished in the presence of 50-fold molar excess GRP94.NTD or 50-fold molar excess endogenous GRP94. However, neither of these

ligands inhibited GRP94.NTD/ova20 cross-presentation. This indicates that DC2.4 cells can internalize GRP94.NTD/ova20 through a non-RME mechanism such as fluid-phase uptake.

To distinguish between the RME- and fluid phase-mediated components of GRP94.NTD internalization, a modified internalization competition was conducted. Unlike the previously described internalization competition experiments, which measured a single round of receptor-mediated endocytosis, these experiments did not include a pre-incubation step. Instead, labeled GRP94.NTD was placed directly in the internalization buffer and DC2.4 cells were allowed to continuously internalize GRP94.NTD at 37°C for either 5 or 20 min. Endocytosis was then arrested by the addition of ice cold buffer. As a control, these experiments were first conducted using RAP, which is known to be primarily internalized via RME. As can be observed in figure 24a, 10-fold excess unlabeled RAP inhibited labeled RAP internalization/processing by 80% after 5 min of internalization. An identical inhibition was observed after 20 min of internalization (data not shown). These data confirm that DC2.4 cells internalize extracellular RAP almost exclusively through RME.

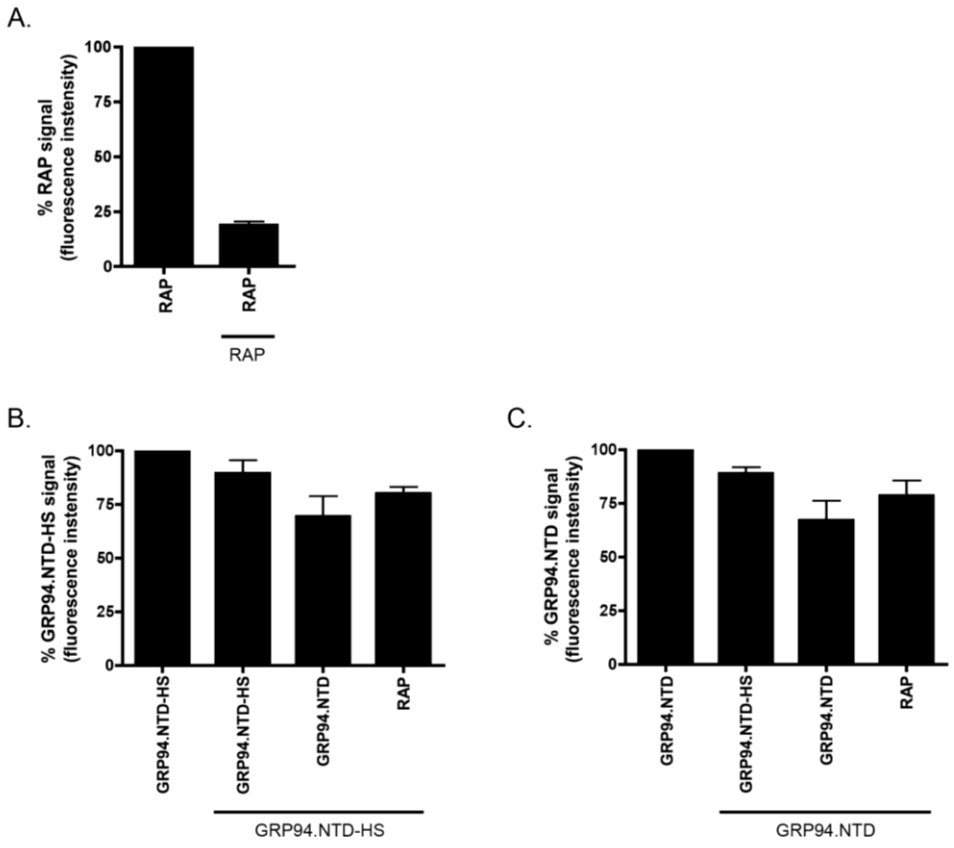

Figure 24: DC2.4 cells internalize GRP94.NTD and GRP94.NTD-HS through both receptor-mediated and fluid phase endocytosis.

A. DC2.4 cells were incubated with 10 μg/mL RAP in the absence or presence of 100 μg/mL unlabeled RAP for 5 min. B & C. DC2.4 cells were incubated with either 10 μg/mL GRP94.NTD (B) or 10 μg/mL GRP94.NTD-HS (C) in the absence or presence of 250 μg/mL GRP94.NTD, 250 μg/mL GRP94.NTD-HS, or 100 μg/mL RAP for 5 min. Cells were then placed on ice to arrest endocytosis, rinsed with cold buffer, and subsequently analyzed by flow cytometry. Samples were normalized to their respective no competitor controls. Data and error bars indicate SD of two experiments.

In contrast, 25-fold excess unlabeled GRP94.NTD only inhibited labeled GRP94.NTD internalization/processing by 40% after 5 min of internalization (Figure 24b). An identical inhibition was observed after 20 min of internalization (data not shown). These data are dramatically different from what was observed for RAP internalization, and suggest that DC2.4 cells internalize >50% of GRP94.NTD through fluid-phase uptake.

Because the GRP94.NTD/peptide complexes were generated by heat-shock, which creates a complex mixture of GRP94.NTD oligomers (Figure 11), both the cross-presentation and modified internalization competition experiments were conducted using heat-shocked GRP94.NTD (GRP94.NTD-HS). Similar to what was observed with GRP94.NTD, GRP94.NTD-mediated ova20 cross-presentation was not inhibited by 50-fold molar excess GRP94.NTD-HS (Figure 23b). In the modified internalization assay, GRP94.NTD-HS internalization was only marginally inhibited by unlabeled GRP94.NTD-HS (Figure 24c). This suggests that DC2.4 cells internalize >70% of extracellular GRP94.NTD-HS by fluid-phase uptake during the first 5 min of endocytosis. An identical inhibition was observed after 20 min of internalization (data not shown). Interestingly, unlabeled monomeric GRP94.NTD was more efficient at competing for GRP94.NTD-HS uptake than GRP94.NTD-HS itself (40% vs. 20%). This is most likely due to the fact that GRP94.NTD-HS samples contain some lower-order

GRP94.NTD oligomers that could be more readily competed by monomeric GRP94.NTD.

Ten-fold RAP inhibited both GRP94.NTD and GRP94.NTD-HS internalization by approximately 20%. This is similar to what was observed with the internalization competition studies presented earlier (Figure 21b), suggesting that CD91 may indirectly modulate to GRP94.NTD internalization/processing in DC2.4 cells. Further studies are required to determine if this is the case.

In summary, previous studies have shown that various CD91 ligands can inhibit GRP94-mediated cross-presentation. However, the data presented in this section demonstrate that neither RAP nor α_2M* inhibited GRP94.NTD binding to DC2.4 cells. RAP modestly reduced GRP94.NTD internalization/processing by DC2.4 cells, suggesting that CD91 may indirectly influence GRP94.NTD internalization/processing by DC2.4 cells. However, both RAP and α_2M* failed to significantly inhibit the cross-presentation of GRP94.NTD/SIINFEKL and GRP94.NTD/ova20 complexes in the DC2.4/OT-1 system. This demonstrates that CD91 does not significantly contribute to GRP94.NTD-mediated peptide cross-presentation by DC2.4 cells. Combined with the modified internalization competition experiments, these studies also demonstrate that DC2.4 cells can internalize and process significant amounts of GRP94.NTD and GRP94.NTD/peptide complexes through fluid-phase endocytosis.

Chapter 4: Identification of cell surface heparan sulfate proteoglycans (HSPGs) as a novel class of GRP94 surface binding sites

In order to conduct the binding competition studies outlined in chapter 3, it was essential to determine how much RAP and GRP94.NTD were necessary to saturate cell surface receptors. To this end, binding titrations were used to characterize the interactions of RAP and GRP94.NTD with MEF-1 and PEA-13 cells. RAP displayed high-affinity, saturable binding to MEF-1 cells, with the binding isotherm approximating the expected rectangular hyperbola (Figure 25a, b). In contrast, GRP94.NTD binding was linear at concentrations up to 25 μg/ml, and essentially linear up to 100 μg/ml (Figure 25c, d). These titrations suggest that GRP94.NTD interacts with low-affinity/high-capacity binding sites on MEF-1 and PEA-13 cells.

The GRP94.NTD binding characteristics are similar to the low-affinity/high-capacity binding interactions observed for numerous cell surface heparan sulfate proteoglycan (HSPG) ligands. Cell surface HSPGs are ubiquitously expressed, structurally diverse proteoglycans that consist of highly heterogeneous, sulfated polysaccharide side chains attached to one of various core proteins (Figure 5). Interestingly, it is well established that GRP94 interacts heparin, a macromolecules that is structurally similar to HSPG polysaccharide side chains (Menoret and Bell, 2000; Reed et al., 2002; Riera et al., 1999). Because heparin-binding is also a common feature of

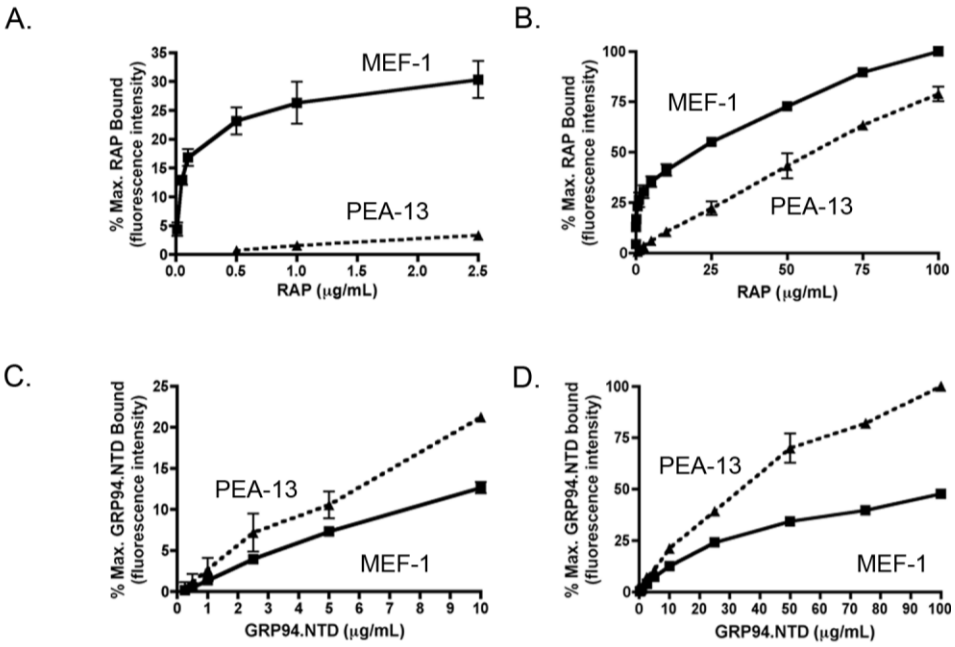

Figure 25: Binding characteristics of RAP and GRP94.NTD to MEF-1 and PEA-13 cells.

MEF-1 and PEA-13 cells were incubated with increasing concentrations of RAP (A and B) and GRP94.NTD (C and D). Cells were subsequently washed and analyzed by flow cytometry. Samples were normalized to highest signal of each titration. Error bars indicate the SD of three experiments.

HSPG-binding proteins, I hypothesized that GRP94.NTD could interact with cell surface HSPGs on MEF-1 and PEA-13 cells.

In this chapter, I identify cell surface HSPGs as a previously unknown class of GRP94.NTD binding sites. I show that disruption of HSPG surface structures results in a marked decrease in GRP94.NTD surface binding to both MEF-1 and PEA-13 cells, but

not RAW264.7 macrophage and DC2.4 dendritic cells. Although this suggests that GRP94.NTD binds a specific class of HSPG that is not expressed by RAW264.7 cells, further investigations suggest that GRP94.NTD interacts with a more than one class of cell surface HSPGs. Together these studies imply that GRP94-HSPG interactions are mediated by the HSPG glycosaminoglycan (GAG) side chains rather than the expression of an individual core protein.

A. HSPGs mediate GRP94.NTD surface binding to MEF-1 and PEA-13 cells

To determine whether cell surface HSPGs contribute to GRP94.NTD surface binding on MEF-1 and PEA-13 fibroblasts, three experimental approaches were used. First, as a means of disrupting HSPG-dependent surface interactions, MEF-1 and PEA-13 cells were placed on ice and incubated with increasing concentrations of heparin. Cells were then washed and examined for GRP94.NTD and RAP binding activity using flow cytometry. As shown in figure 26a, heparin treatment effectively reduced GRP94.NTD surface binding to both MEF-1 and PEA-13 cells. The heparin-dependent inhibition of GRP94.NTD binding was saturable, with near-maximal inhibition occurring at 10 μg/ml heparin. In contrast, RAP binding was insensitive to heparin treatment, even at heparin concentrations two orders of magnitude higher than those needed to inhibit GRP94.NTD binding (Figure 26b).

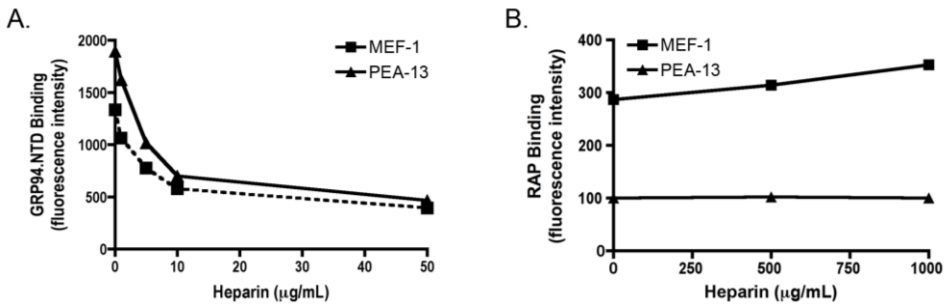

Figure 26: Heparin treatment reduces GRP94.NTD surface binding to MEF-1 and PEA-13 cells.

MEF-1 and PEA-13 cells were incubated with increasing concentrations of soluble heparin, washed, incubated with 25 μg/mL GRP94.NTD (A) or 10 μg/mL RAP (B), and analyzed by flow cytometry. Data presented are representative of two independent replicates.

In an alternative experimental approach, MEF-1 and PEA-13 cells were treated with sodium chlorate. Sodium chlorate competitively inhibits the formation of the cellular sulfate donor 3'-phosphoadenosine 5'-phosphosulfate (PAPS), and thereby reduces the sulfation of HSPG GAG chains during their biosynthesis (Baeuerle and Huttner, 1986; Burnell and Roy, 1978; Conrad, 1998; Farley et al., 1978; Keller et al., 1989). After culturing cells in sodium chlorate-supplemented media for 24 hours, GRP94.NTD and RAP binding were examined by flow cytometry. This treatment resulted in a nearly complete loss of GRP94.NTD binding activity to both MEF-1 and PEA-13 cells, but had no significant effect on RAP binding (Figure 27a). Following sodium chlorate treatment, a substantial (>90%) reduction in HSPG sulfation was

confirmed using the monoclonal anti-heparan sulfate antibody 10E4 (Figure 27b). 10E4 showed significantly higher binding than the IgM isotype control (Figure 27c).

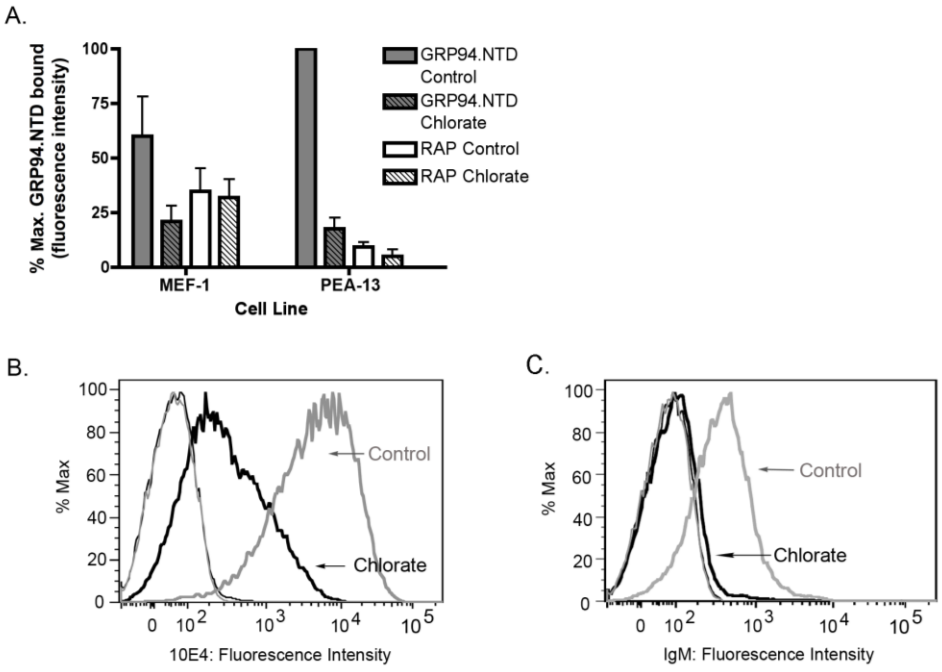

Figure 27: MEF-1 and PEA-13 cells incubated with sodium chlorate bind significantly less GRP94.NTD.

A. MEF-1 and PEA-13 cells were grown in the absence (solid) or presence (striped) of 20 mM sodium chlorate. Cells were incubated with 25 μg/mL GRP94.NTD (grey) or 10 μg/mL RAP (white), washed, and analyzed by flow cytometry. Error bars indicate SD of triplicate measurements.
B & C. To confirm that sodium chlorate treatment reduced HSPG sulfation, MEF-1 cells were incubated with the anti-heparan sulfate antibody 10E4 (B) or an IgM isotype control (C). Cells were then washed, incubated with a fluorescent secondary, and analyzed by flow cytometry: unstained cells (thin lines), stained cells (bold lines), un-treated control cells (grey), and sodium chlorate-treated cells (black).

Lastly, MEF-1 and PEA-13 cells were incubated with 0.01 IU/mL heparinase II, which specifically cleaves sulfated GAG chains. Cells were then washed, placed on ice, and assayed for GRP94.NTD and RAP surface binding. Similar to what was seen with the sodium chlorate treatment, digestion of MEF-1 and PEA-13 cells with heparinase II resulted in a substantial reduction in GRP94.NTD binding at all concentrations examined (Figure 28a). It did not, however, alter RAP binding to MEF-1 cells (Figure 28b). A substantial (>90%) decrease in cell surface HSPG sulfation was confirmed using the anti-heparan sulfate antibody 10E4 (Figure 28c). 10E4 showed significantly higher binding than the IgM isotype control (Figure 28d).

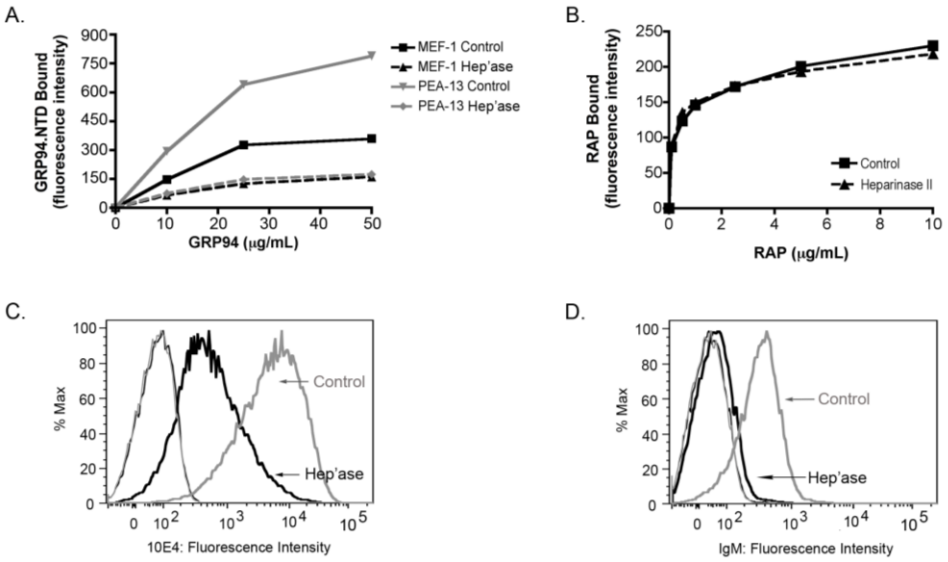

Figure 28: Heparinase II digestion of MEF-1 and PEA-13 cell significantly decreases GRP94.NTD surface binding.

A & B. MEF-1 and PEA-13 cells were incubated in the absence or presence of 0.01 IU/mL heparinase II (Hep'ase) for 90 min at 37°C. Cells were then washed, placed on ice, incubated with increasing concentrations of GRP94.NTD (A) or RAP (B), and analyzed by flow cytometry. C & D. To confirm efficient desulfation by heparinase II, MEF-1 cells were incubated with the anti-heparan sulfate antibody 10E4 (C) or an IgM isotype control (D). Cells were then washed, incubated with a fluorescent secondary, and analyzed by flow cytometry: unstained cells (thin lines), stained cells (bold lines), un-treated control cells (grey), and heparinase II-treated cells (black). All data presented are representative of three independent replicates.

B. GRP94.NTD interacts with multiple classes of cell surface HSPGs on MEF-1 cells

The aforementioned studies establish that GRP94.NTD interacts with cell surface HSPGs expressed by MEF-1 and PEA-13 cells. Although there is no precedence in the literature for an immunologically-important interaction between GRP94 and non-immune cells, it is well established that pAPCs are necessary for GRP94-mediated immune responses. Given that these immune cells also express cell surface HSPGs, experiments were conducted to investigate GRP94.NTD-HSPG interactions using RAW264.7 mouse macrophage-like cells.

To disrupt cell surface HSPG-dependent interactions, RAW264.7 cells were treated with heparin, sodium chlorate, and heparinase II. Similar to what was observed with the MEF-1 and PEA-13 fibroblast cell lines, heparin inhibited GRP94.NTD binding to RAW264.7 cells, with near-maximal inhibition occurring at 25 μg/ml heparin (Figure 29a). However, treatment with sodium chlorate or heparinase II did not significantly reduce GRP94.NTD or RAP binding to RAW264.7 cells (Figure 29b, c).

These studies demonstrate that RAW264.7 and MEF-1 cells differ in their ability to bind GRP94.NTD via cell surface HSPGs. This suggests that MEF-1 cells express more cell surface HSPGs than RAW264.7 cells, or that MEF-1 cells express a specific class of cell surface HSPGs that are not expressed by RAW264.7 cells. To test the first hypothesis,

heparan sulfate expression was quantified using the anti-heparan sulfate antibody 10E4. As can be seen in figure 30, MEF-1 cell bound significantly more 10E4 than RAW264.7 cells, indicating that MEF-1 cells express substantially more cell surface HSPGs than RAW264.7 and DC2.4 cells.

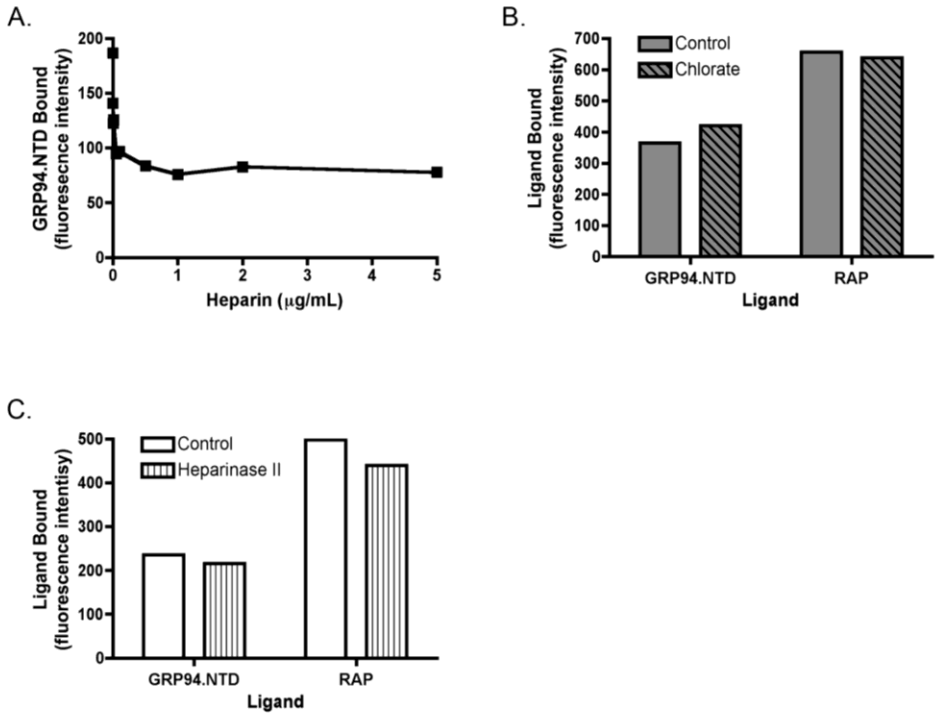

Figure 29: Modulation of HSPGs surface structures does not significantly affect GRP94.NTD binding to RAW264.7 cells.

A. RAW264.7 cells were incubated with increasing concentrations of soluble heparin, washed, incubated with 25 μg/mL GRP94.NTD, and analyzed by flow cytometry. B. RAW264.7 cells were grown in the absence (solid) or presence (striped) of 20 mM sodium chlorate. Cells were incubated with 25 μg/mL GRP94.NTD or 10 μg/mL RAP, washed, and analyzed by flow cytometry. C. RAW264.7 cells were incubated in the absence or presence of 0.01 IU/mL heparinase II for 90 min at 37°C. Cells were then washed, incubated with 25 μg/mL GRP94.NTD or 10 μg/mL RAP, and analyzed by flow cytometry.

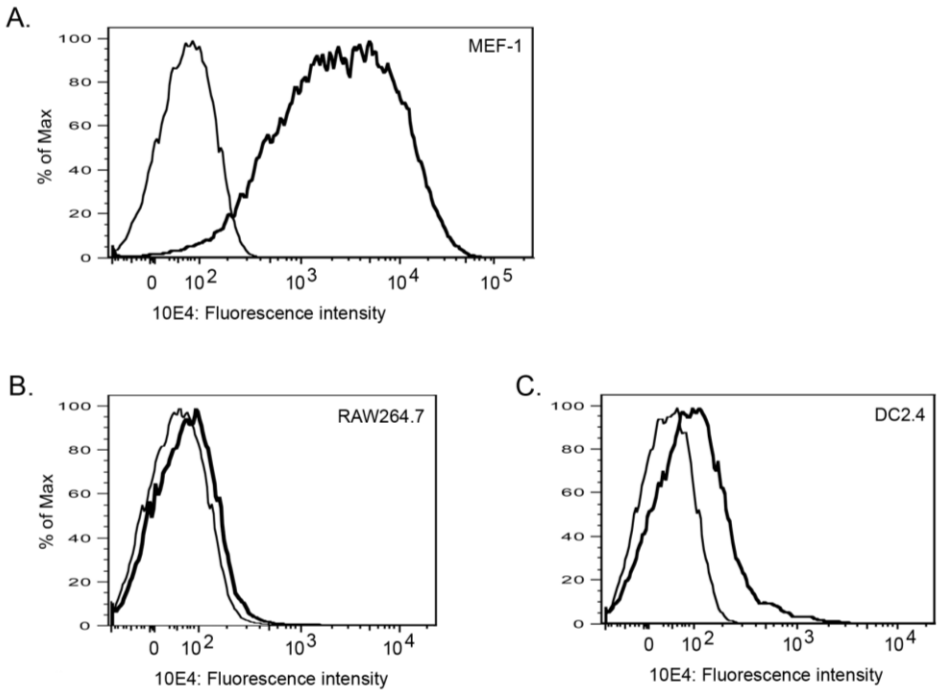

Figure 30: Comparison of cell surface HSPG expression levels by MEF-1, RAW264.7, and DC2.4 cells.

MEF-1 (A), RAW264.7 (B), and DC2.4 (C) cells were incubated with the anti-heparan sulfate antibody 10E4, washed, incubated with a fluorescent secondary, and analyzed by flow cytometry: unstained cells (thin lines) and stained cells (bold lines).

Alternately, but not exclusively, GRP94.NTD may bind a specific class of cell surface HSPG that is expressed by MEF-1 cells, but not RAW264.7 cells. Of the four classes of cell surface HSPGs, only syndecans and glypicans continuously bear heparan sulfate in their side chains. For this reason, MEF-1 and RAW264.7 cells were examined for difference in syndecan and glypican expression using RT-PCR. mRNA was isolated from MEF-1 and RAW264.7 cells, reverse transcribed, and then analyzed for the

expression of syndecan (Sdc) 1-4, and glypicans (Gpc) 1-6 using previously published primer sets. While MEF-1 and RAW264.7 cells share expression of several cell surface HSPG core proteins, RAW264.7 cells were deficient in *Gpc4* and *Gpc6* expression (Table 1, Figure 31). This suggested that Gpc4 and Gpc6 may be responsible for the high level of HSPG -dependent GRP94.NTD binding by MEF-1 cells.

Unlike other cell surface HSPGs, glypicans are tethered to the cell membrane via a glycosylphosphatidylinisotol (GPI) anchor (Figure 5). To further examine the contribution of glypicans to HSPG-dependent GRP94.NTD binding, MEF-1 cells were treated with PI-PLC, an enzyme that cleaves GPI-anchored proteins. Following digestion with 0.05 units/mL PI-PLC for 45 min at 37°C, cells were examined for GRP94.NTD surface binding activity. Compared to the un-digested control cells, PI-PLC digestion reduced GRP94.NTD binding by 35% and 10E4 binding by 25% (Figure 32). 10E4 showed significantly higher binding than the IgM isotype control (data not shown). Digestion with 0.5 units/mL PI-PLC reduced GRP94.NTD and 10E4 binding to a similar extent, indicating that 0.05 U PI-PLC had completely digested GPI-anchored surface proteins (data not shown). Even though numerous proteins contain GPI anchors, the observed 35% decrease in GRP94.NTD binding was significantly less than the 60% decrease observed following sodium chlorate and heparinase II treatments (Figure 27).

This strongly suggests that while glypicans may bind GRP94.NTD on MEF-1 cells, they are not the only class of cell surface HSPGs that interact with GRP94.NTD.

Table 1: Syndecan (Sdc) and glypican (Gpc) messages expressed by MEF-1 and RAW264.7 cells.

HSPG:	Gpc1	Gpc2	Gpc3	Gpc4	Gpc5	Gpc6	Sdc1	Sdc2	Sdc3	Sdc4
MEF-1	+	-	+	**+**	**-**	**+**	+	-	+	+
RAW264.7	+	-	+	**-**	**-**	**-**	+	-	+	+

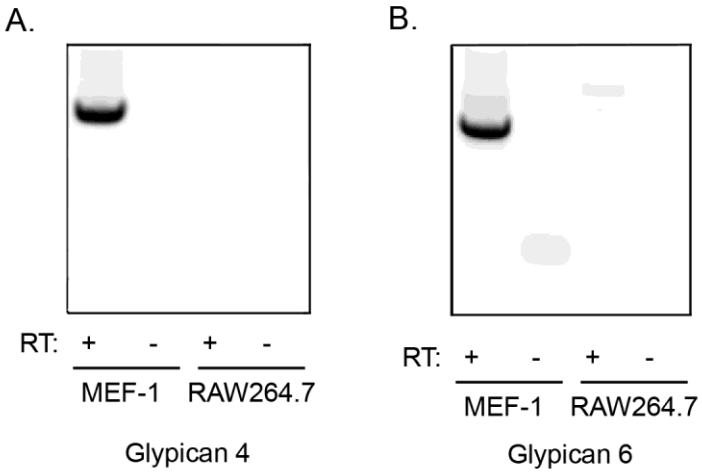

Figure 31: MEF-1 and RAW264.7 cells differ in *Gpc4* and *Gpc6* expression.

Total RNA samples were isolated from MEF-1 and RAW264.7 cells, and cell surface HSPG mRNA expression was determined via RT-PCR. MEF-1 and RAW264.7 cells were found to differ significantly in the expression of *Gpc4* (A) and *Gpc6* (B). All samples were tested for DNA contamination using a paired transcriptase-deficient (RT -) reaction, and were examined for off-target effects to 18S rRNA (data not shown).

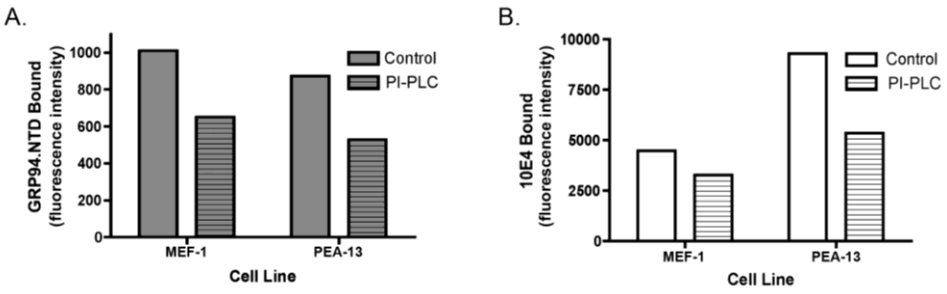

Figure 32: PI-PLC digestion partially inhibits GRP94.NTD surface binding to MEF-1 cells.

MEF-1 and PEA-13 cells were incubated in the absence (solid) or presence (striped) 0.05 units/mL PI-PLC for 45 min at 37°C. Cells were then incubated with GRP94.NTD (A) or 10E4 (B). Samples stained with 10E4 were rinsed and incubated with a fluorescent secondary prior to analysis by flow cytometry.

In summary, these studies demonstrate that cell surface HSPGs are responsible for a significant portion of GRP94.NTD binding to MEF1 and PEA-13 cells, but not RAW264.7 or DC2.4 cells. Although MEF-1 and RAW264.7 cells differ in *Gpc4* and *Gpc6* expression, PI-PLC digestion of MEF-1 cells suggests that GRP94.NTD interacts with multiple classes of cell surface HSPGs. Additionally, because GRP94.NTD binding is decreased following treatment with sodium chlorate and heparinase II, it is likely that GRP94.NTD preferentially interacts with cell surface HSPG side chains rather than a specific cell surface HSPG core protein.

Chapter 5: Discussion

A. Overview

The ability of CD91 to function as a GRP94 endocytic receptor was examined in the context of GRP94.NTD surface binding, endocytosis, and intracellular processing. Using previously characterized CD91+/+ and CD91-/- mouse embryonic fibroblast (MEF) cell lines, I demonstrate that CD91 expression was required for the surface binding and endocytic uptake of the CD91 ligand RAP, but not GRP94.NTD. These data are inconsistent with a role for CD91 in GRP94.NTD endocytosis, and strongly suggest that CD91 does not directly bind or internalize GRP94.NTD.

The ability of CD91 to indirectly affect GRP94-mediated peptide cross-presentation was examined in the context of a pAPC cell line. Using DC2.4 mouse dendritic cells, I demonstrate that CD91 ligands do not inhibit GRP94.NTD binding to DC2.4 cells. However, RAP modestly inhibited GRP94.NTD internalization/processing, suggesting that CD91 may indirectly effect GRP94.NTD internalization/processing by an indirect post-uptake mechanism. To further examine this possibility, the ability of CD91 to modulate GRP94.NTD-mediated peptide cross-presentation was examined. Using the DC2.4/OT-1 system, I demonstrate that CD91 ligands RAP and activated α2-macroglobulin (α2M*) did not significantly inhibit GRP94.NTD/peptide cross-

presentation. I also demonstrate that that DC2.4 cells internalize heat-shocked GRP94.NTD via fluid-phase uptake.

Finally, I identify cell surface HSPGs as a novel class of GRP94 binding sites on MEF cells. This conclusion was established using three distinct experimental approaches. While the biological significance of this interaction remains unknown, cell surface HSPGs do not significantly contribute to GRP94.NTD surface binding to RAW264.7 or DC2.4 cells. Additional studies suggest that the interaction between GRP94.NTD and cell surface HSPGs is mediated through the heparan sulfate GAG chains rather than requiring the expression of a specific class of cell surface HSPG.

In the following section, I will discuss the ramifications of my research, including: 1) a re-evaluation of CD91-mediated GRP94.NTD internalization, and 2) the identification of cell surface HSPGs as GRP94.NTD binding sites. This will be followed by a brief discussion of how cell surface HSPGs may contribute to GRP94.NTD-mediated immune responses.

B. Examination of GRP94.NTD-CD91 interactions at the cell surface: GRP94.NTD binds cells independently of CD91 expression

To determine if CD91 functions as an endocytic receptor for GRP94, I first examined if CD91 directly binds GRP94.NTD at the cell surface. As demonstrated in chapter 3, GRP94.NTD surface binding was not reduced in MEF-1 cells that had been treated with CD91-directed siRNA. Additionally, GRP94.NTD surface binding was not reduced in the paired PEA-13 cell line, which is genetically deficient in CD91 expression. Reduction/deletion of CD91 expression did, however, significantly reduce RAP surface binding. Furthermore, GRP94.NTD binding to MEF-1 cells was not significantly reduced by excess RAP, a universal CD91 ligand binding inhibitor. The CD91 ligands RAP and α_2M* were also unable to significantly inhibit GRP94.NTD binding to DC2.4 mouse dendritic cells. Together, these studies show that CD91 expression does not correlate with GRP94.NTD surface binding, and that CD91 ligands do not significantly compete with GRP94.NTD for occupation of surface receptors. This suggests that CD91 does not directly bind GRP94.NTD at the cell surface.

These findings are in agreement with several past reports concluding that CD91 does not contribute to the surface recognition of GRP94, calreticulin, or Hsp70 (Berwin et al., 2002a; Theriault et al., 2005; Walters and Berwin, 2005). Experiments conducted by Berwin et al. and Binder and Srivastava demonstrated that neither 100-fold molar excess

RAP nor 100-fold molar excess α_2M* significantly reduced GRP94 binding to unfixed elicited peritoneal macrophages or unfixed RAW264.7 mouse macrophage-like cells, respectively (Berwin et al., 2002a; Binder and Srivastava, 2004). However, Binder and Srivastava claim that pre-fixation is necessary to prevent the rapid "measureable internalization" of CD91 while cells are incubated at 4°C. Following pre-fixation, 100-fold excess RAP and α_2M* partially (60%) inhibited GRP94 surface binding to fixed RAW264.7 cells (Binder and Srivastava, 2004). While pre-fixation may be necessary to stabilize highly dynamic CD91 surface interactions, studies conducted by the Nicchitta laboratory show no evidence of this rapid internalization of CD91. If cells internalize CD91 while on ice, surface-bound RAP should also rapidly internalize. However, data presented in chapters 2 and 3 establish that digestion with extracellular proteases significantly reduces the amount of RAP bound to MEF-1, RAW264.7, and DC2.4 cells. This strongly suggests that CD91 is not rapidly endocytosed by cells being incubated on ice, and that pre-fixation is not necessary to stabilize CD91 at the cell surface.

At present, I cannot reconcile the data presented in chapter 3 with some past reports. In particular, Binder and Srivastava claim that siRNA-mediated loss of CD91 expression blocks both GRP94 surface binding and GRP94-mediated peptide cross-presentation by RAW264.7 cells (Binder and Srivastava, 2004). While these data suggest that CD91 directly recognizes GRP94, it is not clear how the investigators obtained a

complete loss of CD91 expression. RAW264.7 cells are traditionally difficult to transfect, but can have an average plasmid transfection efficiency of up to 50% using specialized transfection reagents such as GenePORTER. Even with this level of transfection efficiency, a complete knock-down of CD91 expression would require selection of siRNA-positive cells. However, no selection process is reported. The authors also utilized an actin-directed siRNA to test for off-target effects, and report a complete knock-down of actin expression. Although cells treated with this actin-directed siRNA bound significantly less GRP94 than untransfected cells, this observation is never addressed. For these reasons, it is difficult to interpret the meaning of these siRNA-based studies.

C. Examination of GRP94.NTD internalization/processing pathways: MEF cells internalize RAP and GRP94.NTD via spatially and kinetically distinct routes

Previous studies have focused on the ability of CD91 to either bind GRP94 at the cell surface or to influence GRP94-mediated peptide cross-presentation. However, none of these studies thoroughly examined the ability of CD91 to facilitate GRP94.NTD internalization and/or processing. This is a crucial consideration when studying CD91 endocytic capacities because CD91 binding and internalization activities can function independently of each other. There are several examples where CD91 is not necessary for ligand binding to the cell surface, but is essential for ligand internalization and/or

metabolism (Mahley and Ji, 1999; Nykjaer and Willnow, 2002; Sarafanov et al., 2001). For example, Sarafanov et al. demonstrated that CD91 was necessary for the internalization and metabolism of coagulation factor VIII complexed to von Willebrand factor (fVIII-vWF), but did not contribute to fVIII-vWF surface binding. This suggests that fVIII-vWF initially binds a non-CD91 receptor at the cell surface, and is subsequently internalized via a CD91-dependent mechanism. Therefore, to fully examine the ability of CD91 to function as an endocytic receptor, it is necessary to specifically assess its contribution to ligand internalization.

To examine if CD91 facilitates GRP94.NTD endocytosis, I first compared the uptake kinetics and trafficking itineraries of RAP and GRP94.NTD. CD91 ligands are rapidly endocytosed and many are shunted to the lysosome (Krieger and Herz, 1994). Therefore, if CD91 functions in GRP94 endocytosis, GRP94.NTD and RAP should have similar uptake kinetics and trafficking itineraries. However, MEF-1 cells internalized GRP94.NTD and RAP via pathways that were kinetically and spatially distinct. This indicates that RAP and GRP94.NTD follow divergent mechanisms of uptake and intracellular sorting in MEF-1 cells. GRP94.NTD uptake kinetics were also nearly identical in MEF-1 and PEA-13 cells, thereby establishing that CD91 expression does not enhance GRP94.NTD internalization by MEF-1 cells. Consistent with these results, Berwin et al. demonstrated that GRP94 did not co-localize with an anti-CD91 antibody

seven minutes post-uptake, or with the CD91 ligand *Pseudomonas* exotoxin A 30 min post-uptake by RAW264.7 cells (Berwin et al., 2002a). Furthermore, several investigators have observed that, unlike most CD91 ligands, GRP94 does not traffic to the lysosome during the first 60 min of internalization (Berwin et al., 2002a; Singh-Jasuja et al., 2000b; Wassenberg et al., 1999).

Previous studies have demonstrated that CD91 can facilitate ligand internalization and metabolism without directly binding the ligand at the cell surface (reviewed in Mahley and Ji, 1999). For this reason, I examined the ability of CD91 to endocytose GRP94.NTD independently of surface binding. Cell surface CD91 molecules were blocked with RAP prior to GRP94.NTD surface binding, and excess unlabeled RAP was included in the internalization buffer. This ensured that empty, recycling CD91 molecules would be occupied with RAP instead of potentially interacting with surface-bound GRP94.NTD. These internalization competition studies demonstrate that continuous competition with RAP had no significant effect on either the quantity or rate of GRP94.NTD internalization/processing by MEF-1 cells. Together, these data strongly suggest that CD91 does not directly contribute to GRP94.NTD endocytosis.

D. Examination of GRP94-mediated peptide cross-presentation: GRP94.NTD/peptide complexes are internalized and processed through fluid-phase uptake.

Previous studies have shown that CD91 ligands can significantly inhibit GRP94-mediated peptide cross-presentation (Basu et al., 2001; Binder et al., 2000; Binder and Srivastava, 2004). Yet the surface binding and internalization/processing studies conducted with MEF-1 cells clearly demonstrate that CD91 does not directly bind or endocytose GRP94.NTD. How, then, could CD91 ligands influence GRP94-mediated peptide cross-presentation? Because cross-presentation is restricted to pAPCs, it is possible that CD91 could interact with surface receptors that are restricted to pAPCs. Alternately, CD91 could mediate downstream signaling pathways without contributing to ligand binding at the cell surface. For example, studies by Takayama et al. suggest that CD91 can indirectly influence PDGFR turnover and signaling by modulating c-Cbl activity (Takayama et al., 2005). This raises the possibility that CD91 could indirectly affect GRP94-mediated peptide cross-presentation through a post-uptake phenomenon.

To examine these possibilities, the ability of CD91 to bind, endocytose, and process GRP94.NTD was assessed using DC2.4 mouse dendritic cells. In surface binding studies, RAP and α_2M* did not compete with GRP94.NTD for surface binding. However, in internalization competition studies, RAP modestly inhibited GRP94.NTD internalization/processing after 60 min of internalization. This suggests that CD91 may

indirectly affect GRP94.NTD processing through a pAPC-specific, post-uptake mechanism. To examine this hypothesis, the ability of CD91 to influence GRP94-mediated peptide cross-presentation was assessed. In these cross-presentation studies, neither excess α_2M* nor excess RAP inhibited GRP94.NTD-mediated peptide cross-presentation. Together, these studies demonstrate that CD91 does not significantly contribute to GRP94.NTD surface binding, or to GRP94-mediated peptide cross-presentation in the DC2.4/OT-1 system. However, these experiments cannot exclude the possibility that CD91 influences GRP94.NTD internalization/processing independently of the MHCI cross-presentation pathway.

The results of these cross-presentation experiments are in agreement with several other reports. It has been previously shown that neither RAP nor α_2M* inhibit GRP94/SIINFEKL cross-presentation by RAW264.7 macrophage cells (Berwin et al., 2002a; Binder and Srivastava, 2004). However, because free SIINFEKL can directly charge empty MHCI receptors at the cell surface, it has been proposed that the SIINFEKL peptide should not be used to analyze GRP94-mediated peptide cross-presentation (Binder and Srivastava, 2004). While the potential for surface charging is a valid concern, previous publications have demonstrated that GRP94/peptide complexes generated by heat shock are extremely stable (Blachere et al., 1997; Suto and Srivastava, 1995; Vogen et al., 2002; Wearsch and Nicchitta, 1997). Furthermore, elicited peritoneal

macrophages that were incubated with GRP94/SIINFEKL on ice did not bind significant levels of the 25-D1.16 antibody, which specifically recognizes SIINFEKL in the context of H-2K^b MHCI receptor (Berwin et al., 2002a). Therefore, it is unlikely that these heat-shocked GRP94/SIINFEKL complexes can directly load surface MHCI molecules unless free SIINFEKL is present.

Two different approaches were utilized to formally address the concern about surface charging. First, GRP94.NTD/SIINFEKL complexes were dialyzed to remove any residual un-complexed SIINFEKL. Although this procedure would have reduced any potentially un-complexed SIINFEKL by 20,000-fold, pre- and post-dialyzed GRP94.NTD/SIINFEKL complexes stimulated DC2.4/OT-1 cells to the same extent. Second, the cross-presentation studies were also conducted using a 20 residue ovalbumin peptide (ova20) that cannot be directly loaded onto MHCI receptors. Even though ova20 cross-presentation requires GRP94.NTD/ova20 internalization and processing, RAP and α2M* did not inhibit GRP94.NTD/ova20 cross-presentation. Cumulatively, these studies illustrate that CD91 does not significantly contribute to GRP94.NTD-mediated peptide cross-presentation in the DC2.4/OT-1 system.

It is important to note that GRP94.NTD-mediated ova20 cross-presentation was not inhibited in the presence of 50-fold excess GRP94.NTD, heat-shocked GRP94.NTD

(GRP94.NTD-HS), or endogenous GRP94. Combined with the internalization competition experiments, these studies establish that DC2.4 cells can internalize and process GRP94.NTD/ova20 through a pathway other than receptor mediated endocytosis (RME). Therefore, while CD91 ligands do not reduce GRP94-mediated ova20 cross-presentation by DC2.4 cells, these studies cannot definitively exclude the possibility that CD91 contributes to GRP94.NTD-mediated peptide cross-presentation.

To determine if CD91 fractionally contributes to GRP94-mediated peptide cross-presentation, the present experimental system must be modified to eliminate/significantly reduce the fluid-phase uptake component of cross-presentation. This could be accomplished with various pharmacological compounds, such as dimethylamiloride or rottlerin. However, because many of these agents alter cellular functions other than fluid-phase endocytosis, the effect of these compounds on GRP94.NTD surface binding and internalization/processing would need to be carefully analyzed. Alternately, the fluid-phase uptake component of GRP94.NTD/peptide cross-presentation may be reduced by utilizing a GRP94-peptide fusion protein (see discussion below).

It was surprising to find that GRP94-mediated ova20 cross-presentation could occur through fluid phase uptake because several previous works have demonstrated

that GRP94-mediated peptide cross-presentation occurs primarily through RME. Notably, Singh-Jasuja et al. demonstrated that GRP94 derived from E1B-expressing RMA-S lymphocyte cells could activate E1B-specific CTL clones (Singh-Jasuja et al., 2000b). However, this cross-presentation was significantly reduced by two-fold excess RMA-S-derived GRP94. Later studies also demonstrated that both the scavenger receptor ligand fucoidan and the RME-inhibitor MDC could partially block GRP94-mediated peptide cross-presentation (Berwin et al., 2002a).

Although these studies provide evidence that GRP94-mediated peptide cross-presentation can occur through RME, the contribution of fluid-phase uptake to GRP94-mediated peptide cross-presentation has not been widely discussed. Several studies have observed that GRP94 can be internalized though fluid-phase endocytosis by elicited peritoneal macrophages and immature DCs (Berwin et al., 2002b; Wassenberg et al., 1999). Additionally, it is well established that pAPCs constitutively internalize exogenous ligand through fluid-phase uptake, and that exogenous antigens can access the cross-presentation pathway through this pathway (Brossart and Bevan, 1997; Norbury et al., 1995; Sallusto et al., 1995; Swanson and Watts, 1995). These observations further substantiate the cross-presentation and internalization studies outlined in chapter 3, and establish a role for fluid-phase endocytosis in GRP94.NTD-mediated peptide cross-presentation.

But is the contribution of fluid-phase uptake physiologically significant for GRP94-mediated peptide cross-presentation? Fluid phase endocytosis is an inefficient means of accessing the cross-presentation pathway, and generally requires large quantities of the soluble antigen (reviewed in Kovacsovics-Bankowski et al., 1993; Norbury et al., 1995; Rock et al., 1990; Rock and Shen, 2005). RME, on the other hand, is an extremely efficient means of accessing the cross-presentation pathway, and is capable of ligand recognition event at low concentrations. Therefore, in situations where there is a limited amount of necrotic cell death, RME would likely play a more prominent role *in vivo*. However, relatively high concentrations of GRP94 could be released into the extracellular environment following tissue injury or viral infection. Under these circumstances, fluid-phase uptake may play a significant role in GRP94-mediated peptide cross-presentation. Additional studies are required to determine the contribution of fluid-phase endocytosis to GRP94-mediated immune responses, as well as examine how GRP94-associated peptides are processed through both RME and fluid-phase internalization pathways.

Interestingly, the modified internalization competition assays demonstrate that the amount of GRP94.NTD internalized through RME is significantly greater than the amount of GRP94.NTD-HS internalized through RME. This suggests that DC2.4 cells preferentially internalize GRP94.NTD-HS through a fluid-phase pathway. These studies

also indicate that GRP94.NTD-HS surface binding and internalization are more efficiently competed by GRP94.NTD than the heat-shocked form itself. As displayed in figures 6 and 7, exposing GRP94.NTD to elevated temperatures results in the formation of higher-order GRP94.NTD oligomers. These heat-shocked complexes do, however, contain some monomeric and lower-order GR94.NTD oligomers that migrate similarly to un-heat-shocked GRP94.NTD on native PAGE. Therefore, if DC2.4 cells internalize the monomeric portion of GR94.NTD-HS through RME, this internalization would be more efficiently competed by GRP94.NTD.

Because the GRP94.NTD/peptide complexes utilized for these cross-presentation experiments were created by heat-shock, they also contain higher-order oligomers (Figure 11). If these higher-order GRP94.NTD/ova20 oligomers are preferentially cross-presented through a fluid-phase pathway, any subtle RME-dependent component of cross-presentation could be difficult to detect. This is especially important to consider because some particulate antigens are more efficiently cross-presented than soluble antigens (reviewed in Rock and Shen, 2005). To determine if these higher-order GRP94.NTD/peptide oligomers are preferentially cross-presented through a fluid-phase pathway, it would be necessary to individually examine the ability of monomeric and oligomeric GRP94/peptide complexes to mediate peptide cross-presentation. While separation of monomeric and oligomeric complexes could be accomplished through

ultracentrifugation, the recovery of monomeric GRP94.NTD/peptide complexes would be extremely low. It would be much more efficient to create a GRP94.NTD-peptide fusion protein with a SIINFEKL-containing region. GRP94.NTD-SIINFEKL fusions could be purified in a primarily monomeric form and heat-shocked to create higher-order oligomers. The cross-presentation capacities of monomeric and heat-shocked GRP94.NTD-SIINFEKL fusion proteins could then be compared in the DC2.4/OT-1 system. Similar Hsp70-ovalbumin fusion constructs have been shown to successfully deliver antigen to the MHCI cross-presentation pathway (Suzue et al., 1997; Takemoto et al., 2009). Additionally, because the GRP94.NTD-SIINFEKL fusion protein must be internalized and processed prior to MHCI loading, surface changing should not be a concern.

The data included in this dissertation clearly demonstrate that GRP94.NTD-mediated peptide cross-presentation is facilitated through both RME and fluid-phase endocytosis. In light of this finding, it is unclear how CD91 ligands could ablate GRP94-mediated peptide cross-presentation in RAW264.7 cells. These cells are known to constitutively sample the environment through fluid-phase uptake, and should be competent to cross-present GRP94/peptide complexes through this pathway (Gerondopoulos et al., 2010; Peppelenbosch et al., 2000; Yao et al., 2009). Therefore, it is likely that CD91 ligands influence GRP94-mediated peptide cross-presentation via an

indirect, post-uptake mechanism rather than directly competing for RME. It should also be noted that while the cross-presentation studies conducted for this dissertation expose DC2.4 to GRP94.NTD/peptide complexes for four hours, the assay utilized by Binder and Srivastava expose cells to both GRP94 and CD91 ligands for 20 hours (Binder et al., 2000; Binder and Srivastava, 2004). Therefore, the ablation of cross-presentation could be the result of prolonged exposure to high concentration of various CD91 ligands. Alternately, RAW264.7 cells could differ from DC2.4 cells in their ability to process GRP94/peptide constructs endocytosed via fluid-phase uptake. Additional studies are required to differentiate between these models.

Cumulatively, the studies included in this dissertation clarify the conflicting data on CD91 function in GRP94 surface binding and endocytic uptake. They demonstrate that CD91 does not directly bind or endocytose GRP94.NTD, and that CD91 does not significantly contribute to GRP94.NTD-mediated peptide cross-presentation. However, these studies cannot exclude the possibility that CD91 can indirectly modulate GRP94.NTD internalization/processing by DC2.4 cells. Additional studies are required to examine this possibility. The challenge now confronting the field is to understand the precise molecular mechanism(s) of GRP94-mediated peptide cross-presentation, as well as its physiological implications.

E. Cell surface heparan sulfate proteoglycans (HSPGs): identification of a novel binding site for extracellular GRP94.

Over the course of these studies, I have identified cell surface HSPGs as binding sites for extracellular GRP94.NTD on MEF-1 and PEA-13 cells. This conclusion was derived from three distinct experimental approaches. First, disrupting cell surface HSPG interactions with heparin severely diminished GRP94.NTD binding. Second, disrupting HSPG sulfation by culturing cells in sodium chlorate-supplemented media resulted in the dramatic loss of GRP94.NTD surface binding activity. Third, altering cell surface HSPG structures by digestion with exogenous heparinase II resulted in decreased GRP94.NTD surface binding.

These experiments demonstrate that cell surface HSPGs are necessary for >50% GRP94.NTD surface binding to MEF-1 and PEA-13 cells. With such a prominent contribution to GRP94.NTD surface binding, it is curious that this interaction was not previously reported. Unlike the high-affinity/low-capacity interactions observed between GRP94 and SR-A or SREC-I, the data in chapter 4 indicate that HSPG-dependent GRP94.NTD surface binding is the result of low-affinity/high-capacity interactions (Berwin et al., 2004; Berwin et al., 2003). Additionally, RAW264.7 and DC2.4 cells bind the 10E4 anti-heparan sulfate antibody at substantially lower levels than MEF-1 cells, indicating that these pAPC cell lines express substantially lower levels of cell surface HSPGs. If the pAPCs used for previous studies also expressed low levels of cell

surface HSPGs, any contributions of these low-affinity/high-capacity binding sites could have gone unnoticed. These interactions would have only been evident if extensive binding titrations were performed.

Alternatively, but not exclusively, the pAPC cells used in previous studies may not have expressed the specific class(es) of HSPGs that contribute to GRP94.NTD surface binding on MEF-1 and PEA-13 cells. In support of this hypothesis, conventional methods of disrupting HSPG interactions did not reduce GRP94.NTD binding to RAW264.7 cells. MEF-1 and RAW264.7 cells were also found to differ in the expression of two different cell surface HSPGs: *Gpc4* and *Gpc6*. Although this suggests that GRP94.NTD-HSPG interactions may be mediated by various types of glypicans, PI-PLC digestion studies indicate that GRP94.NTD also interacts with non-glypican cell surface HSPGs. Furthermore, GRP94.NTD binding to MEF-1 cells was reduced following treatment with sodium chlorate and heparinase II, both of which modify HSPG side chains and leave the individual core proteins intact. These data suggest that GRP94.NTD preferentially interacts with heparan sulfate GAGs, and that GRP94-HSPGs interactions do not rely on the expression of a specific cell surface HSPG core protein. Differences in CD44 and betaglycan expression were not examined in these studies.

F. An alternate model of GRP94-mediated immune stimulation: cell surface HSPGs in the formation of GRP94 signaling gradients.

It is well accepted that GRP94 is released into the extracellular environment following non-apoptotic cell death (Basu et al., 2000; Berwin et al., 2001). The prevalent model of GRP94-mediated immune stimulation predicts that this extracellular GRP94 is then bound by high-affinity receptors expressed by pAPCs, and subsequently stimulates innate and adaptive immune responses. However, research conducted during the past decade has revealed that GRP94 and other stress proteins are recognized by receptors expressed by a variety of non-immune cell types. For example, the Hsp70 receptor LOX-1 is expressed by macrophages, vascular smooth muscle cells, endothelial cells, and intestinal cells (Westerweel and Verhaar, 2010). The GRP94 receptor SREC-I is expressed by both macrophages and endothelial cells (Berwin et al., 2004). In addition to these, I have shown that GRP94.NTD can bind another class of widely-expressed receptors: cell surface HSPGs.

The diversity of cells and tissues that express these GRP94 receptors seems to contradict the present model of how extracellular GRP94 initiates immune responses. Indeed, it is unlikely that extracellular GRP94 would encounter a pAPCs when the local environment is populated with a variety of other cells, many of which express GRP94 surface receptors. For this reason, the present model must be expanded to include the

immunological implications of GRP94 interactions with non-immune cells. Interestingly, recent data from the Podack laboratory hint at an alternate model of GRP94-mediated immune stimulation. Using a previously characterized EG7 tumor cell line that had been engineered to secrete a GRP94-Ig fusion protein (EG7-gp96-Ig), Oizumi et al. demonstrated that DCs and natural killer cells are recruited to the site of EG7-gp96-Ig injection four days post-injection, and that CTL expansion can occur locally (Oizumi et al., 2007). The authors then propose that secretion of EG7-gp96-Ig can "transmit signals that result in the local recruitment and activation of innate and adaptive immune cells." In other studies, the cytosolic paralog of GRP94, Hsp90, has been shown to promote epidermal and dermal cell migration when present in the extracellular space (Cheng et al., 2008; Woodley et al., 2009).

Based on this information, it is plausible that extracellular GRP94 could promote pAPC migration to a site of traumatic cell death by behaving as a chemoattractant for local immune cells. In this modified model, extracellular GRP94 would first interact with cell surface receptors expressed by non-immune cells in the local environment. If GRP94 remained at the cell surface for prolonged periods of time, as has been seen with MEF-1 and PEA-13 cells, this interaction could create a GRP94 gradient that would guide immune cells to the site of injury. Although it is possible that pAPCs could respond to this gradient, it is more likely that surface-bound GRP94 would first be detected by local

immune cells (Radsak et al., 2003). These non-pAPC immune cells comprise the majority of immune cells that are recruited from the blood to the site of tissue damage, and are known to rapidly extravasate into inflamed tissues (Ben-Baruch et al., 1995; Lloyd and Oppenheim, 1992; Van Furth et al., 1973). Additionally, local immune cells, such as polymorphonuclear neutrophils (PMNs) and monocytes, are known to express GRP94 surface receptors (Radsak et al., 2003). PMNs, in particular, have been shown to secrete the attractant cytokine IL-8 in response to extracellular GRP94 (Radsak et al., 2003). The interaction of GRP94 with these immune cells could then facilitate the recruitment of pAPCs. Finally, the subsequent interaction of GRP94 with pAPCs could further stimulate the release of pro-inflammatory cytokines, and initiate a much broader immune response.

The formation of a GRP94 gradient could be facilitated by cell surface HSPGs. Unlike previously identified GRP94 receptors, cell surface HSPGs bind extracellular GRP94.NTD in a low-affinity/high-capacity manner, which would allow GRP94 to form a gradient over greater distances than would be possible for high-affinity/low-capacity GRP94 receptors. Furthermore, cell surface HSPGs are the only known GRP94 binding site that have an established role in the formation of morphogen and chemokine gradients. For example, Drosophila cell surface HSPGs are essential for the formation of Wnt, Hh, Fgf, and BMP gradients (Yan and Lin, 2009). In mammalian models it is well

established that cell surface HSPGs facilitate the formation of various chemokine gradients by sequestering chemokines at the cell surface (Taylor and Gallo, 2006). Similarly, MEF-1 and PEA-13 cells slowly internalize extracellular GRP94.NTD, with GRP94.NTD remaining sensitive external proteases for more than 10 min. Sequestering GRP94 at the cell surface for such extended periods of time would enhance the chance of local immune cells being recruited to the site of insult. For these reasons, I propose that cell surface HSPGs could facilitate the formation of a GRP94 gradient following necrotic cell death, and that these GRP94-HSPG interactions could be necessary for the formation of a localized GRP94-mediated immune response.

To test this alternate model of GRP94-mediated immune stimulation, future studies will need to address: a) the ability of GRP94 to function as a chemoattractant and b) the contribution of cell surface HSPGs to the formation of a GRP94 gradient. These studies would need to encompass both *in vitro* and *in vivo* migration studies and would require the use of highly purified, endotoxin-free GRP94. The most direct means of assessing the ability of GRP94 to stimulate immune cell migration *in vitro* is to measure the movement of tissue culture APCs through a fine matrix towards a source of GRP94. This could be accomplished using a standard Boyden chamber or cell invasion assay. The contribution of cell surface HSPGs to this migration would be more challenging to study *in vitro* and may need to be analyzed *in vivo*. These studies would need to first

establish an assay to measure APC migration to a site of GRP94 release, such as those described by Oizumi et al. (Oizumi et al., 2007). Once this has been accomplished, mice could be injected with heparinase a few min prior to the injection of GRP94. Heparinase treatment effectively cleaves sulfated glycan chains and has been shown to alter various HSPG-dependent processes *in vivo* (Mahley and Ji, 1999). By comparing control and heparinase-treated animals, it should then be possible to determine if cell surface HSPGs are necessary for the formation of localized GRP94-mediated immune responses.

These studies extend the diversity of surface receptors that recognize GRP94, and suggest that HSPG-dependent interactions may contribute to the biology of GRP94-elicited immune responses. Further examination into HSPG-GRP94 interactions could influence both the design and modes of administration of GRP94-based vaccines.

References

Anderson, G.P., and N.L. Nerurkar. 2002. Improved fluoroimmunoassays using the dye Alexa Fluor 647 with the RAPTOR, a fiber optic biosensor. *J Immunol Methods*. 271:17-24.

Argon, Y., and B.B. Simen. 1999. GRP94, an ER chaperone with protein and peptide binding properties. *Semin Cell Dev Biol*. 10:495-505.

Arnold-Schild, D., D. Hanau, D. Spehner, C. Schmid, H.G. Rammensee, H. de la Salle, and H. Schild. 1999. Cutting edge: receptor-mediated endocytosis of heat shock proteins by professional antigen-presenting cells. *J Immunol*. 162:3757-60.

Baeuerle, P.A., and W.B. Huttner. 1986. Chlorate--a potent inhibitor of protein sulfation in intact cells. *Biochem Biophys Res Commun*. 141:870-7.

Baker-LePain, J.C., M. Sarzotti, T.A. Fields, C.Y. Li, and C.V. Nicchitta. 2002. GRP94 (gp96) and GRP94 N-terminal geldanamycin binding domain elicit tissue nonrestricted tumor suppression. *J Exp Med*. 196:1447-59.

Baker-LePain, J.C., M. Sarzotti, and C.V. Nicchitta. 2004. Glucose-regulated protein 94/glycoprotein 96 elicits bystander activation of CD4+ T cell Th1 cytokine production in vivo. *J Immunol*. 172:4195-203.

Basu, S., R.J. Binder, T. Ramalingam, and P.K. Srivastava. 2001. CD91 is a common receptor for heat shock proteins gp96, hsp90, hsp70, and calreticulin. *Immunity*. 14:303-13.

Basu, S., R.J. Binder, R. Suto, K.M. Anderson, and P.K. Srivastava. 2000. Necrotic but not apoptotic cell death releases heat shock proteins, which deliver a partial maturation signal to dendritic cells and activate the NF-kappa B pathway. *Int Immunol*. 12:1539-46.

Ben-Baruch, A., D.F. Michiel, and J.J. Oppenheim. 1995. Signals and receptors involved in recruitment of inflammatory cells. *J Biol Chem*. 270:11703-6.

Berwin, B., Y. Delneste, R.V. Lovingood, S.R. Post, and S.V. Pizzo. 2004. SREC-I, a type F scavenger receptor, is an endocytic receptor for calreticulin. *J Biol Chem*. 279:51250-7.

Berwin, B., J.P. Hart, S.V. Pizzo, and C.V. Nicchitta. 2002a. Cutting edge: CD91-independent cross-presentation of GRP94(gp96)-associated peptides. *J Immunol*. 168:4282-6.

Berwin, B., J.P. Hart, S. Rice, C. Gass, S.V. Pizzo, S.R. Post, and C.V. Nicchitta. 2003. Scavenger receptor-A mediates gp96/GRP94 and calreticulin internalization by antigen-presenting cells. *EMBO J*. 22:6127-36.

Berwin, B., and C.V. Nicchitta. 2001. To find the road traveled to tumor immunity: the trafficking itineraries of molecular chaperones in antigen-presenting cells. *Traffic*. 2:690-7.

Berwin, B., R.C. Reed, and C.V. Nicchitta. 2001. Virally induced lytic cell death elicits the release of immunogenic GRP94/gp96. *J Biol Chem*. 276:21083-8.

Berwin, B., M.F. Rosser, K.G. Brinker, and C.V. Nicchitta. 2002b. Transfer of GRP94(Gp96)-associated peptides onto endosomal MHC class I molecules. *Traffic*. 3:358-66.

Bevan, M.J. 1976a. Cross-priming for a secondary cytotoxic response to minor H antigens with H-2 congenic cells which do not cross-react in the cytotoxic assay. *J Exp Med*. 143:1283-8.

Bevan, M.J. 1976b. Minor H antigens introduced on H-2 different stimulating cells cross-react at the cytotoxic T cell level during in vivo priming. *J Immunol*. 117:2233-8.

Binder, R.J., D.K. Han, and P.K. Srivastava. 2000. CD91: a receptor for heat shock protein gp96. *Nat Immunol*. 1:151-5.

Binder, R.J., and P.K. Srivastava. 2004. Essential role of CD91 in re-presentation of gp96-chaperoned peptides. *Proc Natl Acad Sci U S A*. 101:6128-33.

Binder, R.J., R. Vatner, and P. Srivastava. 2004. The heat-shock protein receptors: some answers and more questions. *Tissue Antigens*. 64:442-51.

Biswas, C., U. Sriram, B. Ciric, O. Ostrovsky, S. Gallucci, and Y. Argon. 2006. The N-terminal fragment of GRP94 is sufficient for peptide presentation via professional antigen-presenting cells. *Int Immunol*. 18:1147-57.

Blachere, N.E., Z. Li, R.Y. Chandawarkar, R. Suto, N.S. Jaikaria, S. Basu, H. Udono, and P.K. Srivastava. 1997. Heat shock protein-peptide complexes, reconstituted in vitro, elicit peptide-specific cytotoxic T lymphocyte response and tumor immunity. *J Exp Med*. 186:1315-22.

Bowers, E.V., J.J. Horvath, J.E. Bond, G.J. Cianciolo, and S.V. Pizzo. 2009. Antigen delivery by alpha(2)-macroglobulin enhances the cytotoxic T lymphocyte response. *J Leukoc Biol*. 86:1259-68.

Brossart, P., and M.J. Bevan. 1997. Presentation of exogenous protein antigens on major histocompatibility complex class I molecules by dendritic cells: pathway of presentation and regulation by cytokines. *Blood*. 90:1594-9.

Bu, G., and A.L. Schwartz. 1998. RAP, a novel type of ER chaperone. *Trends Cell Biol*. 8:272-6.

Burnell, J.N., and A.B. Roy. 1978. Purification and properties of the ATP sulphurylase of rat liver. *Biochim Biophys Acta*. 527:239-48.

Calderwood, S.K., S.S. Mambula, and P.J. Gray, Jr. 2007. Extracellular heat shock proteins in cell signaling and immunity. *Ann N Y Acad Sci*. 1113:28-39.

Chen, B., D. Zhong, and A. Monteiro. 2006. Comparative genomics and evolution of the HSP90 family of genes across all kingdoms of organisms. *BMC Genomics*. 7:156.

Cheng, C.F., J. Fan, M. Fedesco, S. Guan, Y. Li, B. Bandyopadhyay, A.M. Bright, D. Yerushalmi, M. Liang, M. Chen, Y.P. Han, D.T. Woodley, and W. Li. 2008. Transforming growth factor alpha (TGFalpha)-stimulated secretion of HSP90alpha: using the receptor LRP-1/CD91 to promote human skin cell migration against a TGFbeta-rich environment during wound healing. *Mol Cell Biol*. 28:3344-58.

Conrad, H.E. 1998. Heparin-Binding Proteins. Academic Press, San Diego, CA.

Delneste, Y., G. Magistrelli, J. Gauchat, J. Haeuw, J. Aubry, K. Nakamura, N. Kawakami-Honda, L. Goetsch, T. Sawamura, J. Bonnefoy, and P. Jeannin. 2002. Involvement of LOX-1 in dendritic cell-mediated antigen cross-presentation. *Immunity*. 17:353-62.

Demine, R., and P. Walden. 2005. Testing the role of gp96 as peptide chaperone in antigen processing. *J Biol Chem*. 280:17573-8.

Farley, J.R., G. Nakayama, D. Cryns, and I.H. Segel. 1978. Adenosine triphosphate sulfurylase from Penicillium chrysogenum equilibrium binding, substrate hydrolysis, and isotope exchange studies. *Arch Biochem Biophys*. 185:376-90.

Foley, E.J. 1953. Antigenic properties of methylcholanthrene-induced tumors in mice of the strain of origin. *Cancer Res*. 13:835-7.

Gerondopoulos, A., T. Jackson, P. Monaghan, N. Doyle, and L.O. Roberts. 2010. Murine norovirus-1 cell entry is mediated through a non-clathrin-, non-caveolae-, dynamin- and cholesterol-dependent pathway. *J Gen Virol*. 91:1428-38.

Gromme, M., F.G. Uytdehaag, H. Janssen, J. Calafat, R.S. van Binnendijk, M.J. Kenter, A. Tulp, D. Verwoerd, and J. Neefjes. 1999. Recycling MHC class I molecules and endosomal peptide loading. *Proc Natl Acad Sci U S A*. 96:10326-31.

Guyre, C.A., M.E. Barreda, S.L. Swink, and M.W. Fanger. 2001. Colocalization of Fc gamma RI-targeted antigen with class I MHC: implications for antigen processing. *J Immunol*. 166:2469-78.

Heath, W.R., and F.R. Carbone. 2001. Cross-presentation in viral immunity and self-tolerance. *Nat Rev Immunol*. 1:126-34.

Herz, J., J.L. Goldstein, D.K. Strickland, Y.K. Ho, and M.S. Brown. 1991. 39-kDa protein modulates binding of ligands to low density lipoprotein receptor-related protein/alpha 2-macroglobulin receptor. *J Biol Chem*. 266:21232-8.

Herz, J., and D.K. Strickland. 2001. LRP: a multifunctional scavenger and signaling receptor. *J Clin Invest*. 108:779-84.

Hilf, N., H. Singh-Jasuja, P. Schwarzmaier, C. Gouttefangeas, H.G. Rammensee, and H. Schild. 2002. Human platelets express heat shock protein receptors and regulate dendritic cell maturation. *Blood*. 99:3676-82.

Huang Q, S.R., Jockheck-Clark A.R., Shi B, Mandelin II A.M., Tak P.P., Haines G.K., Nicchitta C.V., and Pope R.M.. 2009. Heat Shock Protein 96 Is Elevated in Rheumatoid Arthritis and Activates Macrophages Primarily via TLR2 Signaling. *J Immunol*. 182.

Iadonato, S.P., G. Bu, E.A. Maksymovitch, and A.L. Schwartz. 1993. Interaction of a 39 kDa protein with the low-density-lipoprotein-receptor-related protein (LRP) on rat hepatoma cells. *Biochem J*. 296 (Pt 3):867-75.

Keller, K.M., P.R. Brauer, and J.M. Keller. 1989. Modulation of cell surface heparan sulfate structure by growth of cells in the presence of chlorate. *Biochemistry*. 28:8100-7.

Kleijmeer, M.J., J.M. Escola, F.G. UytdeHaag, E. Jakobson, J.M. Griffith, A.D. Osterhaus, W. Stoorvogel, C.J. Melief, C. Rabouille, and H.J. Geuze. 2001. Antigen loading of MHC class I molecules in the endocytic tract. *Traffic*. 2:124-37.

Klein, G., H.O. Sjogren, E. Klein, and K.E. Hellstrom. 1960. Demonstration of resistance against methylcholanthrene-induced sarcomas in the primary autochthonous host. *Cancer Res*. 20:1561-72.

Koch, G., M. Smith, D. Macer, P. Webster, and R. Mortara. 1986. Endoplasmic reticulum contains a common, abundant calcium-binding glycoprotein, endoplasmin. *J Cell Sci*. 86:217-32.

Kounnas, M.Z., R.E. Morris, M.R. Thompson, D.J. FitzGerald, D.K. Strickland, and C.B. Saelinger. 1992. The alpha 2-macroglobulin receptor/low density lipoprotein receptor-related protein binds and internalizes Pseudomonas exotoxin A. *J Biol Chem*. 267:12420-3.

Kozutsumi, Y., M. Segal, K. Normington, M.J. Gething, and J. Sambrook. 1988. The presence of malfolded proteins in the endoplasmic reticulum signals the induction of glucose-regulated proteins. *Nature*. 332:462-4.

Kramer, K.L., and H.J. Yost. 2003. Heparan sulfate core proteins in cell-cell signaling. *Annu Rev Genet*. 37:461-84.

Krieger, M., and J. Herz. 1994. Structures and functions of multiligand lipoprotein receptors: macrophage scavenger receptors and LDL receptor-related protein (LRP). *Annu Rev Biochem*. 63:601-37.

Laskowitz, D.T., A.D. Thekdi, S.D. Thekdi, S.K. Han, J.K. Myers, S.V. Pizzo, and E.R. Bennett. 2001. Downregulation of microglial activation by apolipoprotein E and apoE-mimetic peptides. *Exp Neurol*. 167:74-85.

Li, Y., W. Lu, M.P. Marzolo, and G. Bu. 2001. Differential functions of members of the low density lipoprotein receptor family suggested by their distinct endocytosis rates. *J Biol Chem*. 276:18000-6.

Li, Z., and P.K. Srivastava. 1993. Tumor rejection antigen gp96/grp94 is an ATPase: implications for protein folding and antigen presentation. *EMBO J*. 12:3143-51.

Lillis, A.P., L.B. Van Duyn, J.E. Murphy-Ullrich, and D.K. Strickland. 2008. LDL receptor-related protein 1: unique tissue-specific functions revealed by selective gene knockout studies. *Physiol Rev*. 88:887-918.

Liu, B., J. Dai, H. Zheng, D. Stoilova, S. Sun, and Z. Li. 2003. Cell surface expression of an endoplasmic reticulum resident heat shock protein gp96 triggers MyD88-dependent systemic autoimmune diseases. *Proc Natl Acad Sci U S A*. 100:15824-9.

Lloyd, A.R., and J.J. Oppenheim. 1992. Poly's lament: the neglected role of the polymorphonuclear neutrophil in the afferent limb of the immune response. *Immunol Today*. 13:169-72.

Mahley, R.W., and Z.S. Ji. 1999. Remnant lipoprotein metabolism: key pathways involving cell-surface heparan sulfate proteoglycans and apolipoprotein E. *J Lipid Res*. 40:1-16.

Maki, R.G., L.J. Old, and P.K. Srivastava. 1990. Human homologue of murine tumor rejection antigen gp96: 5'-regulatory and coding regions and relationship to stress-induced proteins. *Proc Natl Acad Sci U S A*. 87:5658-62.

Matzinger, P. 1994. Tolerance, danger, and the extended family. *Annu Rev Immunol*. 12:991-1045.

Maynard, J.C., T. Pham, T. Zheng, A. Jockheck-Clark, H.B. Rankin, C.B. Newgard, E.P. Spana, and C.V. Nicchitta. 2010. Gp93, the Drosophila GRP94 ortholog, is required for gut epithelial homeostasis and nutrient assimilation-coupled growth control. *Dev Biol*. 339:295-306.

Mazzarella, R.A., and M. Green. 1987. ERp99, an abundant, conserved glycoprotein of the endoplasmic reticulum, is homologous to the 90-kDa heat shock protein (hsp90) and the 94-kDa glucose regulated protein (GRP94). *J Biol Chem*. 262:8875-83.

Menoret, A., and G. Bell. 2000. Purification of multiple heat shock proteins from a single tumor sample. *J Immunol Methods*. 237:119-30.

Nair, S., P.A. Wearsch, D.A. Mitchell, J.J. Wassenberg, E. Gilboa, and C.V. Nicchitta. 1999. Calreticulin displays in vivo peptide-binding activity and can elicit CTL responses against bound peptides. *J Immunol*. 162:6426-32.

Nicchitta, C.V. 2003. Re-evaluating the role of heat-shock protein-peptide interactions in tumour immunity. *Nat Rev Immunol*. 3:427-32.

Nicchitta, C.V., D.M. Carrick, and J.C. Baker-Lepain. 2004. The messenger and the message: gp96 (GRP94)-peptide interactions in cellular immunity. *Cell Stress Chaperones*. 9:325-31.

Nieland, T.J., M.C. Tan, M. Monne-van Muijen, F. Koning, A.M. Kruisbeek, and G.M. van Bleek. 1996. Isolation of an immunodominant viral peptide that is endogenously bound to the stress protein GP96/GRP94. *Proc Natl Acad Sci U S A*. 93:6135-9.

Norbury, C.C., L.J. Hewlett, A.R. Prescott, N. Shastri, and C. Watts. 1995. Class I MHC presentation of exogenous soluble antigen via macropinocytosis in bone marrow macrophages. *Immunity*. 3:783-91.

Nykjaer, A., and T.E. Willnow. 2002. The low-density lipoprotein receptor gene family: a cellular Swiss army knife? *Trends Cell Biol*. 12:273-80.

Oizumi, S., N. Strbo, S. Pahwa, V. Deyev, and E.R. Podack. 2007. Molecular and cellular requirements for enhanced antigen cross-presentation to CD8 cytotoxic T lymphocytes. *J Immunol*. 179:2310-7.

Peppelenbosch, M.P., M. DeSmedt, G. Pynaert, S.J. van Deventer, and J. Grooten. 2000. Macrophages present pinocytosed exogenous antigen via MHC class I whereas antigen ingested by receptor-mediated endocytosis is presented via MHC class II. *J Immunol*. 165:1984-91.

Pimpaneau, V., P. Midoux, G. Durand, P. De Baetselier, M. Monsigny, and A.C. Roche. 1989. Endocytosis of alpha 1-acid glycoprotein variants and of neoglycoproteins containing mannose derivatives by a mouse hybridoma cell line (2C11-12). Comparison with mouse peritoneal macrophages. *Glycoconj J*. 6:561-74.

Prehn, R.T., and J.M. Main. 1957. Immunity to methylcholanthrene-induced sarcomas. *J Natl Cancer Inst*. 18:769-78.

Radsak, M.P., N. Hilf, H. Singh-Jasuja, S. Braedel, P. Brossart, H.G. Rammensee, and H. Schild. 2003. The heat shock protein Gp96 binds to human neutrophils and monocytes and stimulates effector functions. *Blood*. 101:2810-5.

Randow, F., and B. Seed. 2001. Endoplasmic reticulum chaperone gp96 is required for innate immunity but not cell viability. *Nat Cell Biol*. 3:891-6.

Reed, R.C., B. Berwin, J.P. Baker, and C.V. Nicchitta. 2003. GRP94/gp96 elicits ERK activation in murine macrophages. A role for endotoxin contamination in NF-kappa B activation and nitric oxide production. *J Biol Chem*. 278:31853-60.

Reed, R.C., T. Zheng, and C.V. Nicchitta. 2002. GRP94-associated enzymatic activities. Resolution by chromatographic fractionation. *J Biol Chem*. 277:25082-9.

Riera, M., N. Roher, F. Miro, C. Gil, R. Trujillo, J. Aguilera, M. Plana, and E. Itarte. 1999. Association of protein kinase CK2 with eukaryotic translation initiation factor eIF-2 and with grp94/endoplasmin. *Mol Cell Biochem*. 191:97-104.

Rock, K.L., and L. Shen. 2005. Cross-presentation: underlying mechanisms and role in immune surveillance. *Immunol Rev*. 207:166-83.

Sallusto, F., M. Cella, C. Danieli, and A. Lanzavecchia. 1995. Dendritic cells use macropinocytosis and the mannose receptor to concentrate macromolecules in the major histocompatibility complex class II compartment: downregulation by cytokines and bacterial products. *J Exp Med*. 182:389-400.

Sarafanov, A.G., N.M. Ananyeva, M. Shima, and E.L. Saenko. 2001. Cell surface heparan sulfate proteoglycans participate in factor VIII catabolism mediated by low density lipoprotein receptor-related protein. *J Biol Chem*. 276:11970-9.

Shaknovich, R., G. Shue, and D.S. Kohtz. 1992. Conformational activation of a basic helix-loop-helix protein (MyoD1) by the C-terminal region of murine HSP90 (HSP84). *Mol Cell Biol*. 12:5059-68.

Singh-Jasuja, H., H.U. Scherer, N. Hilf, D. Arnold-Schild, H.G. Rammensee, R.E. Toes, and H. Schild. 2000a. The heat shock protein gp96 induces maturation of dendritic cells and down-regulation of its receptor. *Eur J Immunol*. 30:2211-5.

Singh-Jasuja, H., R.E. Toes, P. Spee, C. Munz, N. Hilf, S.P. Schoenberger, P. Ricciardi-Castagnoli, J. Neefjes, H.G. Rammensee, D. Arnold-Schild, and H. Schild. 2000b. Cross-presentation of glycoprotein 96-associated antigens on major histocompatibility complex class I molecules requires receptor-mediated endocytosis. *J Exp Med*. 191:1965-74.

Soldano, K.L., A. Jivan, C.V. Nicchitta, and D.T. Gewirth. 2003. Structure of the N-terminal domain of GRP94. Basis for ligand specificity and regulation. *J Biol Chem*. 278:48330-8.

Srivastava, P. 2002. Roles of heat-shock proteins in innate and adaptive immunity. *Nat Rev Immunol*. 2:185-94.

Srivastava, P.K. 1993. Peptide-binding heat shock proteins in the endoplasmic reticulum: role in immune response to cancer and in antigen presentation. *Adv Cancer Res*. 62:153-77.

Srivastava, P.K., Y.T. Chen, and L.J. Old. 1987. 5'-structural analysis of genes encoding polymorphic antigens of chemically induced tumors. *Proc Natl Acad Sci U S A*. 84:3807-11.

Srivastava, P.K., A.B. DeLeo, and L.J. Old. 1986. Tumor rejection antigens of chemically induced sarcomas of inbred mice. *Proc Natl Acad Sci U S A*. 83:3407-11.

Srivastava, P.K., and R.G. Maki. 1991. Stress-induced proteins in immune response to cancer. *Curr Top Microbiol Immunol*. 167:109-23.

Suto, R., and P.K. Srivastava. 1995. A mechanism for the specific immunogenicity of heat shock protein-chaperoned peptides. *Science*. 269:1585-8.

Suzue, K., X. Zhou, H.N. Eisen, and R.A. Young. 1997. Heat shock fusion proteins as vehicles for antigen delivery into the major histocompatibility complex class I presentation pathway. *Proc Natl Acad Sci U S A*. 94:13146-51.

Swanson, J.A., and C. Watts. 1995. Macropinocytosis. *Trends Cell Biol*. 5:424-8.

Takayama, Y., P. May, R.G. Anderson, and J. Herz. 2005. Low density lipoprotein receptor-related protein 1 (LRP1) controls endocytosis and c-CBL-mediated ubiquitination of the platelet-derived growth factor receptor beta (PDGFR beta). *J Biol Chem*. 280:18504-10.

Takayama, Y., and T. Takezawa. 2006. Lactoferrin promotes collagen gel contractile activity of fibroblasts mediated by lipoprotein receptors. *Biochem Cell Biol*. 84:268-74.

Takemoto, S., M. Nishikawa, T. Otsuki, A. Yamaoka, K. Maeda, A. Ota, and Y. Takakura. 2009. Enhanced generation of cytotoxic T lymphocytes by increased cytosolic delivery of MHC class I epitope fused to mouse heat shock protein 70 via polyhistidine conjugation. *J Control Release*. 135:11-8.

Theriault, J.R., H. Adachi, and S.K. Calderwood. 2006. Role of scavenger receptors in the binding and internalization of heat shock protein 70. *J Immunol*. 177:8604-11.

Theriault, J.R., S.S. Mambula, T. Sawamura, M.A. Stevenson, and S.K. Calderwood. 2005. Extracellular HSP70 binding to surface receptors present on antigen presenting cells and endothelial/epithelial cells. *FEBS Lett*. 579:1951-60.

Udono, H., D.L. Levey, and P.K. Srivastava. 1994. Cellular requirements for tumor-specific immunity elicited by heat shock proteins: tumor rejection antigen gp96 primes CD8+ T cells in vivo. *Proc Natl Acad Sci U S A*. 91:3077-81.

Vabulas, R.M., S. Braedel, N. Hilf, H. Singh-Jasuja, S. Herter, P. Ahmad-Nejad, C.J. Kirschning, C. Da Costa, H.G. Rammensee, H. Wagner, and H. Schild. 2002. The endoplasmic reticulum-resident heat shock protein Gp96 activates dendritic cells via the Toll-like receptor 2/4 pathway. *J Biol Chem*. 277:20847-53.

Van Furth, R., M.C. Diesselhoff-den Dulk, and H. Mattie. 1973. Quantitative study on the production and kinetics of mononuclear phagocytes during an acute inflammatory reaction. *J Exp Med*. 138:1314-30.

Vogen, S., T. Gidalevitz, C. Biswas, B.B. Simen, E. Stein, F. Gulmen, and Y. Argon. 2002. Radicicol-sensitive peptide binding to the N-terminal portion of GRP94. *J Biol Chem*. 277:40742-50.

Walters, J.J., and B. Berwin. 2005. Differential CD91 dependence for calreticulin and Pseudomonas exotoxin-A endocytosis. *Traffic*. 6:1173-82.

Wanderling, S., B.B. Simen, O. Ostrovsky, N.T. Ahmed, S.M. Vogen, T. Gidalevitz, and Y. Argon. 2007. GRP94 is essential for mesoderm induction and muscle development because it regulates insulin-like growth factor secretion. *Mol Biol Cell*. 18:3764-75.

Warger, T., N. Hilf, G. Rechtsteiner, P. Haselmayer, D.M. Carrick, H. Jonuleit, P. von Landenberg, H.G. Rammensee, C.V. Nicchitta, M.P. Radsak, and H. Schild. 2006. Interaction of TLR2 and TLR4 ligands with the N-terminal domain of Gp96 amplifies innate and adaptive immune responses. *J Biol Chem*. 281:22545-53.

Wassenberg, J.J., C. Dezfulian, and C.V. Nicchitta. 1999. Receptor mediated and fluid phase pathways for internalization of the ER Hsp90 chaperone GRP94 in murine macrophages. *J Cell Sci*. 112 (Pt 13):2167-75.

Wearsch, P.A., and C.V. Nicchitta. 1996. Purification and partial molecular characterization of GRP94, an ER resident chaperone. *Protein Expr Purif*. 7:114-21.

Wearsch, P.A., and C.V. Nicchitta. 1997. Interaction of endoplasmic reticulum chaperone GRP94 with peptide substrates is adenine nucleotide-independent. *J Biol Chem*. 272:5152-6.

Wearsch, P.A., L. Voglino, and C.V. Nicchitta. 1998. Structural transitions accompanying the activation of peptide binding to the endoplasmic reticulum Hsp90 chaperone GRP94. *Biochemistry*. 37:5709-19.

Westerweel, P.E., and M.C. Verhaar. 2010. LOX-1: luring ox-LDL into the arterial wall. *J Hypertens*. 28:1127-8.

Wiech, H., J. Buchner, R. Zimmermann, and U. Jakob. 1992. Hsp90 chaperones protein folding in vitro. *Nature*. 358:169-70.

Willnow, T.E., and J. Herz. 1994. Genetic deficiency in low density lipoprotein receptor-related protein confers cellular resistance to Pseudomonas exotoxin A. Evidence that this protein is required for uptake and degradation of multiple ligands. *J Cell Sci*. 107:719-26.

Woodley, D.T., J. Fan, C.F. Cheng, Y. Li, M. Chen, G. Bu, and W. Li. 2009. Participation of the lipoprotein receptor LRP1 in hypoxia-HSP90alpha autocrine signaling to promote keratinocyte migration. *J Cell Sci*. 122:1495-8.

Yao, W., K. Li, and K. Liao. 2009. Macropinocytosis contributes to the macrophage foam cell formation in RAW264.7 cells. *Acta Biochim Biophys Sin (Shanghai)*. 41:773-80.

Ying, M., and T. Flatmark. 2006. Binding of the viral immunogenic octapeptide VSV8 to native glucose-regulated protein Grp94 (gp96) and its inhibition by the physiological ligands ATP and Ca2+. *FEBS J*. 273:513-22.

Biography

Angela was born in Ridgewood, New Jersey on April 30, 1982. Although her father was stationed in several different places before he retired from the Army, she claims Redfield, South Dakota as her hometown. After graduating from Redfield High School in 2000, Angela attended the University of South Dakota (USD) in Vermillion, SD. She graduated Summa Cum Laude in 2004 with a BS in Biology and Chemistry. Angela completed her honors thesis under the direction of Dr. Robert Noiva at the USD Medical School, Department of Basic Biomedical Sciences. In Dr. Noiva's lab, Angela studied the effects of redox conditions on the ability of protein disulfide isomerase to catalyze proper substrate folding. Other highlights of her undergraduate research career included working with Dr. Miles Koppang (USD Chemistry Department) on the electrochemical analysis of amino acids using a diamond thin film electrode, and working with Dr. Kevin Shey (Cell and Molecular Pharmacology, Medical University of South Carolina) on the proteomic analysis of steroid-induced human trabecular meshwork cells.

Angela entered graduate school through the Cell and Molecular Biology Program at Duke University in the fall of 2004. After joining the laboratory of Dr. Christopher Nicchitta, Angela focused her research on the mechanisms of extracellular GRP94 immune stimulation. Specifically, she examined the interaction of GRP94 with

cell surface receptors. When Angela is not at the bench, she enjoys playing the piano and spending time with her husband, James.

Publications:

Angela R. Jockheck-Clark, Mariam B. Totonchy, Edith V. Bowers, Julie Neubauer, Salvatore V. Pizzo, and Christopher V. Nicchitta. HEAT SHOCK PROTEIN RECEPTORS: Analysis of CD91 and identification of heparan sulfate proteoglycans as novel GRP94 cell surface receptors. *J. Immunol.* (in submission).

Jason C. Maynard, Trang Pham, Tianli Zheng, **Angela R. Jockheck-Clark**, Helen B. Rankin, Christopher B. Newgard, Eric P. Spana, and Christopher V. Nicchitta. *Gp93*, the *Drosophila GRP94* ortholog, is required for gut epithelial homeostasis and nutrient assimilation-coupled growth control. *Dev Biol.* 2010(339): 295-306.

Qi-Quan Huang, Rudina Sobkoviak, **Angela R. Jockheck-Clark**, Arthur M. Mandelin II, Paul Peter Tak, G. Kennith Haines, Christopher V. Nicchitta, and Richard M. Pope. Heat Shock Protein 96 is Elevated in Rheumatoid Arthritis and Activates Macrophages via TLR2 Signaling. *J. Immunol.* 2009 (182): 4965-73.